INFORMATION TO USERS

This manuscript has been reproduced from the microfilm master. UMI films the text directly from the original or copy submitted. Thus, some thesis and dissertation copies are in typewriter face, while others may be from any type of computer printer.

The quality of this reproduction is dependent upon the quality of the copy submitted. Broken or indistinct print, colored or poor quality illustrations and photographs, print bleedthrough, substandard margins, and improper alignment can adversely affect reproduction.

In the unlikely event that the author did not send UMI a complete manuscript and there are missing pages, these will be noted. Also, if unauthorized copyright material had to be removed, a note will indicate the deletion.

Oversize materials (e.g., maps, drawings, charts) are reproduced by sectioning the original, beginning at the upper left-hand corner and continuing from left to right in equal sections with small overlaps. Each original is also photographed in one exposure and is included in reduced form at the back of the book.

Photographs included in the original manuscript have been reproduced xerographically in this copy. Higher quality 6" x 9" black and white photographic prints are available for any photographs or illustrations appearing in this copy for an additional charge. Contact UMI directly to order.

UMI

A Bell & Howell Information Company
300 North Zeeb Road, Ann Arbor MI 48106-1346 USA
313/761-4700 800/521-0600

Université d'Ottawa · University of Ottawa

Andrei S. Rosen

Effects of brief anoxia on the electrophysiology of neocortical neurons *in vitro*

Andrei S. Rosen

University of Ottawa, Ottawa, Canada

MCMXCVI

ABSTRACT

Although the function of all mammalian central neurons is destroyed by prolonged lack of O_2, during briefer exposures neurons from different regions show differential vulnerability. Pyramidal neurons from the neocortex are reported as some of the most sensitive to anoxia. Using intracellular recording techniques in current clamp mode, the effects of brief anoxia (4–6 min replacement of O_2 by N_2) were studied in pyramidal neurons of layers II–III from adult rat neocortical slices. Changes of passive membrane properties (V_R and R_N) and of synaptic potentials (EPSPs and IPSPs) induced by anoxia have been investigated together with the possible mechanisms underlying these changes. Characteristically, brief anoxia induced in all tested neurons a moderate depolarization (AD) (3–5 mV), accompanied by a small to moderate (20%) decrease in R_N.

The ionic substrate of AD has not been entirely elucidated, but the results of experiments involving the Na^+ channel blocker TTX, Na^+ substitution, and excitatory amino acid (EAA) antagonists (KYN, DL–APV, MCPG) strongly suggest that a major factor responsible for AD is a Na^+ influx, mainly through EAA-activated channels of the "non-NMDA" (AMPA/kainate) type. However, since it is most probable that AD is a mixed ionic phenomenon, other conductances and intracellular cation accumulation are likely to be involved.

Anoxia invariably induced a reversible depression of the evoked postsynaptic potentials, with both fast and slow IPSPs showing an increased sensitivity as compared to the EPSPs. Among the latter, the polysynaptic late EPSP component was more sensitive (reversible block) than the monosynaptic early EPSP (60–70% reduction). The mechanisms responsible for PSP depression were shown to be both pre- and post-synaptic in origin, with a more important contribution of the former—the process most likely involved being presynaptic inhibition mediated by adenosine activation of A_1 receptors, as shown by the protective effect of the A_1 antagonist, 8-CPT.

Among other protective antianoxic measures investigated, creatine pre–incubation and attempts to activate the ATP–sensitive K^+ channels with diazoxide were shown to be ineffective. Changes in temperature between 26 and 37.5°C (from the control temperature of 33.5°C) showed, however, a good correlation with the anoxic events (i.e. warming accentuated and cooling diminished the effects of anoxia). Therefore, relative hypothermia (26°C) proved to be the only measure capable of fully stabilizing the membrane potential and preserving the PSP amplitude during the anoxic challenge.

Everything should be made as simple as possible, but not simpler.

ACKNOWLEDGEMENTS

... to Dr. Mary Morris, my friend ...

... to Drs. Ken Marshall, Michel Désilets and Kresimir Krnjevic, for their invaluable suggestions (and questions) ...

... to the Medical Research Council of Canada, for making this research possible...

... to Mr. Simon Nsonwah, for constant help and positive complicity...

... to Dr. Gabriela Obrocea, for preparing and calibrating the potassium-sensitive microelectrodes ...

... to my wife, for her patience ...

Andrei S. Rosen MD, MSc

LIST OF PUBLICATIONS RELATED TO PhD RESEARCH

1. ABSTRACTS

Rosen, A.S. and Morris, M.E. (1990). Anoxic depolarization of neocortical pyramidal neurons in vitro. Soc. Neurosci. Abstr. 16: 277.

Rosen, A.S. and Morris, M.E. (1991). Anoxic depression of neocortical synaptic potentials. Soc. Neurosci. Abstr. 17: 1079.

Rosen, A.S. and Morris, M.E. (1991). Decreased synaptic activation during anoxia in neocortex. Can. J. Physiol. Pharmacol. 69: Axxviii.

Rosen, A.S.and Morris, M.E. (1992). Role of post-synaptic mechanisms in anoxia-induced depression of neocortical synaptic transmission. Soc. Neurosci. Abstr. 18: 1580.

Morris, M.E., Baimbridge, K.G.B., El-Beheiry, H., Magnuson, D.S.K., Obrocea, G.V. and **Rosen, A.S.** (1992). Correlation of calbindin and neu ronal anoxic responses. Soc. Neurosci. Abstr. 18: 1588.

Rosen, A.S. and Morris, M.E. (1993). Sustained depolarizing response during brief anoxia in CA1 and CA2 hippocampal pyramidal neurons. Can. J. Physiol. Pharmacol. 71: Axix-Axx.

Rosen, A.S. and Morris, M.E. (1993). Ionic mechanisms underlying neocorti cal anoxic depolarization. Soc. Neurosci. Abstr. 19: 1668.

2. PAPERS

Rosen, A.S. and Morris, M.E. (1991). Depolarizing effects of anoxia on pyramidal cells of rat neocortex. Neurosci. Lett. 124: 169–173.

Rosen, A.S. and Morris, M.E. (1993). Anoxic depression of excitatory and inhibitory postsynaptic potentials in rat neocortical slices. J. Neurophysiol. 69 (1): 109–117.

Rosen, A.S. and Morris, M.E. (1994). Influence of temperature on anoxic responses of neocortical pyramidal neurons. Neuroscience 63(4): 949–955.

Morris, M.E., Baimbridge, K.G., El-Beheiry, H., Obrocea, V.G. and **Rosen, A.S.** (1995). Correlation of anoxic responses and calbindin-D_{28k} localization in stratum pyramidale of rat hippocampus. Hippocampus 5: 25–39.

TABLE OF CONTENTS

LIST OF ABBREVIATIONS

[...]	concentration (ion, gas)
$[...]_o$	extracellular concentration (ion, gas)
$[...]_i$	intracellular concentration (ion, gas)
ACSF	artificial cerebrospinal fluid
AD	anoxic depolarization
AMPA	a-amino-3-hydroxy-5-methyl-4-isoxazolepropionic acid
AP	action potential
DL-APV	DL-2-amino-5 phosphonovaleric acid
ATP	adenosine triphosphate
ATPase	adenosine triphosphatase
BMI	bicuculline methiodide
CNQX	6-cyano-7-nitroquinoxaline-2,3-dione
CNS	central nervous system
8-CPT	8-cyclopentyl-1,3-dimethylxanthine
E_K	potassium-dependent potential
E_{REV}	reversal potential
EPSP	excitatory postsynaptic potential
e EPSP	early excitatory postsynaptic potential
l EPSP	late excitatory postsynaptic potential
mepsp	miniature excitatory postsynaptic potential
GABA	γ-aminobutyric acid
ID	inner diameter
IPSP	inhibitory postsynaptic potential
f IPSP	fast inhibitory postsynaptic potential
s IPSP	slow inhibitory postsynaptic potential
KYN	kynurenic acid
LY	Lucifer Yellow
MCPG	(+)-methyl-4-carboxyphenyl-glycine
mGLU	metabotropic glutamate receptor
NMDA	N-methyl-D-aspartate
OD	outer diameter
PAH	postanoxic hyperpolarization
PSP	postsynaptic potential

PTX	picrotoxin
QUIS	quisqualic acid
R_N	input resistance
S.E.M.	standard error of the mean
T	threshold stimulus
TTX	tetrodotoxin
V_m	membrane potential
V_R	resting membrane potential
V-I	voltage-current (curve, relationship etc.)
WM	(subcortical) white matter

LIST OF TABLES AND FIGURES

1.TABLES

2. FIGURES

INTRODUCTION

Oxygen-dependent life has its disadvantages.

Lack of adequate O_2 delivery to cells, either in isolation (hypoxia/anoxia), or accompanying a reduced inflow of cell nutrients and delayed removal of toxic metabolites (ischemia), results sooner or later in cell deterioration and death. In many instances, this may have extreme consequences on the functionality of a whole population of cells, organ, or system, and if unopposed, may lead to the death of the entire organism (Raichle, 1983; Rothman, 1983, 1984; Rothman and Olney, 1986; Choi, 1988; Siesjö, 1988; Siesjö and Bengtsson, 1989; Choi and Rothman, 1990).

The finding that various cell types show differential sensitivities to these injuries (Choi and Rothman, 1990) shows that there must exist several ways of coping metabolically with a reduced O_2 supply and/or different defense mechanisms which can protect some cells (if only temporarily) against the lethal changes induced by lack of oxygen. Neurons, especially those from the central nervous system (CNS), are particularly sensitive to anoxia. This, and the fact that neuronal death means more than decrease in cellular mass, but rather a virtually irreplaceable loss of data, patterns, connections and networks, frequently of essence for coordinating vital functions, make neuronal anoxia a profoundly incapacitating, or even life-threatening event.

The commonness of the hypoxic/ischemic injury in the CNS, especially in the brain, has led to sustained research efforts directed towards understanding: (1) the basic cellular mechanisms of hypoxic brain damage, (2) the natural defense mechanisms of these cells against the hypoxic injury, as well as (3) how to develop therapeutic measures against the occurrence and/or extension of the hypoxic injury and neuronal death. Although much progress has been

made in clarifying the cellular pathogenesis of the hypoxic/ischemic brain damage, there is still no effective therapy. The difficulty of accomplishing this task is directly related to two factors. First, the extremely short *time* (few minutes) of lack of O_2 (e.g. after cardiac arrest or stroke), which is sufficient to produce anoxic damage, makes preventive measures almost impossible to initiate, except perhaps in some selected controlled clinical situations (e.g.: during surgery/anaesthesia). Second, the changes which occur during the first few critical minutes of O_2 deprivation, and known to have an impact later as (potentially treatable) *delayed lethal effects* (Rothman and Olney, 1986) have been mostly used to outline a *general* image of the early central nervous system (CNS) anoxic processes. Consequently, the corresponding potential drug therapy would be too non-specific and with too many unacceptable side effects.

More recently, the interest has shifted toward studying and comparing the *specific* mechanisms of anoxic neuronal injury in various groups of neurons. Numerous researchers have concentrated their efforts on the intimate biochemical and electrophysiological mechanisms responsible for the various effects induced in the CNS by O_2 deprivation. Among their targets, the spinal cord, brain stem and especially the cortical regions of the hippocampus and (to a lesser extent) the neocortex, have been the ones that have received the most attention during recent years (Balestrino and Somjen, 1986; Clark and Rothman, 1987; Fowler, 1989; Krnjevic and Leblond, 1989; Krnjevic and Walz, 1990; Krnjevic and Xu, 1989; 1990, Ben Ari, 1990; Haddad and Donnelly, 1990; Luhmann and Heinemann, 1992; Lee and Löwenkopf, 1993; Rosen and Morris, 1990, 1991a, b, c, 1993, 1994). It became more and more evident that understanding the causes of differential sensitivity of these neuronal populations to hypoxic/ischemic damage would be of greater help in devising efficient and safe therapeutic measures. Even brief periods of anoxia ($\leq$ 5 min) elicit

different and frequently mixed responses (hyperpolarization and/or depolarization) in various *in vitro* preparations of cell populations from the neocortex and hippocampal regions; This suggests that *a diversity of intrinsic properties of neurons from the same or separate brain regions may lead to various types of anoxic response*; these appear to be the result of *combined effects of ionic conductances, exchangers and/or pumps*, due to different degrees of sensitivity of ionic mechanisms to lack of O_2 (Hansen et al., 1982; Fujiwara et al., 1987; Krnjevic and Ben-Ari, 1989; Leblond and Krnjevic, 1989; Kass et al., 1989; Krnjevic and Leblond, 1989; Ben-Ari, 1990; Doll et al., 1990; Luhmann and Heinemann, 1992).

The established connection between an excess of excitatory amino acid transmitters and anoxic neuronal injury (Choi, 1988; Rothman, 1984) suggests that *additional factors of synaptic origin may contribute to neuronal vulnerability*. Accordingly, it is possible that different responses of neurons to O_2 deprivation may be correlated with their synaptic architecture.

The present study, therefore, aimed *to investigate and define the changes in membrane parameters of pyramidal neurons of the fronto-parietal neocortex* (which have known sensitivity to anoxia/ischemia, with resultant numerous, clinically important sequelae). Since anoxic synaptic depression has been always regarded as an obvious effect of the decline in adenosine triphosphate (ATP) (Yamamoto and Kurokawa, 1970), and therefore has been no detailed examination of the basic mechanisms of transmission failure, *the fundamental changes in synaptic behaviour during anoxic exposure and the relative contribution of various synaptic factors to these changes were also considered important to elucidate.*

BACKGROUND

A. GENERAL—BRAIN ANOXIA & ISCHEMIA

Brain deprivation of oxygen and nutrients due to reduction or cessation of blood flow (*ischemia)* is a leading cause of neurological disability and death (Raichle, 1983; Choi and Rothman, 1990). This condition can be produced by a general organ failure such as during severe hypotension (cardiac arrest), or locally, as in thrombo-embolism of a cerebral artery (stroke) (Rothman, 1984; Choi and Rothman, 1990). Although the outcome is variable, the underlying events are, however, very similar: lack of perfusion determines a decrease in the oxygen and glucose supply to the neurons, as well as waste product accumulation and results in metabolic imbalance, followed by destruction of tissue elements (neurons and eventually glia) in the affected areas (Landis, 1994). The severity of the insult varies according to the magnitude and duration of ischemia, and the clinical picture can take variable forms, from small zones of selective neuronal destruction to extensive territories of infarct. This picture is in many aspects similar to that occuring in the heart, as a result of coronary occlusion (Raichle, 1983; Choi, 1988; Siesjö, 1988; Choi and Rothman, 1990).

In several special instances, oxygen deprivation can present itself as the sole factor responsible for neuronal injury (*hypoxia / anoxia*). This is represented by a reduced partial pressure of oxygen in the arterial blood, without cessation (at least in the incipient phase) of the blood flow itself. Examples of hypoxic/anoxic states include respiratory arrest, near-drowning, carbon monoxide poisoning or intra-hospital/surgical iatrogenic conditions such as inadequate mechanical ventilation, lack of an open airway, improper usage of respiratory/anaesthetic gases etc (Choi 1988; Choi and Rothman, 1990).

Although seemingly less intricate, if unrecognized and/or untreated, such conditions are nevertheless as ominous as the ischemic state, leading eventually to brain damage or death.

The ultimate purpose of gaining knowledge about the various aspects of the ischemic/hypoxic conditions is evidently to *find an effective way to counteract them*. And the simple (and unfortunate) way of describing the long and painstaking efforts of the medical scientific community in this direction is that *most often it still cannot be done*. The reasons for this reside in the very pathophysiology of brain ischemia/ hypoxia and ultimately in the structure of the brain itself.

B. THE BRAIN AS A CRITICAL FACTOR

The lack of an effective therapy for the hypoxic/ischemic brain damage can be essentially explained by the interaction of three (strongly interconnected) factors: timing, cell vulnerability and organ complexity.

1. The timing

The rapidity (seconds) with which the interruption of oxygen delivery to neurons produces loss of consciousness and cessation of spontaneous and evoked electrical activity has been recognized for a long time (Raichle, 1983). Moreover, once triggered, the pathophysiological processes advance rapidly (minutes) to abnormal ionic conditions (Hansen, 1985; Erecinska and Silver, 1994; Martin et al., 1994; Luhmann, 1996), acidosis and cell death. It is obvious that time becomes a serious limiting factor and, as in so many other supra-acute conditions, the best way to treat them would be to have been able

to prevent them. Although measures of identification and reduction of the risk of brain ischemia and of early detection of pre-ischemic lesions have been specifically addressed, in the majority of cases, patients are still seen and treated only after several minutes to hours following the initial injury.

2. Neuronal vulnerability

The time handicap has deep roots in the sensitivity of neurons to lack of oxygen. The need of a sustained high energetic output derived from the oxidative phosphorylation of glucose, correlated with the relative paucity of immediate reserves of high-energy phosphates and carbohydrates in the brain account for the well recognized neuronal sensitivity to hypoxia–/ischemia (Schmidt-Kastner and Freund, 1991). Although experimental work suggested in some instances that the brain could be more resistant to oxygen deprivation than had been previously suspected (Hossmann and Zimmerman, 1974), there is no argument over the fact that neurons are exquisitely sensitive to hypoxia, that various neuronal populations show different degrees of vulnerability and that, unfortunately, among the most susceptible subpopulations are CA1 hippocampal pyramidal neurons, necortical neurons from layers 3, 5 and 6, and neurons from the entorhinal cortex and thalamus (Siesjö, 1988; Choi and Rothman, 1990, Shimizu et al., 1996), i.e. neurons constituting the "hardware" of some of the highest brain functions, including, according to our current knowledge, the mechanisms of learning and other cognitive processes, memory, and possibly consciousness and awareness.

3. Brain complexity

Due to the complexity of brain organization, the effects of destruction of an isolated neuronal group, nucleus, or region will not be limited to that sector only. The intricacy of inter-neuronal connections (Shaw and Teyler, 1982; Rothman and Samaie, 1985; Aram et al., 1991; Thompson, 1994) will invariably influence the unaffected but dependent neuronal populations, through alterations of the function of various pathways, changes in synaptic input and (if possible) reorganization and re-distribution of functions, in order to replace those of the lost tissue. Such a complex sequence of events, is obviously difficult to effectively and selectively target.

Various attempts to find effective preventive and pharmacological therapeutic measures have therefore been challenged by the combined effects of the acuteness of the evolution of the lesions and extreme sensitivity and complexity of the substrate. Last, but not least, a vast number of studies carried out during the last two decades in order to clarify the basic pathophysiological mechanisms underlying the ischemic/hypoxic changes have emphasized that the crucial factor which contributes to ischemic damage is most probably the very one which normally sustains most of the excitatory functions of the brain (Kass and Lipton, 1982; Robinson et al., 1984; Rothman, 1985; Rothman and Olney, 1987; Choi, 1988; Clark and Rothman, 1987; Kass et al., 1989; Rader and Lanthorn, 1989; Choi and Rothman, 1990; Globus et al., 1990; Graham et al., 1990; Meldrum et al., 1992; Graham et al., 1993; Szatkowski and Attwell, 1994; Mody and MacDonald, 1995). The fact that glutamate, the most widespread excitatory amino acid (EAA) transmitter in the brain manifests neurotoxic properties in high extracellular concentrations, raises a serious obstacle on the path towards finding a specific treatment, i.e. devising

methods of counteracting glutamate neurotoxicity without impeding normal neuronal processes dependent on this substance.

C. PATHOPHYSIOLOGY-ROLE OF GLUTAMATE

1. Landmarks

The idea that glutamate might be implicated in anoxic/ischemic neuronal injury originated with the work of Rothman (1983) who noted the difference in sensitivity to lack of O_2 between young (resistant) and mature (sensitive) hippocampal neurons maintained in cultures. The only difference between the two types of neurons that could explain this observation was the presence of spontaneous synaptic activity in the adult cells. Additional findings, related to the protective role of Mg^{2+} (Nowak et. al., 1984) and postsynaptic amino acid antagonists suggested that the presence of synaptic activity can influence sensitivity to anoxia and that glutamate released synaptically is the most probable cause of neuronal death following anoxic injury. Subsequently, experiments performed in hippocampal slices confirmed the protective role of Mg^{2+} (through a voltage-dependent block of NMDA receptor–activated channels) and of certain EAA receptor antagonists (kynurenic acid—KYN and aminophosphonovaleric acid—APV), in preventing neuronal death in the CA1 region (Kass and Lipton, 1982; Robinson et al., 1984).

2. General picture

It has been established that under ischemic/anoxic conditions glutamate is initially (first few minutes) released from the terminals and accumu-

lates in the extracellular space. The triggering event is probably the cell depolarization induced by the inhibition of the Na^+-K^+ pump, allowing a slow rise in $[K^+]_o$. After a few minutes of ischemia the vesicular release is inhibited, but the transmitter continues to accumulate due to a reversal of the glial uptake mechanism (Szatkowski and Attwell, 1994). Since concomitantly evoked synaptic transmission is strongly suppressed (probably by presynaptic inhibition mediated through adenosine A_1 receptors—see **DISCUSSION**), a paradoxical situation occurs, in which synaptic traffic is decreased in spite of an excess of excitatory amino acids (Martin et al., 1994). Once in the synaptic cleft, glutamate however activates the postsynaptic receptors and induces two sequential processes, which although they involve synaptic receptors, do not manifest as coherent synaptic activity, but rather as "slow" ionic and membrane potential changes :

a. Na^+ and Cl^- influx

In this initial phase, glutamate acting on EAA receptors induces an influx of Na^+ through "non-NMDA" (AMPA/kainate) and NMDA channels. Since Na^+ influx translates into a membrane depolarization, it is subsequently accompanied by passive Cl^- influx and, due to the difference in osmolality, by water entry. This process results in cell swelling and, if not opposed, by lysis and neuronal death. This scenario is supported by experiments in which the toxicity of various EAAs (glutamate, kainate, NMDA) was prevented by blocking Na^+ influx (Boening et al., 1989; Fried et al., 1995), or substitution of Na^+ or Cl^- in the superfusing solution (Rothman, 1985; Rothman and Olney, 1986).

b. Intracellular Ca^{2+} accumulation

The second and possibly more important event is the intracellular Ca^{2+} accumulation. It was shown that Ca^{2+} enters the cell through NMDA channels (Cotman and Iversen, 1987; Kemp et al., 1987; Huntley et al., 1994). This was documented by *in vitro* studies which emphasized the close relationship between delayed neuronal degeneration and extracellular Ca^{2+}, the protective anti-anoxic role of NMDA receptor antagonists (APV) and the potentiating role of glutamate released during early ischemia on the NMDA receptors (Choi, 1988; Siesjo, 1988; Szatkowski and Attwell, 1994).

Although it was initially thought that only NMDA channels are permeable to Ca^{2+}, it is now postulated that, in abnormal conditions, even non-NMDA channels (i.e. AMPA channels) may allow the passage of Ca^{2+}. It was shown that the lack of permeability to Ca^{2+} of the AMPA receptor-channel is determined by the presence of the GluR2 subunit in the receptor-channel complex. If anoxia-ischemia (like other pathological conditions, such as epileptogenesis) are capable of down-regulating the synthesis of GluR2 subunits, AMPA receptors in the affected areas would become permeable to Ca^{2+} and therefore contribute to excessive Ca^{2+} accumulation, excitotoxicity and neuronal death (Huntley et al., 1994; Mody and MacDonald, 1995).

More recently, the role of another class of glutamate receptors, the metabotropic receptors (mGLUs) has been investigated (Hollmann et al., 1991; Hollmann and Heinemann, 1994; Schoepp et al., 1990; Baskys, 1992; Schoepp and Conn, 1993; Jane et al., 1994; Thomsen et al., 1994).

The mGLUs are a family of receptors composed of at least eight types of proteins (mGLU1–8), indirectly coupled to ion channels, or intracellular messenger cascades via G-protein linkage (Hollmann and Heinemann, 1994;

Brown and Reymann, 1995). According to pharmacological criteria, mGLUs have been subdivided in three groups/classes: class I (mGLU1 and mGLU5), which are coupled to phospholipase C, class II (mGLU2 and mGLU3) and class III (mGLU4 and mGLU6–8); the two latter classes comprise receptors negatively linked to adenylate cyclase (Brown and Reymann, 1995).

mGLUs have been shown to be potentially involved in a diversity of neuronal processes, inluding LTP and epileptogenesis (Bashir et al., 1993; Burke and Hablitz, 1994). It was shown in the hippocampus that glutamate binding to these receptors induces (via a GTP-binding (G) protein, coupled to phospholipase C), the formation of intracellular second messengers such as diacylglycerol (DG) and inositol triphosphate (IP_3) followed by intracellular Ca^{2+} mobilization. However the possible role of mGLUs in the occurrence of the early anoxic events is not yet completely understood—various *in vivo* and *in vitro* cortical studies have reported a protective antianoxic action of either mGLU agonists, or antagonists (Luhmann, 1996), whereas other recent experiments, which have tested both agonists (trans-ACPD) and antagonists (MCPG and L–AP3) of mGLUs have reported a lack of effects of all these substances on the anoxic events in the CA1 region of the hippocampus (Tan et. al., 1995).

All these extremely intricate mechanisms, maintained by several positive feed back loops, result essentially in an increase of $[Ca^{2+}]_i$ (Silver and Erecinska, 1990), which eventually becomes cytotoxic through multiple imbalances of intracellular Ca^{2+}-dependent cell structures and processes (Siesjö, 1988). Examples of some of these loops are (1) further increase in glutamate release due to increased $[Ca^{2+}]_i$, (2) glutamate leakage due to structural cell damage (3) potentiation of NMDA receptors by arachidonic acid and (4) potentiation of NMDA receptors by Ca^{2+}-activated protein kinase (Choi, 1988;

Szatkowski and Attwell, 1994). It is important to mention that another possible source of increased $[Ca^{2+}]_i$, namely the voltage dependent Ca^{2+} channels, does not seem to play an important role in these processes. It has been shown for the hippocampus that during anoxia L-type Ca^{2+} currents (and possibly low-threshold transient currents) are strongly blocked, possibly due to the very high $[Ca^{2+}]_i$, or through ATP depletion (Krnjevic and Leblond, 1987, 1989). Last, the possibility of increased $[Ca^{2+}]_i$ through release from internal stores was recognized more recently as a mechanism of significant importance (Belousov et al., 1995; Simpson et al., 1995; Mody and MacDonald., 1995) and is described in more detail in section (**E**).

c. Therapeutic considerations

It is very difficult to choose from these multiple chained events the one(s) which would be optimally counteracted by a potentially effective and safe therapy. Although the use of the various specific and non-specific glutamate antagonists (KYN, ketamine, MK-801, APV, CNQX, etc), proven to be effective in blocking various glutamate-induced anoxic effects in brain slices, may seem to be the obvious choice, these substances are unacceptable for clinical use, due to their significant side effects, the high concentrations needed, or poor penetration through the blood-brain barrier (Rothman and Olney, 1986; Choi, 1988).

An alternative possibility is offered by adenosine agonists, which could be used to block presynaptically the release of glutamate. It has been shown that during ischemic/hypoxic states, one of the effects of ATP breakdown is the release of endogenous adenosine which, acting mainly on A_1 receptors, counteracts various ischemic effects such as depolarization, glutamate release,

increased potassium and chloride conductances, etc. (Rudolphi et al., 1992). Accordingly, in both *in vitro* and *in vivo* experiments, adenosine agonists have been shown to effectively delay the onset of the hypoxic depolarization, whereas adenosine antagonists (theophylline and related agents) preserve synaptic transmission (Fowler, 1989; Gribkoff et al., 1990; Rudolphi et al., 1992; Lee and Löwenkopf; 1993, Manzoni et al., 1994).

Since glutamate and its various classes of receptors are widely distributed in the brain and can be affected by and respond in similar ways to various factors, it is not surprising that pathophysiological mechanisms induced by glutamate neurotoxicity and related to those taking place during ischemia/anoxia, have been shown or postulated to also underlie other abnormal neurological conditions, such as epilepsy, hypoglycemia, direct mechanical trauma or even chronic degenerative disease (Choi, 1988). Consequently, drugs which are used in other conditions in which glutamate toxicity is implicated may be effective in protecting against the ischemic/anoxic neuronal loss. There is evidence that selected neuroleptics, anaesthetics and anticonvulsants may exhibit a protective role against ischemia-induced neuronal death (Balestrino and Somjen, 1986; Bendo et al., 1987; Taft et al., 1989; Boxer et al., 1990; Fried et al., 1995). For example, the still extremely effective and safe "veteran" of antiepileptic drugs, phenytoin (Dilantin), when administered in rats immediately after brief bilateral carotid occlusion was shown to block neuronal destruction in the CA1 sector of the hippocampus (Taft et al., 1989).

Another example is that of the local anaesthetic lidocaine (a Na^+ channel blocker), which used in sub-anaesthetic concentration (i.e. concentration which does not block neuronal transmission: 10 μM), was shown to improve the post-anoxic (5–10 min N_2 exposure) recovery of synaptic activity recorded extracellularly in hippocampal slices, as well as to preserve ATP levels during

anoxia (Fried et al., 1995). These findings can be explained by the effects that high $[Na^+]_i$ would have on the transmembrane movements of Ca^{2+} and glutamate during anoxia, and therefore emphasize the significant role of Na^+ in the anoxic damage. They also suggest that anoxia may alter Na^+ channel properties, since during anoxia Na^+ influx was shown to be blocked by a concentration of lidocaine that normally (i.e. in normoxic conditions) does not alter the neuronal synaptic activity.

Last but not least, the findings that the anoxic intracellular Ca^{2+} accumulation is most probably initiated by the release of Ca^{2+} from internal stores and that pharmacological agents that block the Ca^{2+} release from the endoplasmic reticulum can oppose the changes in membrane potential and input resistance induced by early anoxia (Krnjevic and Xu, 1989; Belousov et al., 1995) (see details in section **(E)**, below and **DISCUSSION**), raise the possibility that drugs which are already in clinical use for other pathological conditions, (e.g. dantrolene sodium), could have their field of indications considerably extended, and be used to prevent or limit glutamate-induced neurotoxicity which occurs during anoxia or other mechanism-related neurological disorders, such as stroke and epilepsy (Mody and MacDonald, 1995; Luhmann, 1996).

D. OTHER AMINO ACID TRANSMITTERS—GABA

The crucial role of γ-aminobutyric acid (GABA) as inhibitory transmitter in the brain is well documented (Krnjevic and Schwartz, 1967; Krnjevic, 1987; Dutar and Nicoll, 1988; McCormick, 1989; Müller et al., 1989; Morrisett et al., 1991; Mody et al., 1994). Numerous studies have investigated the mechanisms of action of GABA, the various classes of GABA receptors, their ago-

nists and antagonists, as well as the correlation between receptor activation and the various types of inhibitory postsynaptic potentials (IPSPs) (Andersen et al., 1980; Alger and Nicoll., 1982; Inoue et al., 1985a-c; Bormann, 1988; Connors et al., 1988; Dutar and Nicoll, 1988; Bonanno and Raiteri, 1993).

Since the reduction of ATP occurring during O_2 deprivation is also likely to affect energy-dependent processes other than glutamate release and reuptake, it is conceivable that the metabolism of other transmitters may be affected by anoxia. Indeed, it was shown in an *in vivo* rat experimental model that during brain ischemia, total tissue levels of GABA may increase up to seven-fold (the largest changes of all measured neurotransmitters) (Graham et al., 1990). It was suggested that these findings may reflect glutamate-stimulated GABA release (Schatzki et al., 1990), and that GABA, by inhibiting EAA release via presynaptic $GABA_B$ receptors, could exert a protective effect against glutamate toxicity.

It is important, however, to mention that since most of the hippocampal and neocortical neurons (especially in *in vitro* preparations) have resting membrane potential (V_R) values close to--, or more negative than the Cl^- equilibrium potential (≈ -70 mV), GABA action at the $GABA_A$ receptors induces membrane depolarization or biphasic responses (Connors et al., 1988). In these instances, the effects of massive GABA release during ischemia/anoxia may have (at least before V_R reaches more depolarized levels) mainly *depolarizing* effects (i.e. similar to those induced by glutamate release and supported by cation influx). The complexity of these phenomena is further demonstrated by the fact that both $GABA_A$ and $GABA_B$-mediated IPSPs are particularly sensitive to anoxia (Leblond and Krnjevic, 1989), which does not entirely support the hypothesis of a GABA protective action through activation of synaptic receptors, at least at the post-synaptic neurons. It becomes evident

that GABA-related events during anoxia may manifest differently in various types of neurons and that they need further investigation.

E. ANOXIC EFFECTS – REGIONAL DIFFERENCES

The chain of events related to glutamate release constitutes only the basic frame underlying the responses of neurons to lack of O_2. The broad scenario, based on data furnished by extensive studies of structural and functional characteristics of glutamate receptors and related substances (Cotman and Iversen, 1987; Sommer et al., 1990; Seeburg, 1993; Hollmann and Heinemann, 1994; Huntley et al., 1994) cannot, however, explain entirely the diversity of electrophysiological responses (and degrees of vulnerability) of various neuronal sub-populations to anoxia. Consequently, detailed electrophysiological studies of various classes of central neurons have been undertaken; among these, hippocampal studies are by far the best represented and it could be said that, with the help of the slice preparation, a veritable "dissection" of the neuronal ionic mechanisms and their relative role in the anoxic changes was performed.

1. Hippocampus

In 1982, Hansen et al. reported that pyramidal neurons from the CA1 and CA3 regions of the hippocampus hyperpolarize ($\approx$ 4–5 mV) in response to brief anoxia (4–6 min). A decrease in input resistance (R_N) by $\approx$ 40% and a disappearance of evoked synaptic activity (excitatory postsynaptic potentials—EPSPs) were also observed. The effect of various channel blockers (TTX, potassium channel blockers [tetra-ethylammonium, 4-aminopyridine],

manganese, magnesium) suggested the presence of a K^+ efflux as a cause of the hyperpolarization, although the mechanism of the K^+ conductance activation has not been determined.

A detailed study focusing on CA1 pyramidal neurons (Fujiwara et al., 1987) confirmed most of these findings, re-emphasized the central role of a K^+ conductance and described the post-anoxic hyperpolarization (PAH), which has been attributed to the re-activation of the Na^+-K^+ ATPase.

All these findings were consolidated and expanded in the fundamental study of CA1 pyramidal neurons by Leblond and Krnjevic (1989). The most plausible underlying mechanism for the anoxic hyperpolarization was narrowed down to the activation of a Ca^{2+}-dependent K^+ conductance. Their experiments confirmed the changes in R_N, the occurrence of PAH, the sensitivity to anoxia of synaptic processes and emphasized the protective role of creatine pre-incubation. Since, however, in a parallel study, Krnjevic and Leblond (1989—voltage clamp) reported the anoxic blockade of certain voltage-dependent Ca^{2+} currents (L-type slow-inactivating), the source of intracellular calcium accumulation, necessary for the activation of the K^+ conductance was sought at a different level. By using dantrolene sodium, Krnjevic and Xu (1989) reinforced the idea that anoxia activates a Ca^{2+} -dependent K^+ conductance, *by releasing Ca^{2+} from internal stores*. (These findings were confirmed by subsequent experiments —Belousov et al., 1995—see **DISCUSSION**). A more complex picture emerged later, when the outward current underlying the anoxic hyperpolarization was shown to be abolished by the atropine-sensitive action of carbachol (suggesting an M current) and when, in the absence of the hyperpolarization, an inward current, possibly chloride mediated, became evident (Krnjevic and Xu, 1990). Moreover, in contrast to the initial negative findings of the effects of tolbutamide (sulphonylurea

known to be an ATP-dependent K^+ channel inhibitor) on the CA1 anoxic hyperpolarization (Leblond and Krnjevic 1989), it has been shown more recently that at least part of the CA1 anoxic hyperpolarization could be indeed due to activation of ATP-dependent K^+ channels, since the outward current generated by anoxia in CA1 pyramidal neurons voltage-clamped in the presence of TTX and KYN was suppressed by tolbutamide (Godfraind and Krnjevic, 1993).

It has been therefore postulated that the CA1 anoxic hyperpolarizing process is in fact a very intricate mixture of hyperpolarizing and depolarizing tendencies which can be summarized as: (1) an early release of Ca^{2+} from internal stores activates Ca^{2+}-sensitive, as well as M-like K^+ channels, (2) a possible implication of some type of ATP-dependent K^+ channel and (3) opposing currents mediated by Cl^- —all accounting for the variable degree of hyperpolarization observed during anoxia.

While CA1 cells seemed to respond characteristically by hyperpolarization (although Leblond and Krnjevic (1989) found depolarization in almost half of the tested neurons—confirmed by Morris et al., 1995), CA3 neurons and dentate granule cells have been shown to exhibit mixed (hyperpolarizing/depolarizing) or, more often, pure depolarizing changes in response to brief periods of anoxia (Ben-Ari and Krnjevic, 1989; Ben-Ari and Lazdunski, 1989; Ben-Ari, 1990; Ben-Ari et al., 1990; Krnjevic, 1990; Shimizu et al., 1996). The depolarization was shown to be sensitive to tetrodotoxin and kynurenic acid and has been attributed to glutamate release. Importantly, the depolarization occuring in CA3 neurons was shown to be counteracted by ATP-dependent K^+ channels activators (galanin) and augmented by ATP-dependent K^+ channels inhibitors (glibenclamide, tolbutamide). These channels seem to be located on granule cell axons/terminals (i.e. pre-synaptically from

CA3 neurons); it is possible that during anoxia, the decrease in ATP levels would relieve the blockade of these channels and the subsequent K^+ efflux may counteract the depolarizing tendencies of the cell, thus providing a natural, region-specific protection against anoxic damage.

It is interesting to note that whole-cell recordings of CA1 pyramidal neurons using patch electrodes (Zhang and Krnjevic, 1993) revealed anoxic changes less prominent and definitely more towards the depolarizing side, than the typical ample hyperpolarizations obtained during intracellular recordings (Leblond and Krnjevic, 1989). The characteristic response was a 2–3 mV depolarization, accompanied by a slight reduction of input resistance (about 12%). These anoxic effects were very similar to the changes described in the present study for neocortical neurons and could raise the question of the real significance of the hyperpolarization, recognized widely as a marker of the anoxic response of CA1 pyramidal cells. However, in a subsequent CA1 study from the same laboratory, using the same methodology (patch-clamp), the authors recorded again hyperpolarizing changes (about 4 mV) and a more significant (i.e. typical) reduction in input resistance (about 20%) (Belousov et al., 1995). These discrepancies have been attributed to the differences in microelectrode filling solutions (K^+ gluconate—in the first study vs. K^+ methylsulphate—in the second study), but is important to note that the recording setup and basic techniques may be crucial in the assessment of electrophysiological mechanisms and labeling a phenomenon.

2. Neocortex

Neocortical neurons, although extremely sensitive to anoxia, were far less studied than the hippocampal cells. The diversity of neocortical cellular

types, their synaptic intricacy, the lack of relative structural "order" (as compared with the hippocampus), and possibly the less well established neocortical slice preparation may all constitute factors which prevented a more extensive approach to the characterization of neocortical responses to brief anoxia. It was reported initially that neocortical neurons respond *in vivo* to anoxia with a *hyperpolarization* (Glötzner, 1967), very similar to that described for the CA1 hippocampal cells (see above). However, subsequent studies (including the present experiments) have shown that, again, it is not possible to define a single type of anoxic response, applicable to all (or even the majority) neurons from a certain brain structure. Doll et al., 1991 reported for rat fronto-parietal neurons a transient *hyperpolarization* followed by a massive spreading-depression-like *depolarization*, together with significant decrease and eventual undetectable R_N. Luhmann and Heinemann (1992), working on somato-sensory pyramidal neurons, reported that *hyperpolarization* (with a reversal potential [E_{REV}] of ≈ -81 mV) and *depolarization* (with E_{REV} of ≈ -58 mV) occurred with equal frequencies and, as in other studies, EPSPs and (especially) IPSPs were reversibly depressed. The hyperpolarization was explained by anoxia-induced activation of an ATP-sensitive K^+ conductance, whereas the depolarization has been attributed to glutamate release. The current study emphasizes the exclusive presence of *depolarization* in fronto-parietal neocortical neurons.

The emerging pattern is that, super-imposed on a quite uniform background, represented by a variable decrease in R_N and significant depression of EPSPs and (especially) IPSPs, there is a multitude of ionic processes which can be affected by anoxia. The combination of the degree of expression of these processes in a given type or sub-population of neurons, and their specific sensitivity to O_2 deprivation determines the type (i.e. polarity) of the

anoxic response and could possibly represent the substrate of differential sensitivity and vulnerability to anoxia.

METHODS

A. DISSECTION AND SLICE PREPARATION

Bilateral coronal slices were obtained from the frontoparietal region of the rat neocortex following a previously developed method (Rosen and Andrew, 1990), that had been adapted from one used for slicing the cingulate cortex (Vogt and Gorman, 1982). Adult male Sprague-Dawley rats (21–50 days old, 50–350 g—30 days/150 g average) were housed in a controlled environment (temperature 25°C, light on 0600–2000 h) and provided with food and water *ad libitum*. Following decapitation, the scalp was incised on the midsagittal line and retracted laterally. The cranium was opened by two parasagittal cuts from the occipital pole to the coronal suture. The bone between the two cuts was removed and the opening was enlarged laterally with rongeurs. The dura mater was carefully excised, using fine forceps and scissors. The cortical surface was thoroughly flushed with ice-cold physiological saline (see below for composition). The frontal bone was removed and the brain was cut rostrally, as close as possible to the frontal pole. Posteriorly, it was separated from the cerebellum. The brain was removed and quickly placed in a beaker containing ice-cold saline for about 20 s. This made the tissue firmer for slicing and probably improved the viability of the slices (Andersen, 1984).

A median block of brain tissue (approximately 15 x 6 x 4 mm) was cut using a single edge razor blade (Fig. 1A–D) and placed cortex down (Alger et al., 1984) on the stage of a tissue slicer (Frederick Haer). Four to six bilateral coronal slices (Fig. 1–D), 400–500 μm thick were cut from the block and transferred with a fine brush to a holding chamber (Medical Instruments), containing oxygenated artificial cerebrospinal fluid (ACSF) at room temperature.

The dissection time from the decapitation to cutting of the last slice never exceeded 10 min.

B. COMPOSITION OF ACSF

The ACSF used to cool the brain, incubate the slices and serve as "control" saline in all experiments was prepared with Millipore-treated water and contained (in mM): NaCl, 120; KCl, 3.3; $NaHCO_3$, 26; $MgSO_4$, 1.3; NaH_2PO_4, 1.23; $CaCl_2$, 1.8; glucose, 11. and was saturated with 95% O_2 / 5% CO_2, at pH 7.3–7.4.

Magnesium free solution was prepared similarly to control ACSF, but omitting $MgSO_4$. The reduction in osmolality was balanced by addition of an equiosmolar concentration of NaCl. Low sodium solution was prepared similarly to control ACSF, but NaCl was omitted and replaced by an equiosmolar concentration of choline Cl. Low chloride solution was prepared by omitting NaCl and replacing it by an equiosmolar concentration of Na methane sulphonate. Calcium free solution was prepared by omitting $CaCl_2$ from the ACSF and replacing it with an equiosmolar concentration of NaCl. Potassium free solution was prepared by omitting KCl from the ACSF and replacing it with an equiosmolar concentration of NaCl. High potassium ACSF (5.0 mM K^+, and 9.0 mM K^+) was prepared by adding the appropriate amounts of KCl to control ACSF.

C. ELECTROPHYSIOLOGICAL PROCEDURES

1. Recording chamber and ACSF delivery

After 1–1.5 h of incubation, slices were transferred one at a time, using a large bore pipette, from the holding chamber onto a lens paper strip placed on the chamber top of a Haas-type recording chamber (Medical Instruments) (Fig. 2), modified for superfusion. The slice was weighted with 2 pieces of 0.38 mm diameter silver wire (3–4 mm length). ACSF was delivered over the slice by a gravity–driven system. The system (Fig. 3), adapted from Barolet et al., 1989, consisted of six plastic reservoirs (60 ml each), placed at about 75 cm above the recording site. Each reservoir was connected through a small bore Teflon® TFE tube (ID = 0.97 mm) (Canlab) to 6 outlets of an 8-way valve (Omnifit Ltd.). One of the valve outlets was connected to a terminal teflon tube to provide inflow to the recording chamber and the last outlet was connected to a suction syringe, used to drain or initiate the filling of the tubes. The ACSF flow from different reservoirs was changed by a six solenoid valve system (General Valve Corporation), placed between the reservoirs and the Omnifit valve and controlled by a battery-powered switch. The flow was maintained at 1.2–1.6 ml/min. Before reaching the slice, the ACSF was warmed to 33.5 ± 0.1°C. This temperature was maintained with a feed-back system consisting of a thermistor in contact with the superfusing ACSF at 2–3 mm from the slice, coupled with a temperature controller (Model BTC–12, John Knowles, McGill University), which warmed the distilled water bath situated beneath the recording chamber and the ACSF line running through it. The slices were transilluminated from below with a fiberoptic light source and viewed through a dissecting microscope.

2. Recording and stimulating equipment and techniques

a. General

Intracellular electrodes were pulled from capillary glass (0.7–0.9 mm ID/1.2 mm OD—Prism™ glass capillaries, Dagan Corporation), using a horizontal micropipette puller (Flaming Brown—Model P80/PC, Sutter Instruments Co.). The microelectrodes were filled with 3M potassium acetate (resistance = 40–80 MΩ) and connected through a Ag/AgCl wire to the probe of an intracellular amplifier (8700 Cell Explorer, Dagan Corporation). A piezoelectric microdrive (Burleigh 6000 inchworm motor/controller) holding the electrode was mounted on a tridimensional manipulator (Narishige Scientific). By adjusting the manipulator, the tip of the electrode was positioned on the surface of the slice and the electrode was advanced through the slice in 4–6 μm steps, until a suitable recording was obtained (see below).

The active bridge circuit of the intracellular amplifier allowed simultaneous passage of current (hyperpolarizing or depolarizing) and the measurement of voltage across the same microelectrode. Negative capacitance was adjusted and gauged by the squareness of a 10 mV, 5ms, internally-generated calibration pulse. The bridge was balanced to remove the rapid voltage transients at the onset and offset of the current pulses which were delivered by a Grass S 44 stimulator connected to a PSIU 6 stimulus isolation unit (Grass Instruments). During intracellular injection of current pulses, the bridge was balanced repeatedly to compensate for changes in the resistance of the microelectrode. The recording set-up, (including the devices for data acquisition and storage—see below) is shown diagramatically in Fig. 4.

Microconcentric bipolar electrodes (model MCE–100. Rhodes Medical

Instruments) placed in the subcortical white matter and/or in layer IV of the slices were used to orthodromically activate the recorded neurons (Fig. 5). A second S44 stimulator coupled to a PSIU 6 stimulus isolation unit (Grass Instruments) delivered monophasic square pulses of 0.1–1.5 mA and 0.05–0.25 ms duration at frequencies of 0.05–0.5 Hz.

The weakest stimulus of given duration, capable of eliciting an AP with every synaptic response, was designated as "threshold" (T), and multiples of T were used to quantify stimulus strength. For most of the anoxic trials in which the synaptic response was tested throughout the experiment, stimuli of constant strength were continuously delivered at 0.1 Hz.

The tip of the recording electrode was visually located through the dissecting microscope and positioned above the superficial layers (II–III) of the cortex, 0.2–0.5 mm from the pial surface; using the micromanipulator, it was then carefully advanced through the ACSF in the superficial portion of the slice. To obtain orthodromic responses at low intensity stimulation, the recording electrode was aligned radially with the stimulating electrode.

b. Intracellular recordings

Single cell impalements were obtained by advancing the microelectrode through the slice in 4–6 μm steps. Each 1–4 steps, a "tickler" switch on the amplifier was activated to inject very briefly a large amount of depolarizing current, clean the microelectrode tip and check for membrane penetration. A drop of potential of at least 40 mV and injury APs signalled a neuronal impalement. Steady hyperpolarizing current injection of 0.8–1.6 nA was continued for 1–5 min, while the membrane potential (V_m) increased. The current was decreased gradually during the next 5 min and the cell was left to stabilize at

resting membrane potential (V_R) for at least another 10 min. Most of the impalements were obtained at 100–200 μm depth. Occasionally, the bridge balance was checked and the AP amplitude was measured by delivering orthodromic stimuli or injecting short suprathreshold depolarizing pulses (50–150 ms). The 20 min period after cell penetration seemed necessary to ensure a stable recording. A stable V_R of at least – 60 mV and AP amplitude (baseline to peak) of ≥ 80 mV were considered prerequisite for adequate impalement. The impalement was discontinued at the first sign of cell deterioration. When the impalement was lost or abandoned, the electrode was retracted 20–50 μm to obtain the zero potential level and was checked for added resistance. Good impalements usually lasted over one hour.

In some preliminary experiments, tissue pO_2 was continuously monitored with O_2-sensitive microelectrodes, placed in the slice close to the recording site (see Fig. 13–A). The O_2-sensitive microelectrode (Diamond General Corporation) was first calibrated in a calibration cell (Transdyne General Corporation), which was maintained at the constant temperature of 33.5°C, using gas mixtures of known concentrations (0%, 20% and 100% O_2 /5% CO_2 in N_2) and an oximeter (Chemical Microsensor, Transdyne General Corporation). The same O_2-sensitive microelectrode, connected to the oximeter was subsequently used to measure pO_2 in the slice and display it expressed as percentage of the atmospheric pressure (760 torr).

c. Extracellular K^+ measurements:

Potassium-sensitive microelectrodes were prepared as previously described (Morris et al., 1991). Briefly, after drilling 3–5 mm of one of the barrels, 60 mm length/ 3.0–3.2 mm OD double–barrel thick septum "theta" glass

capillaries (R&D Scientific Co.) were cleaned (repeated flushing with distilled water followed by phosphoric acid and acetone immersion), heat-dried and stored in hermetically sealed containers. 24 h before the experiment, microelectrodes were pulled using a vertical puller (model PE2—Narishige Instruments) and the inner surface of the shorter barrel was rendered hydrophobic by treatment with vapors of silane (N,N-dimethyltrimethylsilylamine, Fluka Corporation). The tip of the hydrophobic ("exchanger") barrel was backfilled with the liquid K^+ exchanger: K^+ ionophore 60398 (Fluka), followed immediately by filling of the other ("reference") barrel with a 150 mM NaCl solution. Then, the rest of the exchanger barrel was backfilled with a 150 mM KCl solution (Fig 6). Ag/AgCl wires were introduced in each barrel, placed in contact with the ionic solutions, and the openings of the barrels were sealed around the wires with Elephant Wax, to prevent evaporation of the backfilling solutions. The electrode was clamped in a plastic holder, secured on the plate of a microscope and the electrode tip was broken under visual control at low magnification, by contact with a clean plastic rod, mounted on a micromanipulator. This procedure reduced the resistance of the reference barrel of the electrode to 5–15 MΩ. Electrodes were placed in glass containers and stored for 24 h in the refrigerator with their tips placed in millipore water. Before the experiment, the tips of the microelectrodes were checked under the microscope in order to detect a possible "retraction" of the ion exchanger column, due to insufficient hydrophobicity of the exchanger barrel; such electrodes were discarded.

The microelectrode intended for use was calibrated prior to the experiment in a series of ACSF solutions containing increasing concentration of K^+ (as KCl): 1 mM, 2 mM, 3 mM, 5 mM, 10 mM and 20 mM; the decrease/ increase in $[K^+]$ was compensated by an increase/ decrease in NaCl. Calibration was

performed by detecting the K^+-dependent potential (E_K) recorded as the differential potential between the exchanger and the reference barrels of the microelectrode. For this, the Ag/AgCl wires present in the two barrels were connected to a Differential Electrometer Amplifier (model 604—Keithley Instruments). The electrode was then mounted as for intracellular recording (see above) and its tip was successively exposed to the series of calibrating solutions; after stabilization in each solution, E_K values were read from the meter face of the differential amplifier and recorded in parallel on a polygraph (Grass Instruments). These values were used to plot a semi-logarithmic calibration curve, characteristic to that particular electrode, and showing the variation of E_K as a function of $[K^+]$ (Fig. 7; see also Fig. 18–B, C). Calibrations were performed at the recording temperature (33.5°–34°C).

During the experiment, the tip of the microelectrode (mounted as for intracellular recording—see above—and connected to the Keithley Differential Amplifier) was placed in the slice at 150 μm depth (i.e. similar to the depth of most intracellular recordings) and control extracellular E_K was measured after stabilization. Changes in E_K during anoxic trials (see below) were continuosly monitored on the chart recorder (model 2200S, Gould Electronics) and E_K was measured at various moments during anoxia, including at peak anoxic depolarization. These E_K values were then plotted on the calibration curve and used to calculate the corresponding values of extracellular potassium concentration—$[K^+]_o$.

The calibration was repeated at the end of the experiment, in order to detect and correct for changes with time in the electrode response (Fig. 18–B, C).

3. Dye injections

Glass microelectrodes (0.7-0.9 mm ID/1.2 mm OD—Prism™ glass capillaries, Dagan Corporation) pulled with the Flaming Brown horizontal puller were filled with 3–5% solution of the fluorescent dye Lucifer Yellow CH-lithium salt (LY) (Molecular Probes, Inc.), dissolved in 1M lithium chloride. Electrode resistances were 100–120 MΩ. Once a neuron was impaled, if the membrane potential was fluctuating not more than 10 mV and V_R was ≥ –50 mV, the impalement was considered stable and suitable for dye injection. Long and low amplitude hyperpolarizing pulses (200–500 ms, 0.1–0.2 nA) were delivered superimposed on a steady hyperpolarizing injection of 0.8–2.0 nA. The AP amplitude was monitored with suprathreshold orthodromic stimuli. The injection was discontinued after at least 10 min, or when the impalement deteriorated (as evidenced by membrane depolarization, decrease and broadening of the AP). If the impalement was unstable during the first 30 s after cell penetration or deteriorated rapidly in the first 2–3 min, the electrode was withdrawn and a new electrode pass was started at at least 1.0 mm from the previous position. Only one injection was made in a single hemi-slice.

Injected slices were removed from the chamber and placed in a fixative solution of 4% formaldehyde in 0.1 M phosphate buffer. A 0.4 M phosphate buffer stock (see rinsing procedure below) was also prepared by dissolving 8.0 g $NaH_2PO_4 \bullet H_2O$ and 20.2 g $Na_2HPO_4 \bullet H_2O$ in distilled water up to 500 ml.

The slices were fixed for 1 h at room temperature and rinsed in 1/2 diluted phosphate buffer stock for 10 min. Subsequently, the slices were passed through a series of increasing concentrations of dimethyl sulfoxide (DMSO) in water (50% — 70% — 95% — 100%). Ten minutes in each solution gradually dehydrated and cleared the slices (Grace and Llinas, 1985). Slices were

TABLE 1 – Sources for pharmacological agents

	Substance	Abbrev.	Source
1	Bicuculline methiodide	BMI	Sigma
2	Creatin	—	Sigma
3	γ-aminobutyric acid	GABA	Sigma
4	Kynurenic acid	KYN	Sigma
5	Ouabain	—	Sigma
6	Picrotoxin	PTX	Sigma
7	Tetrodotoxin	TTX	Sigma
8	8-cyclopentyl-1,3-dimethylxanthine	8-CPT	ICN Biochemicals
9	Theophylline	—	ICN Biochemicals
10	DL-2-amino-5-phosphonovaleric acid	DL-APV	Tocris Cookson
11	(+)-methyl-4-carboxyphenyl glycine	MCPG	Tocris Cookson
12	Phaclofen	—	Tocris Cookson
13	Quisqualic acid	QUIS	Tocris Cookson
14	Lucifer Yellow	LY	Molecular Probes Inc.

mounted in 100% DMSO in depression slides and visualized and photographed using a Carl Zeiss epifluorescence photomicroscope.

D. PHARMACOLOGICAL TESTS

In most experiments drugs were applied as bath superfusates. In some cases, drugs were pressure-ejected in the slice. The ejection electrode (2–10 MΩ resistance) was pulled with the Flaming Brown horizontal puller from glass capillary (0.9 mm ID/1.2 mm OD—Prism™ glass capillaries, Dagan Corporation). Prior to filling, the tip of the electrode was rendered hydrophobic by dipping it in a 2% solution of butylchlorosilane (Fluka Corporation) in CCl_4. This procedure opposed the dissipation due to surface tension effect of the ejected microdrop on the outer wall of the microelectrode shank, as gauged by direct observation of ejections in the air, under the dissecting microscope. The electrode was filled with the drug dissolved in ACSF and obliquely advanced into the slice to a depth of about 130 μm, as close as possible to the recording electrode. The solution was ejected with pulses of 15–40 psi/5–400 ms from a Picospritzer II (General Valve Corporation). Mechanical artifacts did not occur with these ejection parameters, as gauged by the absence of V_R changes in response to pulses applied through ACSF–filled electrodes.

The ACSF constituents and DMSO were obtained from Fisher Scientific; the sources of the pharmacological agents are shown in Table 1.

E. ANOXIC TRIALS

Brief anoxic episodes (4–7 min duration, 1–6 episodes per impalement, 1–2 impalements per slice) were produced by exposure of the slice to 95%N_2 /5%

CO_2. This was created by switching the superfusate flow to a reservoir of ACSF saturated with this mixture and, after the time lag necessary for the new ACSF to reach the slice (calculated from the total length and internal diameter of the tubing and the delivery rate), by bubbling the same mixture in the warming bath situated beneath the recording chamber (Fig. 2). At the end of the anoxic period, re-oxygenation was induced by switching in the same way to ACSF saturated with 95%O_2/5% CO_2. A recovery period of ≥ 10 min (whose duration was determined by return to control values of V_R, R_N and PSP amplitude) was allowed between two successive anoxic trials.

F. DATA ACQUISITION AND ANALYSIS

The recorded signal was displayed on a storage oscilloscope (model 5103N, Tektronix) and continuously monitored at slow speed on a two-channel chart recorder (model 2200S, Gould Electronics) (Fig. 4). An audio monitor (model AM8—Grass Instruments) was also used to improve detection of spontaneous APs, as well as to monitor responses to current pulses and orthodromic stimulation. The signal gain was increased in parallel by a buffer amplifier (model 3A3—Tektronix) and directed to an analog-to-digital interface (TL–1 DMA—Axon Instruments) for digitization and export to an IBM-compatible computer (PEER-1630—DTK Computer). Acquisition software (Axotape vv. 1.2 and 2.0—Axon Instruments) was used for continuous sampling (5–10 kHz per channel), data storage and subsequent analysis. Diagrams were obtained from segments of computer-stored records exported to a plotter (model 7470A—Hewlett Packard) and chart recorder traces.

Statistical evaluation was performed using a bidirectional Student's t-test for paired comparisons, using the software INSTAT, Graphpad). Due to the

variance of control excitatory postsynaptic potential (EPSP) amplitude, the differences recorded were first normalized as a percent of the average control value. Changes in spontaneous miniature PSP (mpsps) amplitude and frequency were evaluated for each slice with a unidirectional Student's t-test for difference of means (independent samples). In all cases, differences were considered significant at the 95% confidence level and, if found, higher levels of significance are specified in the results.

RESULTS

Intracellular recordings were performed in 146 neurons (in 123 slices from 105 rats) from layers II–III of the neocortex.

A. PASSIVE MEMBRANE PROPERTIES OF NEOCORTICAL PYRAMIDAL NEURONS

1. Resting membrane potential

Resting membrane potential (V_R), determined by measuring the abrupt upward deflection obtained upon microelectrode withdrawal, was – 83.2 ± 2.18 (mean ± S.E.M.; n = 127 neurons). V_R was occasionally as high as – 100 mV and never decreased below – 74 mV. Neurons with more depolarized V_R values usually deteriorated rapidly during the first minutes after impalement (spike broadening, disappearance of synaptic potentials) and were not included in the study.

2. Input resistance

Input resistance (R_N) at resting membrane potential was estimated from the linear portion of the V-I curve (Fig. 8A). This was obtained by injecting 150–200 ms hyper– and depolarizing current pulses (between – 0.5 and + 1.0 nA, in 0.1 nA increments) and measuring the voltage deflection at 100 ms after the onset of the pulse. For 108 neurons, mean R_N was 28.5 ± 2.33 MΩ, ranging from 15 to 53 MΩ. The anomalous (inward) rectification seen in Fig. 8 was present in various degrees in almost all of the neurons tested and was

manifest as an increased voltage response to depolarizing currents at subthreshold level, as compared with similar amounts of hyperpolarizing currents.

In order to detect the dynamics of resistance changes during anoxia (see below), R_N was also monitored continuously during most experiments by injection of small hyperpolarizing pulses (0.2–0.3 nA, 150–250 ms, 0.05–0.2 Hz).

3. Action potentials and rheobase

Single action potentials (APs) were elicited by slowly increasing the intensity of depolarizing current pulses (Fig. 8–B). APs were overshooting (i.e. AP upward deflection raised above 0 mV), with mean baseline to peak amplitude difference of 102.3 ± 5.6 mV (n = 53), and the mean AP duration measured at 1/2 amplitude was 1.07 ± 0.05 ms (n = 46). Suprathreshold pulses (i.e. strong currents, producing more than one AP) elicited trains of APs which showed frequency accommodation. This and other electrophysiological characteristics (together with the microscopic appearance of 15 neurons injected with Lucifer Yellow) helped in classifying all the recorded neurons as regular spiking pyramidal neurons (Connors and Gutnick, 1990; McCormick et al., 1985).

In a representative group of neurons, the firing threshold was estimated by the rheobase (smallest current capable of eliciting an AP), which was found to be 0.52 ± 0.12 nA (n = 38 neurons).

B. NEOCORTICAL SYNAPTIC POTENTIALS

Orthodromic stimuli applied in cortical layer IV and/or the subcortical

white matter (WM) (Fig. 5) evoked compound postsynaptic potentials in all of the neurons tested. These postsynaptic potentials (PSPs) were similar to those described in detail in a series of recent papers (Sutor and Hablitz, 1989a,b; Hablitz and Sutor, 1990).

1. Excitatory postsynaptic potentials

a. Early EPSP

Both WM stimulation (n = 23) and layer IV stimulation (n = 107, including 15 of the neurons which received WM stimulation) (total 115 neurons) elicited early EPSPs (*e* EPSPs). For WM stimulation, good radial alignment between the stimulating and the recording electrodes allowed weaker and/or shorter stimuli to be used. Weak stimuli (0.1–0.3 T) applied in layer IV were sufficient to elicit *e* EPSPs. The *e* EPSP (Fig. 9–A,B) had a steep rise followed by a slower decay to $V_{R,}$ with a stimulus-to-peak latency of 8.2 ± 0.27 ms and a duration of 62 ± 12.5 ms (n = 86). This was evident in the absence of superimposed late EPSP or inhibitory postsynaptic potentials (IPSPs) (i.e. in neurons stimulated from the white matter with subthreshold stimuli). The *e* EPSP amplitude increased gradually with stimulus strength and at stimuli = T the *e* EPSPs elicited single overshooting APs. No double spikes or bursts were generated by suprathreshold stimuli. The *e* EPSP was able to follow stimulation frequencies > 0.5 Hz and was unaffected by the N-methyl-D-aspartate (NMDA) antagonist, DL-APV (50–250 μM) (Fig. 10), showing characteristics similar to those originally described by Sutor & Hablitz (1989a).

b. Late EPSP

Late EPSP (*l* EPSPs) were elicited exclusively by layer IV stimulation in 100% of the neurons tested, usually with stimuli ≥ 0.4 T. Stimulation of WM failed to evoke *l* EPSP in all cases. This was occasionally advantageous to study the other PSPs in relative isolation. However, due to the lack of *l* EPSPs and the need for perfect electrode alignment to obtain good responses with WM stimuli, stimulation of layer IV was chosen as the routine protocol in most of the experiments.

A *l* EPSP was always preceded by an *e* EPSP, had the onset embedded into the *e* EPSP decaying phase, relatively similar time courses of the rising and decaying phases, and had a much longer stimulus-to-peak latency and duration (34.0 ± 1.6 ms and 170.8 ± 16.5 ms, respectively). Characteristically, a gradual increase in stimulus strength up to about 0.8 T induced, concomitantly with *e EPSP* increased amplitude, an increased amplitude of *l* EPSP and a decrease of its latency to peak.

The evolution of *l* EPSP with increased stimuli was variable, and assisted in the classification of the tested neurons into two groups. In 77% of the neurons (n = 89), an increase of the stimulus strength over 0.8 T resulted in a rapid decline in *l* EPSP amplitude, whereas the *e* EPSP continued to increase; at 1.0 T, only the *e* EPSP remained to evoke an AP (Fig. 9–A). This *l* EPSP disappearance with subthreshold stimuli is consistent with previous descriptions (Hablitz and Sutor, 1990; Sutor and Hablitz, 1989a,b) and has been explained by a shunting action of the conductance increase associated with IPSPs (Sutor and Hablitz, 1989a).

In about 23% of the neurons (n = 26) which showed *l* EPSPs, the latter increased steadily over the entire stimulus range (although without a signifi-

cant decrease in latency for stimuli over 0.8 T) and at 1.0 T generated an AP (Fig. 9–B). In these cells, the absolute (i.e. current intensity) thresholds for *l* EPSP and AP generation were low, whereas the threshold for the IPSP was relatively high (≥ 1.0 T). It was assumed that these characteristics, together with the unusually long, relatively fixed latency of the *l* EPSP, rendered the shunting action of the IPSP less effective.

The *l* EPSP was not able to follow stimulation frequencies > 0.5 Hz and was abolished by the N-methyl-D-aspartate (NMDA) antagonist, DL-APV (50–250 μM) (Fig. 10).

2. Inhibitory postsynaptic potentials

Inhibitory postsynaptic potentials (IPSPs) were evoked with stimuli ≥ 0.75 T in 11 neurons stimulated in the WM and in all neurons stimulated in layer IV. Their characteristics were in many respects similar to those described previously for rat primary somatosensory cortical pyramidal neurons (Connors et al., 1988; Howe et al., 1987).

a. Fast IPSP

The Cl^--dependent "fast" IPSP (*f* IPSP) (Fig. 11–A) was inverted (i.e. depolarizing) at V_R, had a reversal potential (E_{REV}) of – 68 mV and could be blocked by the γ-aminobutyric $(GABA)_A$ receptor antagonists picrotoxin (PTX) 100–200 μM (Fig. 12–A) and bicuculline methiodide (BMI) (50-100 μM) (not shown). The *f* IPSP became hyperpolarizing and amenable to study (n = 21 neurons: 9 cells stimulated in the WM and 12 cells stimulated in layer IV) only during injection of strong pulses of depolarizing current (Figs. 11, 12, 24

and 27–A). The relatively rapid onset of *f* IPSP was difficult to separate from the preceding *e EPSP* and the slow decaying phase was superimposed on the initial phase of the following slow IPSP (*s* IPSP) (see below). When the *s* IPSP was blocked (in the presence of phaclofen 0.5 mM) the total duration of the *f* IPSP could be estimated at 62.7 ± 4.5 ms (n = 5 neurons).

b. Slow IPSP

The K^+ -dependent, (Connors et al., 1988) "slow" IPSP (*s* IPSP) was hyperpolarizing at the V_R of these neurons (usually about – 80 mV), had a higher amplitude than the preceding *f* IPSP and a much longer duration (usually exceeding 250 ms). The *s* IPSP was evoked in 9 cells stimulated in the WM and in all neurons stimulated in layer IV, with stimuli of 0.75–1.5 T and as previously described (Soltesz et al., 1988), was eliminated by superfusion of the slice with the $GABA_B$ receptor antagonist, phaclofen (0.5 mM) (Fig.12). The *s* IPSP was not able to follow stimulation frequencies > 0.5 Hz and its E_{REV} was about – 90 mV (Fig. 25).

C. EFFECTS OF ANOXIA ON PASSIVE MEMBRANE PROPERTIES:

1. Oxygen measurements in the slice

Prior to testing the anoxic response of cortical neurons, a preliminary series of experiments (n = 18 cells) attempted to assess the dynamics of changes in $[O_2]$ in the superfusing ACSF and the slice. This was performed in order to establish the degree of O_2 deprivation (hypoxia vs. anoxia) induced by replacement of O_2 by N_2 in the ACSF and warming bath, as well as to

determine the way in which the timing of changing solutions and gases was controlled. As shown in Fig. 13–A the decrease in tissue [O_2], measured with O_2-sensitive microelectrodes, was very fast, falling to zero in the first 70–80 s after switching gases, with 90% of the change occurring during the first 45 seconds. Tissue [O_2] remained at zero level throughout the 4–5 min of N_2 exposure and returned to control values in about 2.5–3 min (158 ± 26 s) after reintroduction of O_2.

2. Anoxic depolarization

In 259 anoxic trials performed in 125 neurons, brief anoxia (4–6 min, 1–6 trials/neuron) resulted in a small to moderate depolarization with a peak amplitude of 3.2 ± 0.86 mV for 4 min exposure, (n = 73 trials in 46 neurons), and 4.1 ± 0.97 mV for 5–6 min exposure, (n = 186 trials in 112 neurons). The anoxic depolarization (AD) started 15 s to 1 min after N_2 exposure and declined within 1–2 min after reintroduction of O_2 (Fig. 13–A, B). In experiments in which [O_2] was simultaneously measured in the slice, the onset of AD correlated well with the time when tissue O_2 levels were close to zero, and the recovery of V_m mirrored the recovery of tissue O_2 levels (Fig. 13–A). Only one cell responded with a brief (1.5 min) hyperpolarization, which was followed by a spreading depression-like depolarization (~ 50 mV, with undetectable R_N, not shown). A pure hyperpolarizing response could not be observed in any of the tested neurons. During early recovery from N_2 exposure, V_m occasionally reached more negative values than V_R, to produce a small (1–3 mV, 60–270 s duration) postanoxic hyperpolarization (PAH) (Fig. 13–B, 15–A, 17, 19–A, 20, 22–C); PAH was continuous with the descending slope of the recovering V_m and was similar to that previously described for

TABLE 2 – Effects of anoxia on neuronal properties

	Normoxic value	Anoxic change (5 min)
V_R	– 82.2 ± 2.18 mV	↑ 4.1 ± 0.97 mV
R_N	28.5 ± 2.33 M	↓ 14.8 ± 3.4%
eEPSP	always present (variable amplitude)	⇓ 67 ± 9 %
lEPSP	always present (variable amplitude)	abolished
fIPSP	sometimes present (variable amplitude	abolished
sIPSP	always present (variable amplitude)	abolished
mpsps	always present (variable frequency)	⇓ 65 %

hippocampal pyramidal cells and attributed to Na^+-K^+ ATPase reactivation during reoxygenation (Fujiwara et al., 1987). No correlation could be established between the amplitude of the AD and the magnitude of PAH. In both the presence and absence of PAH, V_m always returned to control values. V_R recovery times (measured from re-introduction of O_2) were 2.3 ± 0.2 min for 4 min exposure, (n = 70 trials in 44 neurons) and 3.7 ± 0.7 min for 5–6 min exposure, (n = 180 trials in 110 neurons).

R_N was frequently monitored throughout the experiment by injection of hyperpolarizing pulses (0.2–0.3 nA) at 0.1–0.2 Hz (see traces in Figs. 13–A, B, 15, 16, 19–22, 30D). During anoxic episodes, falls of 14.8 ± 3.4% (n = 78) and at most 25% were recorded at the peak of AD. With the decrease in R_N, an

increase in rheobase was detected (Fig. 13–C, right), but AP amplitude and duration were not changed. A transient increase of R_N was observed during repolarization in the early reoxygenation phase (Fig. 13–C, left). The anomalous rectification present in normoxic conditions was not affected by anoxia.

A summary of the changes induced by anoxia in neocortical pyramidal neurons is listed in Table 2.

3. Ionic basis of AD

The reversal potential (E_{REV}) of a given transmembrane electric event can often provide clues about the ionic mechanism underlying that event. A depolarization such as AD could be produced by either an influx of positive ions, or/and an efflux of negative ions. Theoretically, steady injection of hyperpolarizing current is expected to increase the amplitude of AD, whereas depolarizing current would normally decrease AD amplitude, up to a point where no AD can be observed (E_{REV}), beyond which AD should change into a hyperpolarization. Hence, E_{REV} should be tested in the depolarizing range of V_m values.

In 25 neurons, E_{REV} of the anoxic depolarization was tested by performing anoxic trials ($\geq$ 2/neuron), while V_m was kept throughout the trial at a constant value, more negative or more positive than V_R, with the help of continuous injection of hyperpolarizing or depolarizing current, respectively. Due to the relative low R_N of these neurons, large depolarizing currents were necessary to create significant V_m changes. (It can be calculated that for the average V_R and R_N of these cells, a 1.0 nA depolarizing pulse will bring V_m to about – 50 mV.) With these currents, the recording often became unstable and the impalement was soon lost. This procedure could not therefore establish

directly the value of E_{REV} (i.e. no depolarizing current high enough to "flatten" or reverse the AD could be injected without impalement deterioration). Moreover, in some neurons, the inward rectification present in these cells in the – 70 mV to – 50 mV range, tended to obscure the measurements, by accentuating AD amplitude at V_m values at which AD was expected to decrease (Fig. 14). However, by extrapolating the portion of the plots in which AD decreased proportionally with V_m, E_{REV} of the anoxic depolarization was found to be approximately – 40 mV (37.6 ± 4.2 mV, n = 25) (Fig. 14—dotted lines). This value is not typical for any specific ionic species, suggesting that the E_{REV} of AD represents a combination of electrochemical gradients and therefore AD has a mixed ionic substrate. Moreover, this value suggests that a significant component of AD is produced by influx of positive ions, having high positive E_{REV} values, such as Na^+ and Ca^{2+}.

a. Role of Na^+

The importance of Na^+ in the production of AD was tested by partially substituting in the ACSF a non-permeant cation for Na^+. This was realized by replacing NaCl with an equiosmolar concentration of choline chloride, thus replacing about 72% of the total Na^+. Anoxic trials performed in low-Na^+ ACSF (n = 6 neurons) showed a significant decrease in the amplitude of AD (see example of Fig. 15) (26.6 ± 1.4% from control at 60 min exposure, $P \leq 0.0001$, n = 6 trials in 6 neurons) which in 3 cells was reversible upon re-introduction of normal ACSF (not shown). In the other 3 neurons, reversibility could not be tested due to deterioration of the recording (a 45–60 min incubation in low-Na^+ solution was usually needed for equilibration and maximum effect on AD.)

Sodium ions could enter the cells through both voltage-dependent and synaptic channels. The implication of voltage-dependent Na^+ channels was tested by introducing in the ACSF the Na^+–channel blocker tetrodotoxin, (TTX) (Fig. 16). Incubation in 1 μM TTX abolished the AP and PSPs in about 5 min and, upon exposure to N_2, resulted in a decrease in amplitude of AD by 45–50% (46.5 ± 6.5%, n = 21 trials in 10 neurons—see example in Fig. 16–A). The E_{REV} of the AD remaining in the presence of TTX could be directly measured at about – 65 mV (Fig. 16–B). This did not eliminate the possible participation of TTX-insensitive Na^+ channels to AD, but strengthened the possibility that conductances other than Na^+ could also be activated during anoxia.

b. Role of Ca^{2+}

The influx of Ca^{2+}_0 during anoxia was blocked by superfusing slices with "Ca^{2+}-free" ACSF, in which divalent metallic cations such as Mn^{2+} and Co^{2+} were added (n = 10 trials in 6 neurons). ("Ca^{2+}-free" refers to ACSF in which $CaCl_2$ was omitted; this does not preclude the existence of small amounts of Ca^{2+}, in the sub-millimolar range.) In normoxic conditions Ca^{2+}-free ACSF with 2.3 mM Mn^{2+} blocked the evoked PSPs in less than 5 min. However, the amplitude of AD induced under these conditions was not decreased, but rather slightly increased in 2 out of 3 neurons tested (see example in Fig. 17). Co^{2+} (2 mM) had similar effects in 3 other neurons (not shown).

c. Role of K^+

Potassium efflux due to an anoxia-activated K^+ conductance (however

unlikely, due to the absence of a hyperpolarization), or decreased pump activity (see below) could produce extracellular K^+ accumulation and cause depolarization. K^+-selective microelectrodes (Figs. 6,7) were used to measure $[K^+]_o$ changes in layers II–III of the neocortex during anoxic episodes (Fig. 18). The time-course of the anoxic-induced $[K^+]_o$ change was very similar to the time-course of a typical AD (Fig. 18–A), showing a rounded upward slope followed by a plateau phase. Upon reoxygenation, $[K^+]_o$ decreased transiently (30 s–2 min) below the control value. At peak anoxia, the increase in $[K^+]_o$ was 0.94 ± 0.12 mM (n = 23 trials in 10 slices). This value is insufficient to account for the observed AD. Furthermore, slices were incubated in ACSF containing various potassium concentrations: 0 mM (n = 3), 5 mM (n = 3) and 9 mM (n = 2). This resulted in V_R changes of hyperpolarization (– 6.65 ± 0.5 mV for 0 K^+) and depolarization (+ 5.2 ± 0.13 mV for 5 mM and + 9.75 mV for 9 mM K^+). V_R was then re-established with steady intracellular current injection and anoxia was induced, but no significant changes in AD amplitude were observed.

d. Na^+ -K^+ ATPase

Combined intracellular Na^+ accumulation and increased $[K^+]_o$ due to a decrease in Na^+-K^+ ATPase activity during anoxia could account for the observed AD. This mechanism has been suggested for the early depolarization seen in some hippocampal pyramidal cells (Leblond and Krnjevic, 1989). It has been shown that PAH is probably due to pump reactivation during re–oxygenation (Fujiwara et al., 1987), an interpretation which supports the idea of a diminished pump activity during anoxia. The application of a Na^+–K^+ ATPase inhibitor, ouabain (5 µM, 5 min) elicited a depolarizing

response comparable to that of AD, but lacking PAH (3.83 ± 0.22 mV, n = 12 trials in 9 neurons—Fig. 19–A, B); anoxia combined with ouabain treatment resulted at 5 min exposure in additive depolarizing changes (n = 4 trials in 4 neurons—Fig. 19–C). These findings demonstrate that AD and pump inhibition have similar and cumulative effects, but do not substantiate/quantify the possible contribution of pump failure to AD.

e. Role of Cl^-

Five slices were superfused with low-Cl^- ACSF, obtained by replacement of NaCl—corresponding to almost 95% of total [Cl^-]—with an equimolar concentration of Na methane sulphonate. At V_R (about – 80 mV), chloride substitution (30–45 min) resulted in an 18% increase of the amplitude of AD (17.7 ± 3.3%, n = 7 trials in 4 neurons) (see example of Fig. 20), indicating that Cl^- efflux, enhanced by the much smaller concentration gradient, may play a minor role in AD generation. This could explain in part the shift in E_{REV} of the AD towards – 60 mV, recorded in TTX (see ***Role of Na^+*** and Fig.16B). Due to the shift in E_{REV} of Cl^-, towards more depolarized values of V_m, induced by decreased $[Cl^-]_o$. AD was still prominent in cells in which V_m was held with continuous depolarizing current at values of between – 55 and – 60 mV (not shown).

Exposure of slices to the $GABA_A$ receptor antagonists BMI (50–100 μM) and PTX (100–200 μM), although effective in rapidly (≤ 2 min) blocking the *f* IPSP and induced epileptiform synaptic responses to orthodromic stimuli (see Fig. 12–A and **Inhibitory postsynaptic potentials—*f* IPSP**, above), did not influence the magnitude of AD (n = 12 trials in 8 neurons) (not shown). Moreover, in 3 slices incubated first in the non-specific excitatory amino acid

(EAA) receptor antagonist, kynurenic acid (KYN) 1 mM (see ***Excitatory amino acid transmitters***, below) and then in KYN plus BMI 100 μM, the degree of depression of AD recorded under KYN and BMI (54.2 ± 4.0%, n = 8 trials in 3 neurons) was comparable to the depression seen under KYN alone (53.8 ± 2.3%, n = 5 trials in 3 neurons) (not illustrated). These experiments suggest that the potential contribution of Cl^- efflux to the production of AD is most probably not through $GABA_A$-activated channels.

f. Excitatory amino acid transmitters

The effect of TTX on AD could be due to a direct effect on Na^+ channels of the recorded neurons, and/or due to a reduced release of EAA transmitter (glutamate) from the terminals of presynaptic cells. To test the latter possibility, slices were incubated for 20–40 min with KYN prior to anoxic exposure. KYN (1 mM) induced a depression of the amplitude of AD comparable to but slightly larger than that produced by TTX (54.7 ± 6.2%, n = 17 trials in 11 neurons) (see example in Fig. 21). Slice exposure to both KYN (1 mM) and TTX (1 μM) (n = 4) induced an AD depression similar to that seen with KYN alone (53.6 ± 7.1%—not shown), indicating that TTX is most probably effective in decreasing AD amplitude through a presynaptic blockade of APs and subsequent reduction of transmitter release, rather than through a direct effect on Na^+ influx in the postsynaptic cell. Furthermore, slice treatment with the specific NMDA receptor antagonist DL-2–amino-5 phosphonovaleric acid (DL-APV) (50–250 μM, n = 4 cells) had no effect on the amplitude of AD (see example in Fig. 22–A), suggesting that in these neurons, an anoxia–induced glutamate release induces depolarization mainly through Na^+ influx via the "non-NMDA" (AMPA/kainate) activated channels. However, a more specific block-

ade of AMPA/kainate–activated channels with small concentrations (< 10 μM) of CNQX would be useful for strengthening these results).

Another possibility is that anoxia-released glutamate activates metabotropic receptors (mGLU) (i.e. not influenced by KYN) and therefore increases intracellular cation concentration through various mechanisms dependent on mGLU activation (see **BACKGROUND**). Slice exposure to the specific metabotropic receptor antagonist (+)-methyl-4-carboxyphenyl-glycine (MCPG—1mM) (Watkins and Collingridge, 1994) did not have any depressant effect on AD amplitude (n = 5 trials in 3 neurons) (as illustrated in Fig. 22–B). This finding was further confirmed in 2 other neurons, where KYN 1mM reduced the amplitude of AD by 47% and 50% respectively, but the addition of MCPG 1 mM to the KYN-containing ACSF did not further change the amplitude of AD (see example in Fig. 22–C). Since MCPG does not block, however, class III mGLU, more specific blockers should be tested, in order to rule out the possible role of metabotropic receptors. A summary of the ionic mech-

TABLE 3 – Contribution of various ionic mechanisms to AD

Na^+ influx		++++
K^+ efflux & accumulation		±
Cl^- efflux		±
	Passive	+
	Synaptic channels ($GABA_A$)	–
Ca^{2+} influx		–
	Voltage-gated channels	–
	Synaptic channels	–

(+) presence of effect (–) absence of effect

anisms involved in the anoxic depolarization is presented in Table 3.

D. EFFECTS OF ANOXIA ON SYNAPTIC POTENTIALS

A period of 4–6 min of anoxia depressed the synaptic potentials in all tested neurons (n = 115). This effect was not "contaminated" by sensitivity induced by the sustained stimulation at 0.1–0.2 Hz, because for a given cell, the PSPs evoked by stimuli applied at 0.05 Hz, minute intervals, or as a single volley at 5 min anoxia showed identical degrees of depression (n = 9 neurons). However, the various types of synaptic potentials showed differential sensitivity to anoxia.

1. Changes in EPSPs

The *e* EPSP was the component *least sensitive* to anoxia. The peak amplitude of the *e* EPSP decreased by 67 ± 9.0% at 5 min N_2 exposure (n = 74 trials in 44 neurons) (Figs. 23–A, B and 26). The *e* EPSP latency to peak was unchanged, but the rising slope was usually decreased. Because 0.5–0.8 T were used routinely to evoke robust EPSPs throughout the anoxic episode, the possibility that too-strong stimuli might account for the incomplete depression was investigated; it was found that even isolated (i.e. no *l* EPSP), small (2–5 mV) *e* EPSPs evoked by weak (0.1–0.3 T) stimuli were always submaximally depressed at 5 min of anoxia.

The *l* EPSP was always *abolished* during the same period of N_2 exposure (Figs. 23–A, B and 26–A). For 0.5–0.6 T stimuli, *l* EPSP disappearance occurred usually within the first 2 min of anoxia and was graded, typically consisting of progressive decrease of the amplitude and increase of the laten-

cy to peak (Figs. 23 and 27–B). Occasionally this process produced a separation of discrete subcomponents of the *l* EPSP (Fig. 23–B). Therefore, at the end of the anoxic episode, the residual synaptic response in all recorded neurons was a small *e* EPSP. Comparison of the change in amplitude of the early and late components of the EPSP at 1 min 30 s of anoxia (i.e., before the disappearance of the *l* EPSP) showed a significantly greater attenuation of 63 ± 2.5% of control for the *l* EPSP compared with 23 ± 1.4% for the *e* EPSP ($P \leq 0.0001$, n = 44). At the same time, the latency to peak of the *l* EPSP was prolonged (64.0 ± 3.0 ms, cf. control of 34 ± 1.6 ms, $P \leq 0.0001$). whereas that of the *e* EPSP was unchanged (8.3 ± 0.29 ms, cf. control of 8.2 ± 0.27 ms, P = 0.13).

Re-oxygenation induced a complete recovery of the EPSPs in all recorded cells. With longer exposures to O_2 lack, longer times for recovery were observed. For 89 anoxic trials in 53 neurons, the EPSP recovery periods were 5.7 ± 1.9 min (4 min anoxia, n = 15 trials), 7.4 ± 1.5 min (5 min anoxia, n = 50 trials) and 9.8 ± 1.4 min (6 min anoxia, n = 24 trials). The course of recovery mirrored the events during N_2 exposure: an initial increase in the *e* EPSP was followed by the reappearance of a small, delayed *l* EPSP, which gradually reached the control values for amplitude and latency to peak (Figs. 23–A, B and 27–B).

2. Changes in IPSPs

The fast and slow IPSPs were particularly *sensitive* to N_2 and were characteristically abolished during the first 1–1.5 min of anoxia (Fig. 24–A, C). No consistent sequence was noted for the loss of the two types of IPSP, the time of disappearance being 86.2 ± 10.2 s for the *f* IPSP, compared to 98.8 ± 11.4 s

for the *s* IPSP (n = 8, P = 0.14). However, for a given cell, both IPSPs were abolished before the *l* EPSP evoked at the same stimulus strength; the time for failure for the *l* EPSP (131 ± 12.0 s, n = 8) was significantly longer than that of either *f* IPSP or *s* IPSP ($P \leq 0.0005$). The recovery of the IPSP was delayed compared with that of the EPSP (Figs. 24–B, D and 26–B), and in some cases it was incomplete, even after 20 min of re-oxygenation. The effect of N_2 on the IPSPs represented a true suppression of synaptic conductances and was not due to a change in reversal potential (E_{REV}) of the synaptic current (due to ionic redistribution and depolarization). This is illustrated in Fig. 25, which shows the absence of a shift in E_{REV} of the *s* IPSP during anoxia for three different neurons.

3. Consequences of different PSP sensitivity to anoxia

In about 25% of the cells (12 out of 53 neurons) a transient *increase* in excitability could be observed during a 20–30 s interval (i.e., 2–3 responses at 0.1 Hz) of early anoxia. This was represented by more robust EPSPs which, if elicited by stimuli ≥ 1.0 T or evoked superimposed on depolarizing pulses, were capable of generating APs at higher frequency (Fig. 27–A) or in longer trains (not shown). A related effect was the occurrence of APs with stimuli that initially were < 1.0 T in control ACSF. This occurred at the initial value of V_R (i.e., the effect was not related to anoxic depolarization) and was observed during early anoxia, as well as in mid-recovery (Fig. 27–B). The most likely explanation for these phenomena is the early depression and delayed recovery of the IPSPs, although other factors may contribute.

4. Mechanisms of synaptic depression

a. Postsynaptic mechanisms

Changes in V_R and R_N

The finding that both V_m and R_N returned to control values several minutes before PSP recovery testified against a significant effect of these membrane properties upon the PSP depression. To confirm this finding, PSP amplitude was routinely measured at the peak of anoxic depolarization after briefly (for 20–30 s) restoring V_R by injection of hyperpolarizing current (as in example of Fig. 28). Because this procedure neither significantly increased the reduced *e* EPSP, nor restored the *l* EPSP, it indicated that occlusion (a decrease in EPSP amplitude as V_m is depolarized toward E_{REV} of the EPSP), at least at the level of the soma (i.e. region affected by the current injection), was not responsible for the depression of EPSPs. Moreover, the mechanism of occlusion is not applicable to the depression of the IPSPs, which should rather be accentuated by depolarization.

Failure of the Na^+-K^+ ATPase

Since the sodium pump is likely to be depressed during anoxia, the resulting decrease in the transmembrane Na^+ gradient could reduce postsynaptic currents carried by Na^+ and therefore depress the EPSPs. This hypothesis was tested in 9 neurons by comparing the effects on EPSPs of N_2 exposure and bath application of the sodium pump inhibitor, ouabain (5 μM). In all cases, anoxia induced the characteristic membrane depolarization and EPSP depres-

sion (as shown in the recordings from one cell in Fig. 29–A, B); whereas, although ouabain in normoxic ACSF caused a similar depolarization, it did not affect EPSP amplitude even after prolonged exposure (Fig. 29–C, D). Indeed in two neurons, the application of ouabain resulted in increased excitability, which manifested as spontaneous depolarizing events (Fig. 29–C, insets). The similarity of the time course of these small depolarizations to that of the *l* EPSP, together with their sensitivity to N_2 (Fig. 29–E), suggested a synaptic origin involving the activation of excitatory polysynaptic pathways. This effect of ouabain on excitability has been previously described in hippocampal CA1 pyramidal cells and attributed to an enhancement of a Ca^{2+}-dependent conductance (McCarren and Alger, 1987). An additional mechanism may be the release of aspartate and glutamate induced by ouabain exposure (Jacobson et al., 1986).

Postsynaptic receptors

Reduced adenosine triphosphate (ATP) levels, as well as increased concentration of transmitter in the synaptic cleft (Lipton and Whittingham, 1984; Hauptman et al., 1984; Simpson et al., 1991), occur during anoxia and could contribute to synaptic depression through decreased receptor phosphorylation and/or receptor desensitization, respectively. The possibility that anoxia influences postsynaptic receptors was investigated by studying the neuronal response to local applications of the α-amino-3-hydroxy-5-methyl-4-isoxazolepropionic acid (AMPA) receptor agonist quisqualate (QUIS), and of the inhibitory neurotransmitter gamma–aminobutyric acid (GABA).

QUIS (100 μM) was ejected into the slice close to the recording site (at a distance estimated to be < 100 μm). Anoxic trials were started only after

obtaining reproducible responses to the ejected drug (i.e., ≥ 10 min). Since during QUIS ejection, the usually continuous orthodromic stimulation was stopped, the degree of synaptic depression was quantified at the beginning of each experiment, either by pairing a pulse with an orthodromic stimulus, or by performing a separate anoxic trial under continuous layer IV stimulation. QUIS ejection (1 pulse every 30–60 s) elicited strong depolarizing responses (> 20 mV amplitude and 2–6 s duration) that could be abolished by 1 mM kynurenic acid (KYN), but not by 250 μM DL-APV (not shown) and evoked trains of APs (Fig. 30–A). The contribution of the recurrent synaptic circuitry to QUIS responses was eliminated by bathing the slices in 1 μM TTX; each QUIS pulse then elicited a spikeless depolarization, which was reduced by 25.4 ± 3.2% (n = 5 trials in 4 neurons) in the presence of N_2 (see example in Fig. 30–C).

Local application of 1 mM GABA close to the apical side of the soma (1 pulse every 1–2 min) elicited at V_R depolarizing responses (4–10 mV amplitude and 4–8 s duration) that became biphasic with membrane depolarization: the initial phase remained depolarizing up to AP threshold (about – 56 mV), whereas the late phase reversed between – 70 and – 75 mV (Fig. 30–B). These responses were similar to those previously described for a similar position of the ejection microelectrode (Connors et al., 1988), and could be blocked by bath application of the $GABA_A$ receptor antagonists, BMI (100 μM) and PTX (200 μM). Before anoxic exposure, the slices were bathed in 1 μM TTX and 1 mM KYN to eliminate any synaptic contribution to the depolarizing GABA response. Exposure to N_2 reduced the amplitude of GABA-evoked responses by 26.5 ± 1.7% (n = 11 trials in 4 cells) (see example in Fig. 30–D).

b. Presynaptic mechanisms

Since the reduction in amplitude of the depolarizing responses evoked by local application of EAAs does not account for the extent of the synaptic depression (as gauged by the much larger decrease of the *e* EPSP amplitude in the same neurons), a possible involvement of presynaptic mechanisms was also investigated.

Miniature PSPs (mpsps) frequency.

On the basis of the observation that anoxia strongly inhibits voltage-gated Ca^{2+} currents (Young and Somjen, 1991), (possibly through release of Ca^{2+} from internal stores and subsequent increased intracellular [Ca^{2+}] (Krnjevic and Leblond, 1987, 1989; Krnjevic and Xu, 1989), the possibility of a decrease of Ca^{2+} influx in the presynaptic terminals was examined. Presynaptic activity was studied by measuring the frequency of spontaneous miniature postsynaptic potentials (mpsps) in control and anoxic conditions (Fig.30). First, measurements were performed in standard ACSF. After the correction for decrease in amplitude due to anoxia, the frequency of mpsps during the last minute in a 5 min anoxic period was found to be decreased by about 70% (68 ± 4.2 %, n = 5) as compared to control conditions (an example is shown in Fig. 31–A). Since in this model, the presynaptic cell was not isolated from its various synaptic inputs, and therefore some of the observed reduction in mpsps frequency could be the result of a decrease in the synaptic activity impinging on the presynaptic cell, these measurements were also performed in slices incubated in TTX (n = 5). Although TTX greatly reduced the control value of the mpsp frequency (Fig.31–B), exposure to N_2 had an effect similar to that in

standard ACSF (i.e. the mpsp frequency per 1 min decreased by 65 ± 7.3 %). This decrease was large enough to account for the observed anoxic depression of the evoked monosynaptic events (*e* EPSP) recorded in these neurons.

Presynaptic adenosine receptors.

It has been shown that during hypoxia levels of endogenous adenosine increase in various regions of the central nervous system (spinal cord, hippocampus) (Manzoni et al., 1994; Rudolphi et al., 1992) and that adenosine may play a neuroprotective role in hypoxia and ischemia by decreasing neuronal excitability and therefore lowering ATP expenditure. This effect is thought to occur by binding of adenosine to the A_1 receptor subtype, which is present pre-, post- and extrasynaptically on neurons rich in glutamate receptors (Lee and Löwenkopf, 1993; Rudolphi et al., 1992).

The possibility that the observed presynaptic effect of anoxia on PSPs is due to adenosine binding to A_1 presynaptic receptors was tested in the neocortical slice by incubating the slices in adenosine antagonists prior to the anoxic trials. Preliminary experiments, using the non-specific adenosine antagonist, theophylline 200 µM (n = 3 neurons) revealed a strong influence of the drug on the evoked PSP, with burst-like spiking in normoxic conditions and preservation of EPSP amplitude during anoxia (not shown). Since theophylline is a non-specific antagonist, which at high concentrations exerts significant effects on phosphodiesterase activity, the effect of the more selective A_1 antagonist, 8-cyclopentyltheophylline (8-CPT) was subsequently tested (n = 5 neurons in 5 slices). A 10–20 min pre-incubation of the slices in 8-CPT 1 µM did not significantly affect the firing pattern in normoxic conditions, but was effective in all cases in maintaining the evoked PSP amplitude through-

out the 5 min of anoxia (Fig. 32), strongly suggesting that the anoxic PSP depression is mediated by adenosine interaction with A_1 receptors.

Table 4 summarizes the mechanisms contributing to the occurrence of the neocortical synaptic depression during anoxia.

TABLE 4 – Contribution of various mechanisms to synaptic depression

↓ Presynaptic adenosine receptor sensitivity		+++
↓ Postsynaptic receptor sensitivity		+
	AMPA/Kainate	+
	NMDA	–
	mGLU	–
	$GABA_A$	+
↓ E_{REV} EPSP		–
↑ V_R ↓ R_N		–
↓ Na^+-K^+ ATPase		–

(+) presence of effect (–) absence of effect

5. Protective antianoxic measures

a. Creatine pre-incubation

It has been shown that pre-incubation of slices (1–3 h) in Ringer containing creatine protects hippocampal neurons during anoxia (reduction of changes in V_R and R_N, small or no PAH and preservation of PSPs) (Leblond and Krnjevic, 1989; Whittingham and Lipton, 1981), probably through an elevation of tissue phosphocreatine and delay in the fall in ATP during anoxia.

Neocortical slices (n = 8) were pre-incubated in 25 mM creatine for 1.5–2.5 h prior to recording. Since anoxic trials with and without creatine pre–incubation could not be performed in the same neuron, comparisons were made between slices obtained in the same day, from the same animal. In normoxic conditions the effect of creatine pre-incubation was an increase in excitability, manifest as a high amplitude of both *e* and *l* EPSP. The *l* EPSP had almost the appearance of an epileptiform paroxismal depolarizing shift and had a bursting spiking pattern (see lower inset in Fig. 33). Creatine pre-incubation did not, however, influence the anoxic response. The EPSP amplitude decreased and the anoxic depolarization occurred and, in some cases, was significantly accentuated, as compared with the average ADs recorded from control slices from the same animal; in 3/8 neurons a 67.6 ± 4.1 % increase in peak amplitude of AD was recorded (an example of such cell is illustrated in Fig. 33).

b. ATP–sensitive K^+ channels

A potential mechanism which could oppose the anoxic depolarizing tendencies would be an activation of ATP-sensitive K^+ channels. If these channels

would be well represented in these neurons, the fall in ATP induced by anoxia could open them to a certain extent and induce an efflux of K^+ which should counteract the depolarization. Furthermore, if this K^+ current would exist but be surpassed by the depolarizing conductances activated by anoxia, it is conceivable that treating the slices with an ATP-sensitive K^+ channel opener would augment the K^+ efflux and therefore decrease the amplitude of AD.

This hypothesis was tested in 5 neurons from 5 different slices, by superfusing the slices with ACSF containing the ATP-sensitive K^+ channel opener, diazoxide (0.8 mM), followed by 1 to 3 anoxic trials/neuron (total of 9 trials), performed between 10 min and 40 min after exposure to diazoxide. Although in one neuron diazoxide slightly delayed (20 and 35 s) the onset of two successive ADs as compared with control values (not shown), the difference was not statistically significant. No decrease in the amplitude of AD or changes in the decrease of R_N were observed in all neurons tested. Therefore, another documented effect of diazoxide—glutamate receptor de-sensitization (which also could have influenced AD amplitude) was not evident.

c. Temperature effects

Intracellular recordings at control temperature (33.5°C) and during temperature changes to values between 26 and 37.5°C were performed in a group of 22 neurons and electrophysiological properties and anoxic responses were compared. The recorded cells were representative of the entire population included in this study ($V_R = -82.3 \pm 2.8$ mV, $R_N = 25.2 \pm 2.2$ MΩ, and EPSPs and IPSPs were elicited in all neurons by layer IV stimulation).

Effects of temperature in normoxic conditions

When temperature was raised from the control level to 35°C and higher, neurons showed a slight depolarization, which was directly proportional to the change in temperature ($\approx$ 2 mV/°). In order to restore V_m close to V_R prior to the anoxic trial, hyperpolarizing current (0.2–0.6 nA) was steadily injected through the recording microelectrode. R_N decreased at temperatures $\geq$ 36.5°C: 21.2 $\pm$ 2.1 MΩ as compared with 26.3 $\pm$ 1.9 MΩ at 33.5°C (n = 6 trials, $P \leq 0.01$). Brief spontaneous depolarizing events of 1–10 s duration and 5–15 mV amplitude also occurred with warming (Fig. 35–B, inset. These appeared only occasionally between 35 and 36°C (n = 2/10 trials in 8 neurons), but increased in frequency and showed maximal amplitude and duration above 36°C (n = 8/9 trials in 9 neurons). Their time course was very similar to that of interictal discharges in the Mg^{2+}-free epileptic model (Rosen and Andrew, 1990), but they did not generate APs.

EPSPs were depressed with increased temperature. Both early and late components were strongly influenced, showing an decreased latency and a lower peak amplitude (illustrated for *e* EPSP in Fig. 34). The effect of increased temperature on fast and slow IPSPs was even more profound: both IPSPs disappeared at temperatures above 35°C (shown in Fig. 36–B for the *s* IPSP).

The effects of cooling on V_m, R_N and synaptic potentials were opposite to those of warming only in some respects (Fig. 34 B,C). Increases in R_N were recorded when temperature was lowered: 27.6 $\pm$ 0.4 MΩ at 26–27°C compared to 23.3 $\pm$ 0.6 MΩ at 33.5°C (n = 3). Changes in V_m occurred in four out of 14 trials (n = 10 neurons) and consisted of minor hyperpolarizations of 1–2 mV. The latency of the *e* EPSP was increased, but interestingly, as with warming,

the peak amplitudes of both the *e* EPSP (Figs. 34–C, 37) and *l* EPSP (not shown) were reduced. The IPSPs were also attenuated and at temperatures lower than 31.5–32°C were abolished (not shown).

Effects of temperature on anoxic changes

The amplitude of the anoxic depolarization (Fig. 35) was either unaffected by warming, or showed an increase in one third of the trials: 6.6 ± 0.6 mV compared with 4.3 ± 0.6 mV at control temperature (n = 5 trials, $P \leq 0.001$). In 90% of trials the initial slope of the anoxic depolarization was increased: 3.7 ± 0.1 mV/min during the first minute at temperatures over 36.5°C, compared with 1.9 ± 0.1 mV/min at 33.5°C (n = 8 trials, $P \leq 0.0001$). PAH was accentuated: 4.0 ± 0.2 mV at temperatures ≥ 36.5°C as compared to 2.8 ± 0.2 mV at control temperature (n = 8 trials, $P \leq 0.0001$; not illustrated). The duration for postanoxic recovery of V_m was prolonged: 8.8 ± 0.98 min compared with 4.2 ± 0.28 min (n = 8, $P \leq 0.005$; Fig. 35). The brief spontaneous depolarizations which were observed chiefly at temperatures > 36°C were not depressed by anoxia. In fact, they appeared more frequently and were prominent during the anoxic period, probably due to lack of interference from the evoked synaptic potentials (Fig. 35–C, arrowheads).

The anoxic-evoked synaptic depression was accentuated at increased temperature in all recorded neurons (Figs. 35–38). This was manifest as a faster decrease in the amplitude of both early and late EPSPs, a more rapid disappearance of the *l* EPSP and a smaller and briefer residual *e* EPSP at the peak of the anoxic trial (Fig. 36 B). At 36.5°C the amplitude of the *e* EPSP was 32.3 ± 5.2% of control as compared with 58.3 ± 1.2% at 33.5°C (at 5 min of anoxia, n = 5, $P \leq 0.0005$). In 4 cells which were warmed ≤ 37°C, the residual *e*

EPSP at 5 min anoxia was 16.3 ± 2.3%. These effects were fully reversible upon return to control temperature; in some cases, the EPSPs even showed a slightly decreased sensitivity to subsequent anoxias, with a delay and reduction of the depression (Fig. 36 C). For temperatures above 36.5°C the recovery of the compound EPSP took 12.8 ± 0.8 min vs 7.8 ± 0.3 min at 33.5°C ($n = 9$, $P \leq 0.0005$).

Since in most cases IPSPs were abolished at temperatures > 35°C (Fig. 36–B), the influence of warming upon IPSP depression was not amenable to study. In two cells in which *s* IPSPs were present (although reduced to 40%) at 35°C, anoxia induced a rapid disappearance of the IPSP (50–60 s as compared to 90–110 s at 33.5°C) and its recovery was delayed and incomplete.

Cooling had a stabilizing effect on V_R. The anoxic depolarization was consistently reduced in amplitude, its slope during the first minute was decreased from 2.0 ± 0.1 mV/min at 33.5°C to 1.0 ± 0.2 mV/min at 30.5–31°C ($n = 5$ trials, $P < 0.005$) and recovery to control V_R appeared to be hastened. Since PAH was minimally present at 30.5–31°C (and absent at 26–27°C), the duration of postanoxic recovery of V_m was difficult to estimate. Below 31°C the amplitude of the anoxic depolarization never exceeded 1–2 mV and at 26°C ($n = 4$ trials) it was practically nil (not illustrated). The synaptic depression evoked by anoxia was oppositely affected by lowering temperature. Both early and late EPSPs were better and longer preserved during N_2 exposure. At 30.5–31°C, there were minimal changes in the rising slope of the *e* EPSP, a delay and decrease in the reduction in its amplitude (at 5 min of anoxia, 86.5 ± 3.8% vs. 59.8 ± 4.3% of control, $n = 5$ trials, $P \leq 0.005$), and a delayed disappearance of the *l* EPSP. The recovery of the control compound EPSP took 4.2 ± 1.3 min vs 8.0 ± 1.1 min ($n = 5$ trials, $P = 0.056$).

At 26–27°C EPSP preservation was practically complete (Fig. 37). In all

anoxic trials (n = 6) *e* EPSP amplitude remained above 95% of control value (Fig. 37–C) and the *l* EPSP was not abolished. The effects of temperature change, over the range between 26 and 37.5°C, on anoxic depression of the *early* and *late* EPSPs are summarized for all recorded neurons in Fig. 38.

FIGURES

NOTE: in the following section, each figure is *preceded* by its corresponding figure legend.

Figure 1. Blocking and slicing of neocortex. (A) Rat brain removed from the cranium. (fp: frontal pole, cs: cortical surface). (B) Two parasagital cuts separated the median from the lateral regions of the brain. (C) A horizontal cut inferior to corpus callosum separated a neocortical block (nb) from the ventral region of the brain, which was discarded. (D) The block was rotated 180° (cortex down) and sliced.

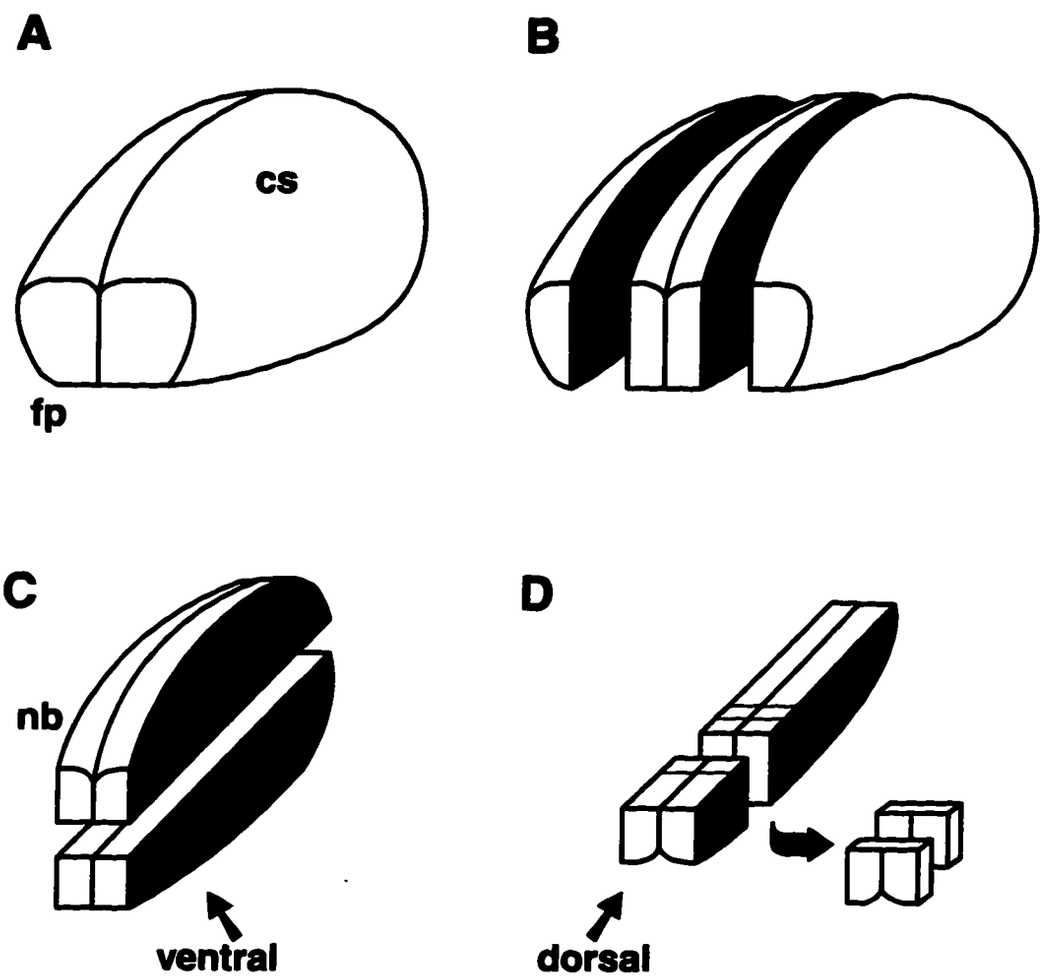

Figure 1

Figure 2. Diagramatic section of the recording chamber assembly showing the temperature controlling system, the ACSF circulation (black arrows), and the oxygenation of the slice surroundings (white arrows). The slice is placed on a lens paper strip which acts as a wick to ensure a continuous flow of ACSF. A cover placed above the slice is essential for maintaining the O_2-rich atmosphere. Note that the recording electrode (R) is placed in the slice through an opening of the cover.

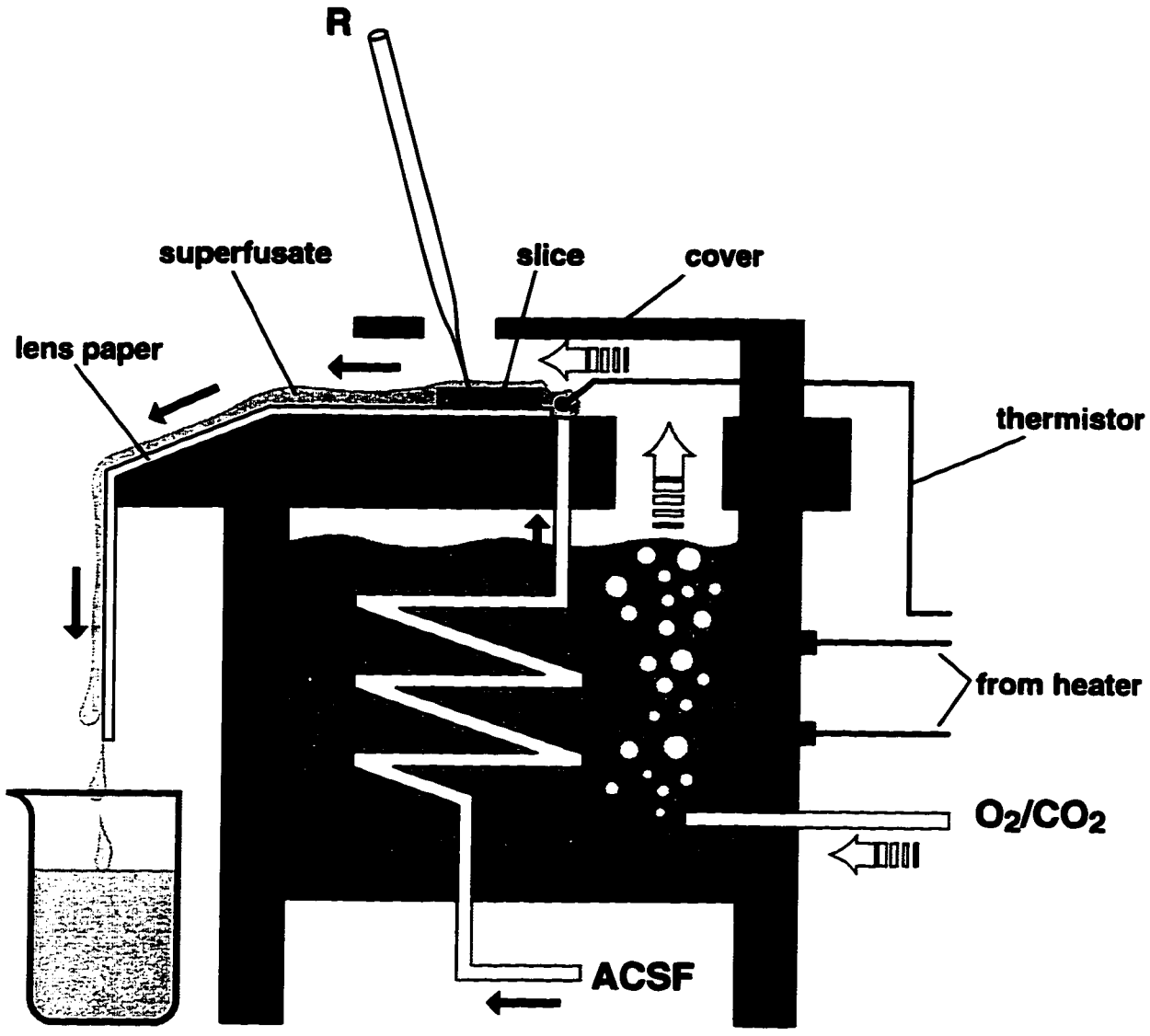
R
superfusate
slice
cover
lens paper
thermistor
from heater
O_2/CO_2
ACSF

Figure 2

Figure 3. Diagram of the superfusion system. In this particular setup, the left three ACSF reservoirs are permanently bubbled (light gray lines) with oxygenated gas mixture (from the tank marked O_2/CO_2) and the right three reservoirs are bubbled with "anoxic" gas mixture (from the tank marked N_2/CO_2). The active ACSF reservoir is the leftmost one: both the solenoid valve and 8–way valve are open in such a way as to allow ACSF from this reservoir to flow (dark gray lines) to the recording chamber. Accordingly, O_2 is directed also to the recording chamber, through the 3-way valve. (See text for a complete description of the system.)

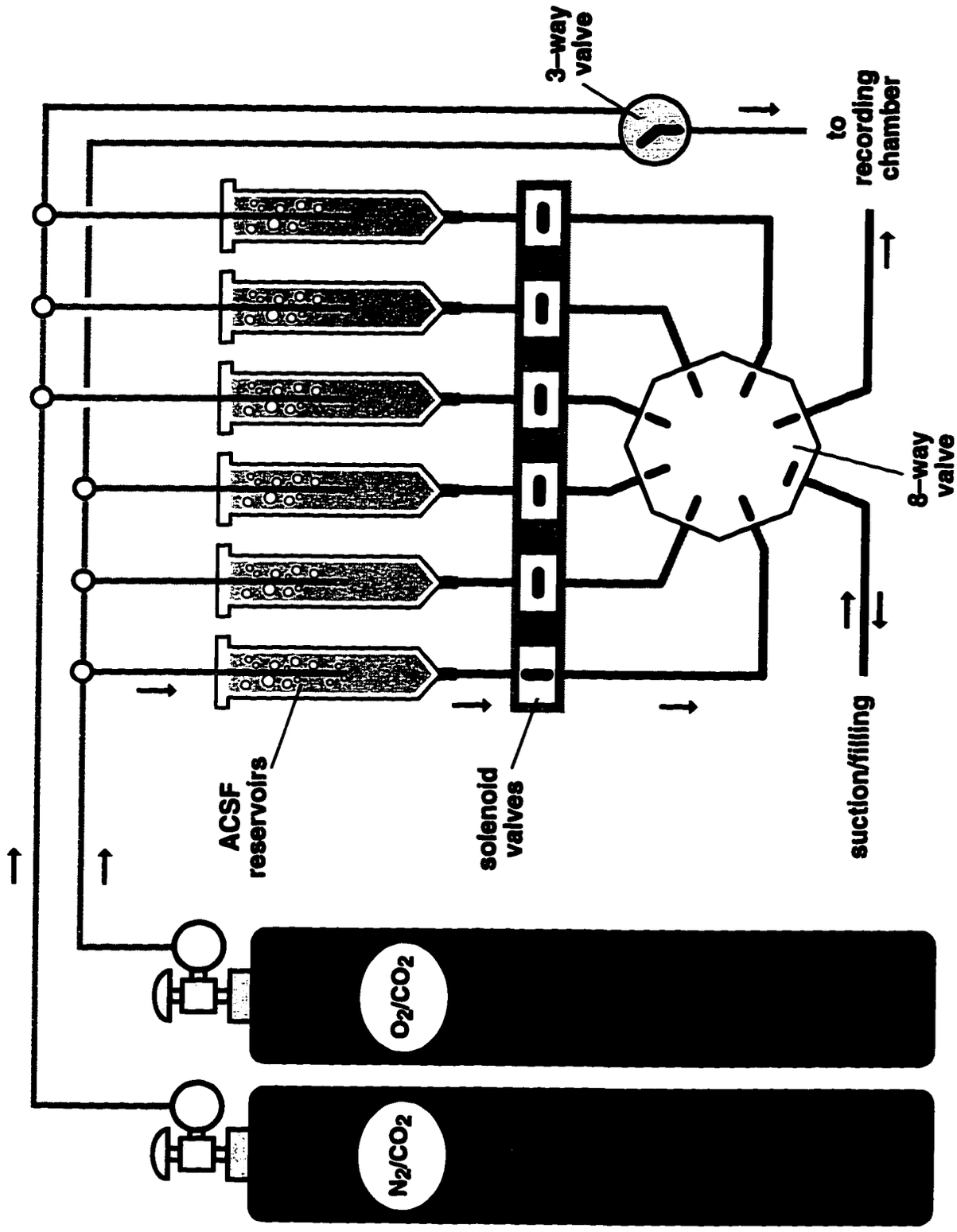
3-way valve
to recording chamber
8-way valve
ACSF reservoirs
solenoid valves
suction/filling
O_2/CO_2
N_2/CO_2

Figure 3

Figure 4. Diagram of the intracellular recording setup. The gray rectangles marked A, B and C represent levels of basic input/stimulation (A), monitoring–transducing (B) and data storage (C). (A) This level is in direct connectivity with the recording chamber (depicted at right). In response to an intracellular current pulse delivered through the microelectrode by the main stimulator (1) the biological signal is picked up and enhanced by the intracellular amplifier (2), which sends it to level B (see the connections of the black circles). The main stimulator (1) serves also as triggering source for other devices which are situated at various levels and require synchronization (see the connections of the gray circles). These include an additional stimulator (10), which is used to deliver orthodromic stimuli (white circle) to the slice. The output of each stimulator is adjusted by a stimulus isolation unit (SIU). (B) At this level, the amplifier/oscilloscope (5) receives both biological and current monitor signals (for convenience, only one line is shown coming out from the intracellular amplifier(1)), enhances them and displays them continuously on the screen. (The biological signal is also monitored through a loud speaker (4)). The signals amplified by (5) are also sent to an analog/digital interface (8) for digitization and computer processing. (C) Data storage and processing level. Both biological and current monitor signals from the intracellular amplifier (2) are displayed on the screen of a storage oscilloscope (6) and chart recorder (7). The digitized signals from the interface (8) are continuously recorded on the hard drive of a computer (9) for subsequent playback and analysis. (See text for a complete description of the hardware, software and intracellular techniques).

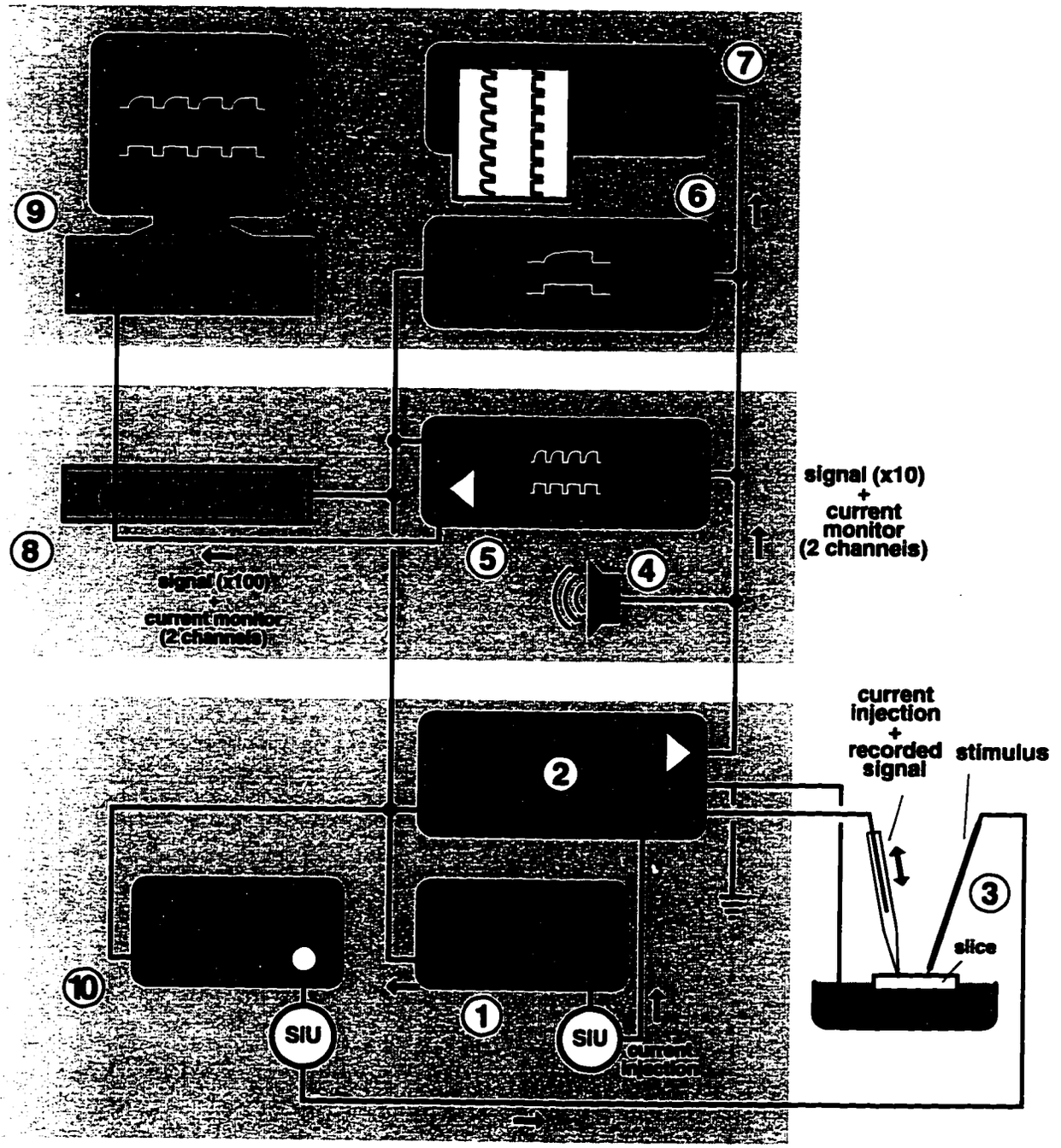
7
6
9
signal (x10)
+
current
monitor
(2 channels)
8
5
4
signal (x100)
+
current monitor
(2 channels)
current
injection
+
recorded
signal
stimulus
2
3
slice
10
SIU
1
SIU

Figure 4

Figure 5. Placement of the stimulation and recording electrodes in the slice. The slice is placed in the recording chamber (not shown) with the cortex oriented opposite to the direction of ACSF flow (gray arrows). (The silver wires used to weigh the slice are not shown.) R: recording microelectrode placed in layer II. S_1, S_2: stimulating electrodes placed in the white matter (corpus callosum—CC) and layer IV, respectively. (C/Pu: caudate/putamen, LS lateral septum, V: lateral ventricle, C: cortex).

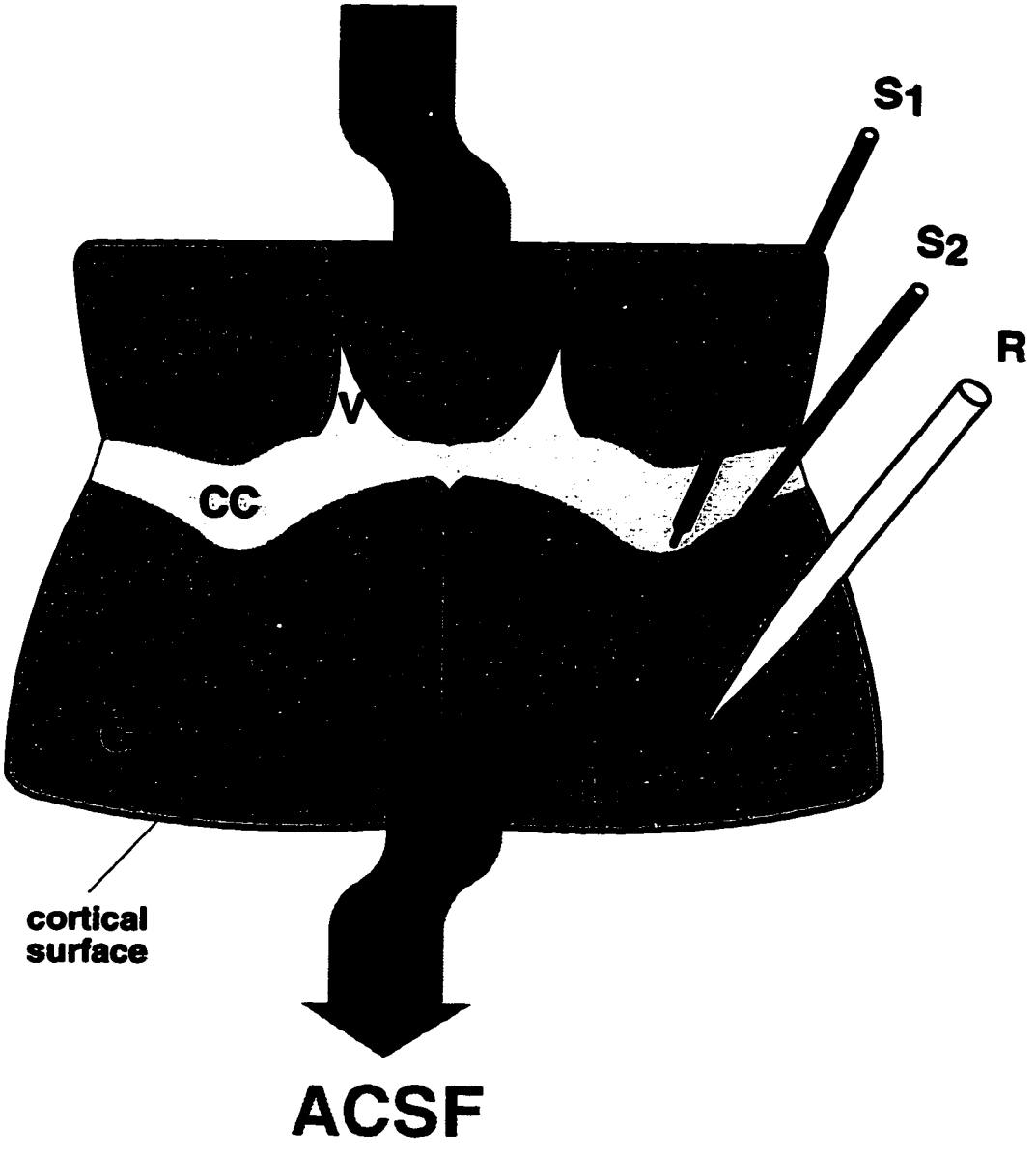

Figure 5

Figure 6. Diagram of a potassium-sensitive microelectrode. At left, a pulled electrode, ready for filling. Note the shorter exchanger barrel (eb), as compared to the reference barrel (rb), as well as the cross-section of the electrode (in the shape of the greek letter "theta"), shown at the top. At right, a finished electrode (see text for details).

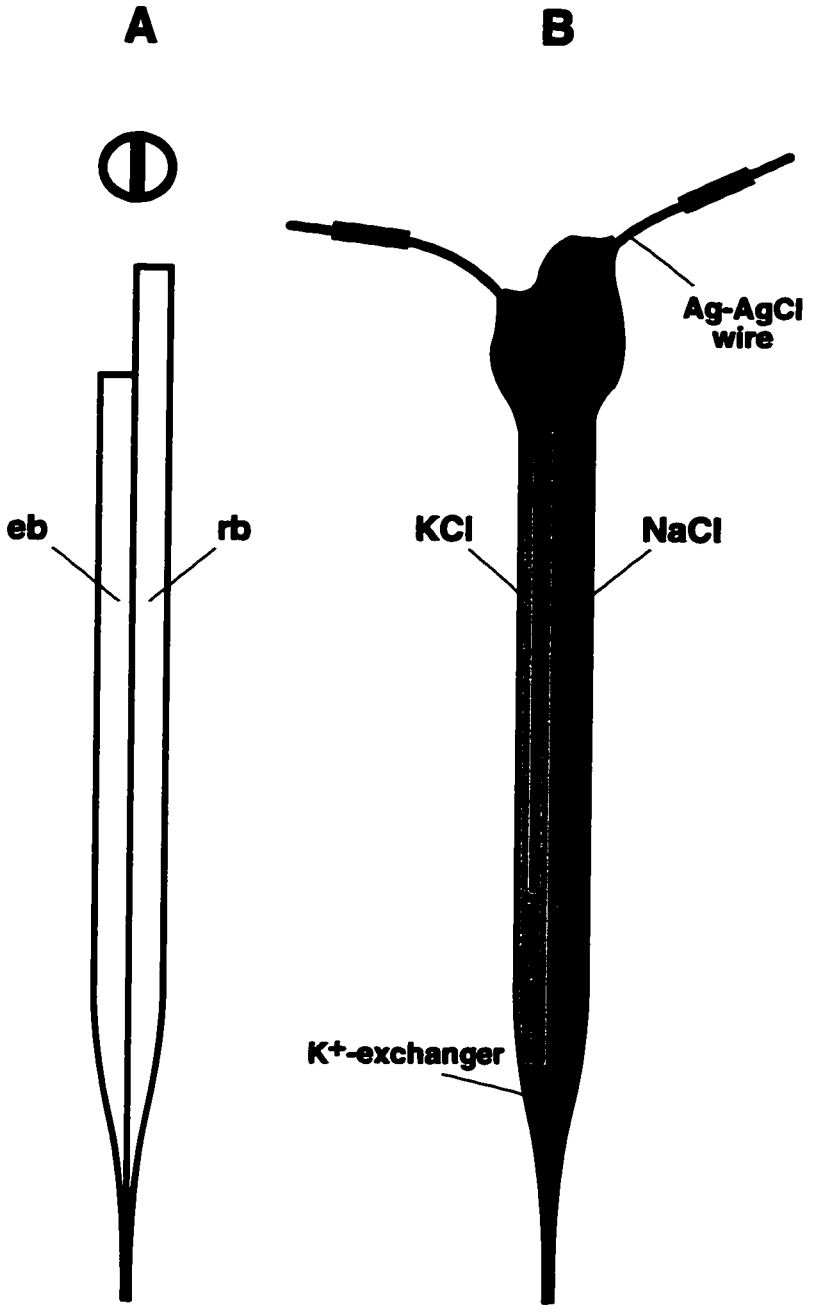

Figure 6

Figure 7. Calibration of a potassium-sensitive microelectrode. (K^+ exchanger—valinomycin, reference barrel resistance—10 MΩ, tip diameter—5 μm). (A) Polygraph recording (note curvilinear scales) of the calibration of the K^+-sensitive microelectrode. The microelectrode tip was successively introduced in ACSF solutions containing 1, 3, 5, 10 and 20 mM KCl. The upper trace represents the response of the K^+-sensitive barrel, the lower trace is the recording obtained from the reference barrel. (B) The E_K values obtained from (A) were used to plot the calibration curve of the electrode. Following an experiment this curve was used to plot values of E_K recorded extracellularly from slices in control or anoxic conditions and obtain the concentrations of K^+ in mM (see Fig. 18).

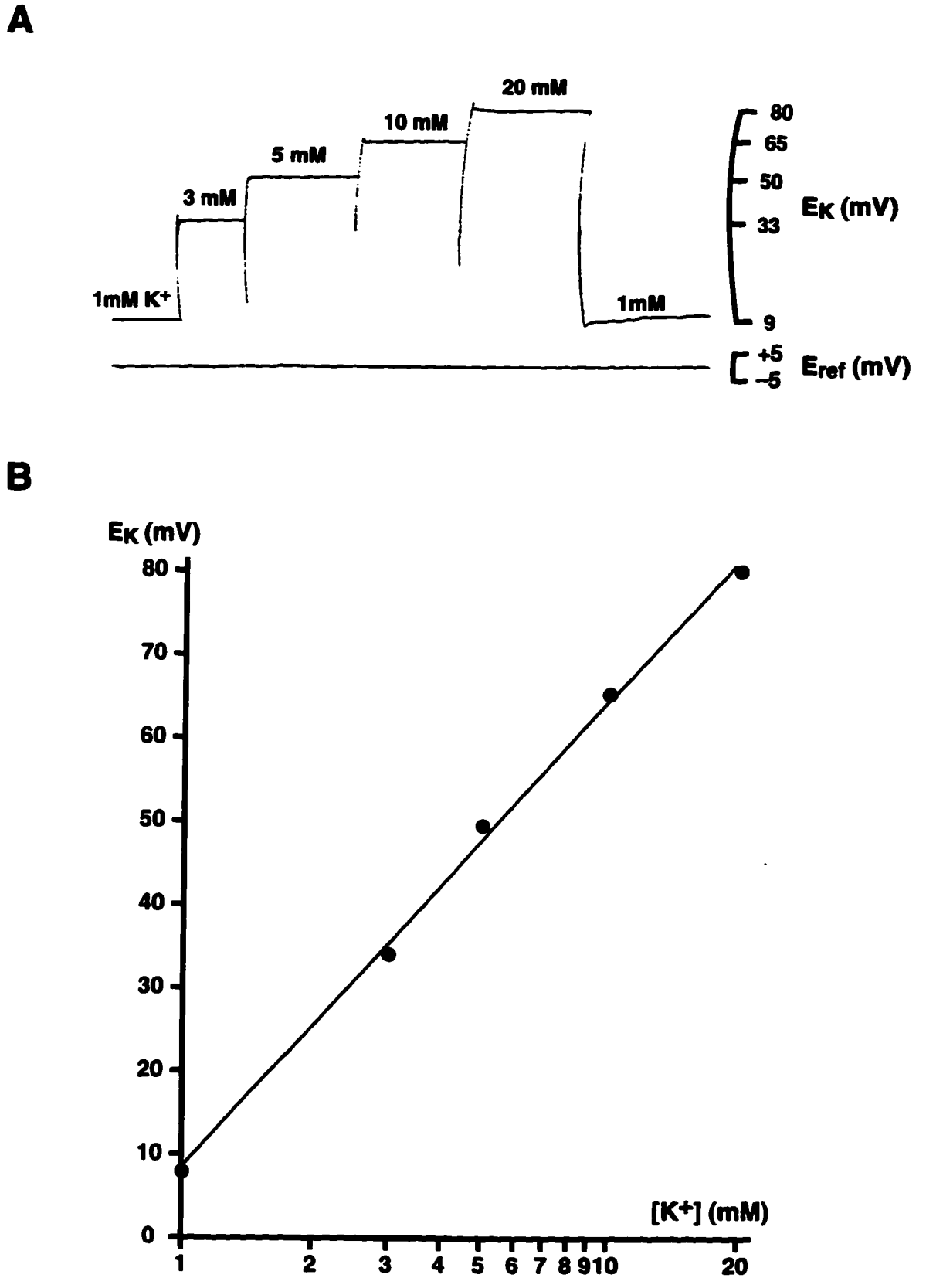
A
20 mM
10 mM
5 mM
3 mM
1mM K+
1mM
80
65
50
33
9
EK (mV)
+5
–5
Eref (mV)
B
EK (mV)
80
70
60
50
40
30
20
10
0
[K+] (mM)
1
2
3
4
5
6
7
8
9
10
20

Figure 7

Figure 8. Input resistance of neocortical pyramidal neurons. (A) V-I curve of a neocortical neuron, obtained by plotting the voltage deflections measured while injecting current pulses between – 0.4 nA and + 0.5 nA through the recording microelectrode. Note the anomalous (inward) rectification (present in most of these neurons), represented by the non-linear portion of the curve (arrow) and produced by disproportionately increased voltage responses to stronger depolarizing pulses in the subthreshold range for AP. (B) Records of R_N measurement trial from the same cell as in A, obtained by superimposition of the voltage deflections (lower traces) obtained in response to the corresponding current pulses (upper traces). (C) Anomalous rectification illustrated here as short traces showing increased input resistance (R_N) with membrane depolarization (downward deflections represent responses to – 0.2 nA pulses of hyperpolarizing current.) Note pronounced anomalous rectification in the neuron from the top panel, compared to minimal rectification in the neuron at bottom.

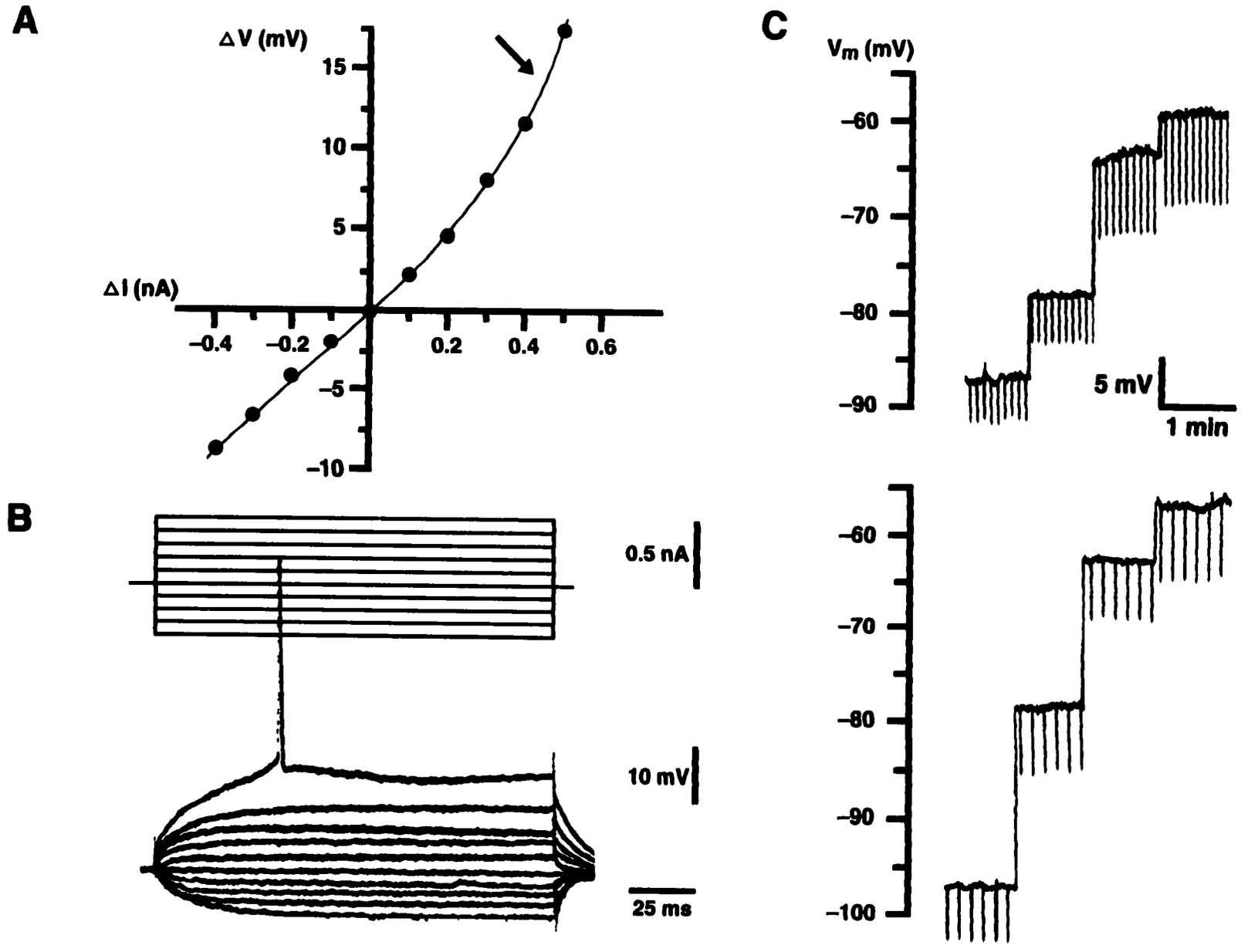
A
ΔV (mV)
15
10
5
ΔI (nA)
-0.4
-0.2
0.2
0.4
0.6
-5
-10
B
0.5 nA
10 mV
25 ms
C
Vm (mV)
-60
-70
-80
-90
5 mV
1 min
-60
-70
-80
-90
-100

Figure 8

Figure 9. Neocortical excitatory postsynaptic potentials (layer IV stimulation). Evolution of early (e) and late (l) EPSPs with increasing stimulus strength in 2 different neurons. (A) Graded increase in amplitude of *e* and *l* EPSPs and decrease in latency of the *l* EPSP. The *l* EPSP disappeared for stimuli > 0.85 T; as defined, the *e* EPSP evoked an AP at 1.0 threshold (T). Note late hyperpolarization [slow inhibitory postsynaptic potential (*s* IPSP)]—dotted lines—for stimuli ≥ 0.75 T and the initial steep descending slope of the EPSP (reversed fast IPSP) at 0.9 and 1.0 T stimuli. (B) Neuron that showed little increase in *e* EPSP amplitude, a large increase in amplitude with minimal change in latency of the *l* EPSP, and absence of IPSP for stimuli ≤ 1.0 T. In contrast to the cell in A, the AP was elicited by the *l* EPSP. Calibration for both A and B is shown in B.

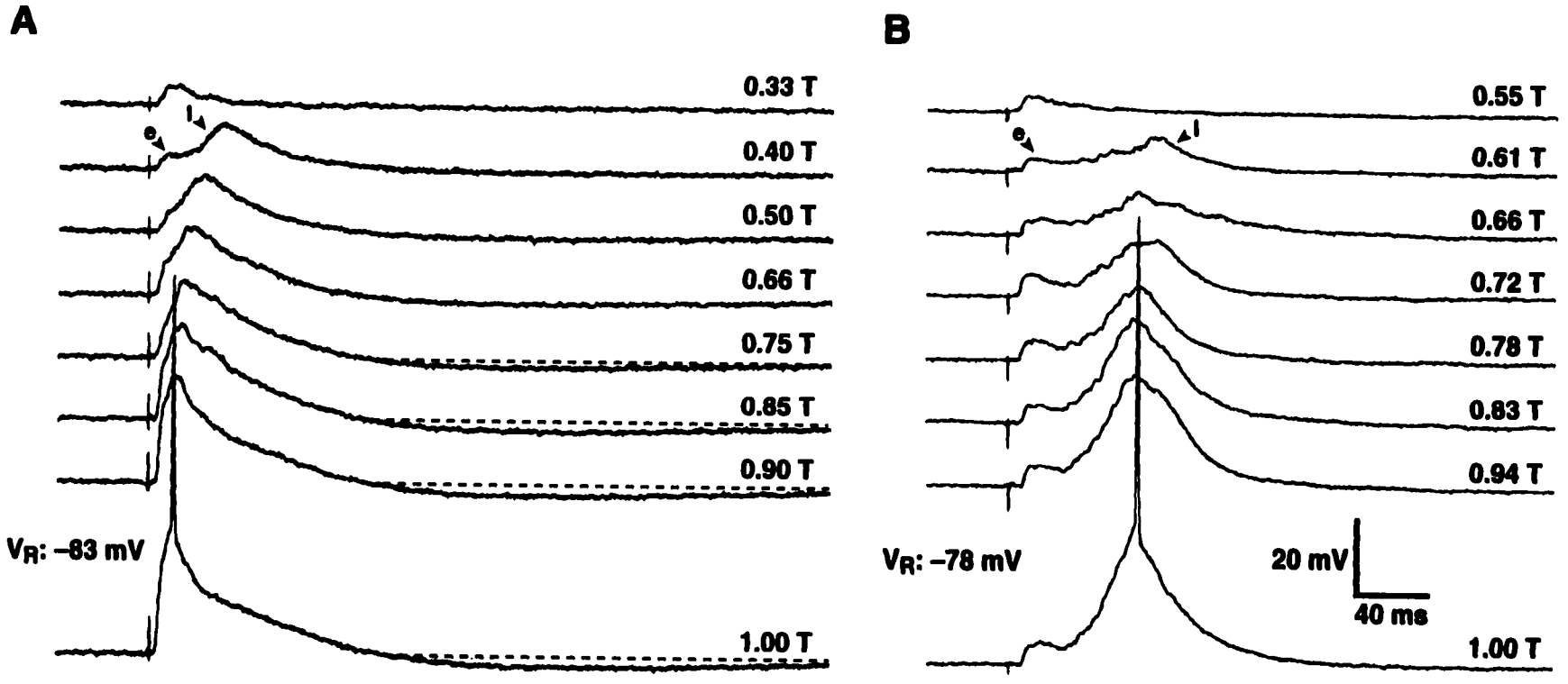
A
0.33 T
e
I
0.40 T
0.50 T
0.66 T
0.75 T
0.85 T
0.90 T
V_R: –83 mV
1.00 T
B
0.55 T
e
I
0.61 T
0.66 T
0.72 T
0.78 T
0.83 T
0.94 T
V_R: –78 mV
20 mV
40 ms
1.00 T

Figure 9

Figure 10. NMDA-dependence of the late EPSP. Superimposed traces showing the early and late components of the EPSP in control ACSF and after 2 min superfusion with the specific NMDA receptor antagonist DL-2-amino-5 phosphonovaleric acid (DL-APV) (50 μM). Note disappearance of the *l* EPSP and preservation of the *e* EPSP.

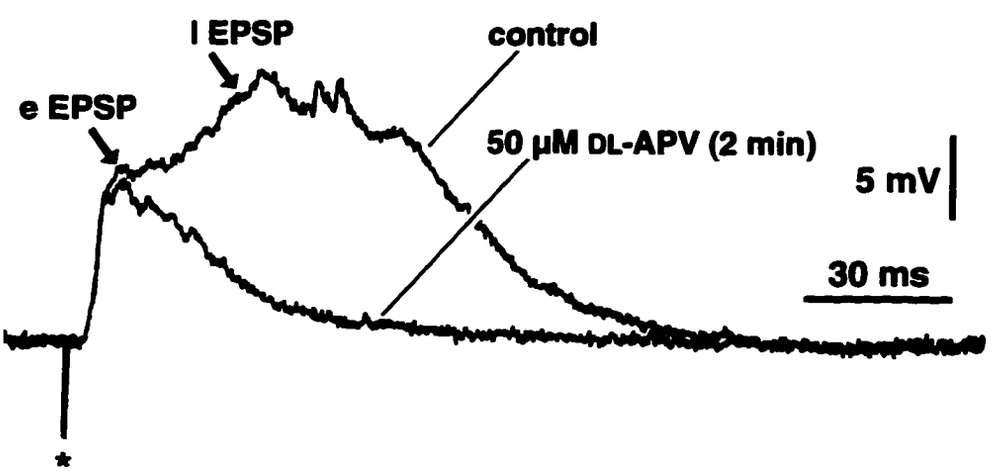

Figure 10

Figure 11. Neocortical inhibitory postsynaptic potentials. (A) Superimposed synaptic responses evoked by layer IV stimulation, recorded at resting membrane potential (V_R) (– 88 mV) and during a 500 ms, 1.5 nA depolarizing pulse to – 58 mV . (B) Illustration of current monitor traces. Note that at – 58 mV (dotted horizontal line) in A, the fast IPSP (f), which corresponds to the steep descending phase of the EPSP as recorded at V_R, became hyperpolarizing. At – 58 mV, the slow IPSP (s) appeared as an ample, prolonged hyperpolarizing event that reversed near V_R.

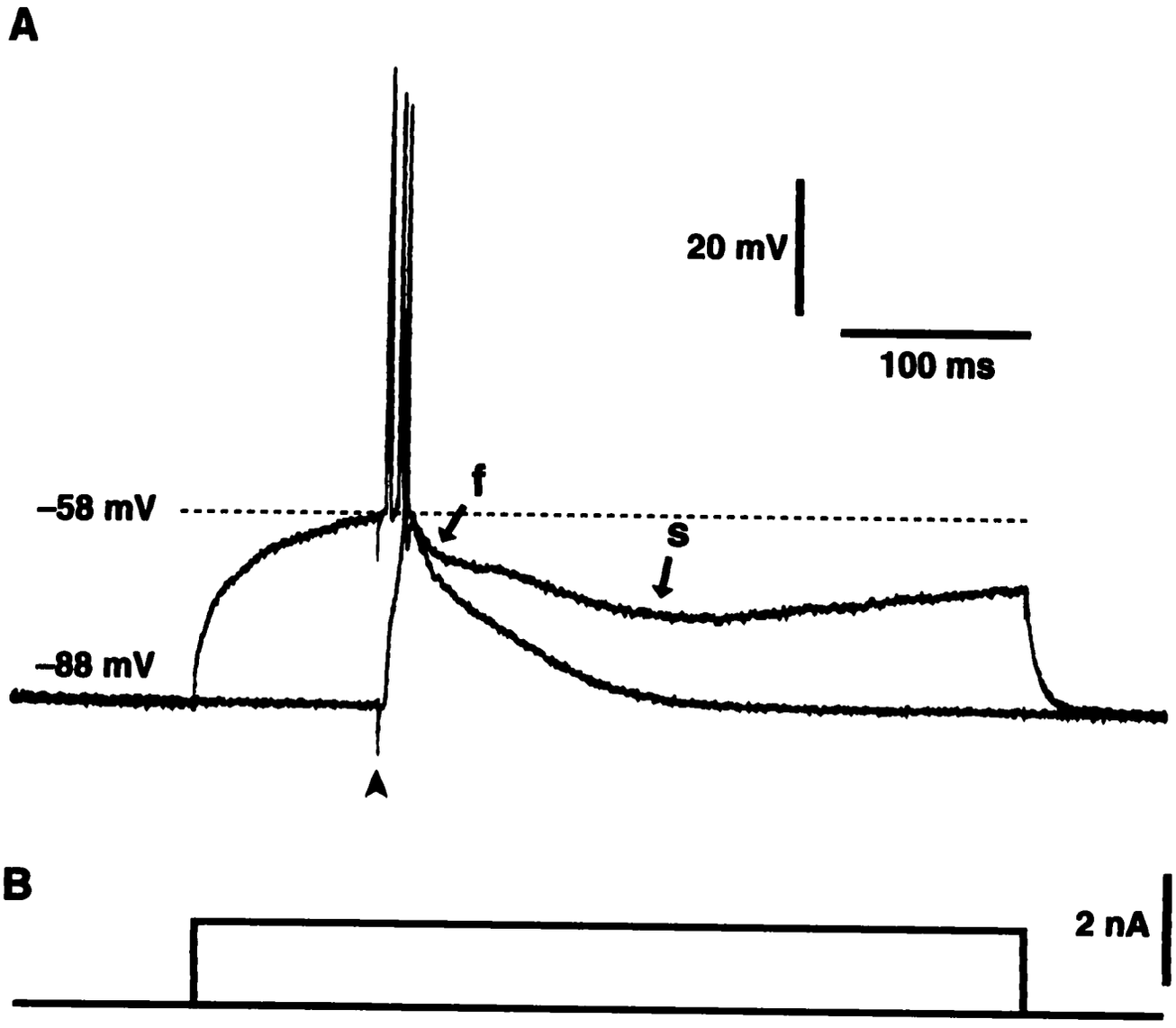

Figure 11

Figure 12. Effects of picrotoxin and phaclofen on neocortical IPSP. Each panel shows orthodromic responses to two sequential stimuli: lower trace at V_R, and upper trace during intracellular injection of depolarizing current (I_D). (A) Effect of the $GABA_A$ antagonist, picrotoxin (PTX) (100 μM) on the fast IPSP (f) (single arrowhead). At 3 min exposure to PTX (middle panel), the *f* IPSP was abolished, the cell responded with a bursting response and the *s* IPSP became more prominent (arrows). At 7 min PTX exposure, the initial part of the prolonged *s* IPSP was obscured by a multispiked paroxysmal depolarizing shift (double arrowhead). The *f* IPSP recovered after re-incubation in control ACSF for 10 min (not shown). (B) Effect of the $GABA_B$ antagonist phaclofen (0.5 mM) on the *s* IPSP (s). After 20 min exposure to phaclofen, the *s* IPSP was completely abolished, whereas the fast IPSP (f) remained intact. The *s* IPSP recovered after 8 min re-incubation in control ACSF (not shown). All panels show superimposition of orthodromic responses evoked during application of depolarizing pulses (**) of 0.6 nA, 500 ms (only initial portion shown, current traces not shown), on responses to pulses alone (*).

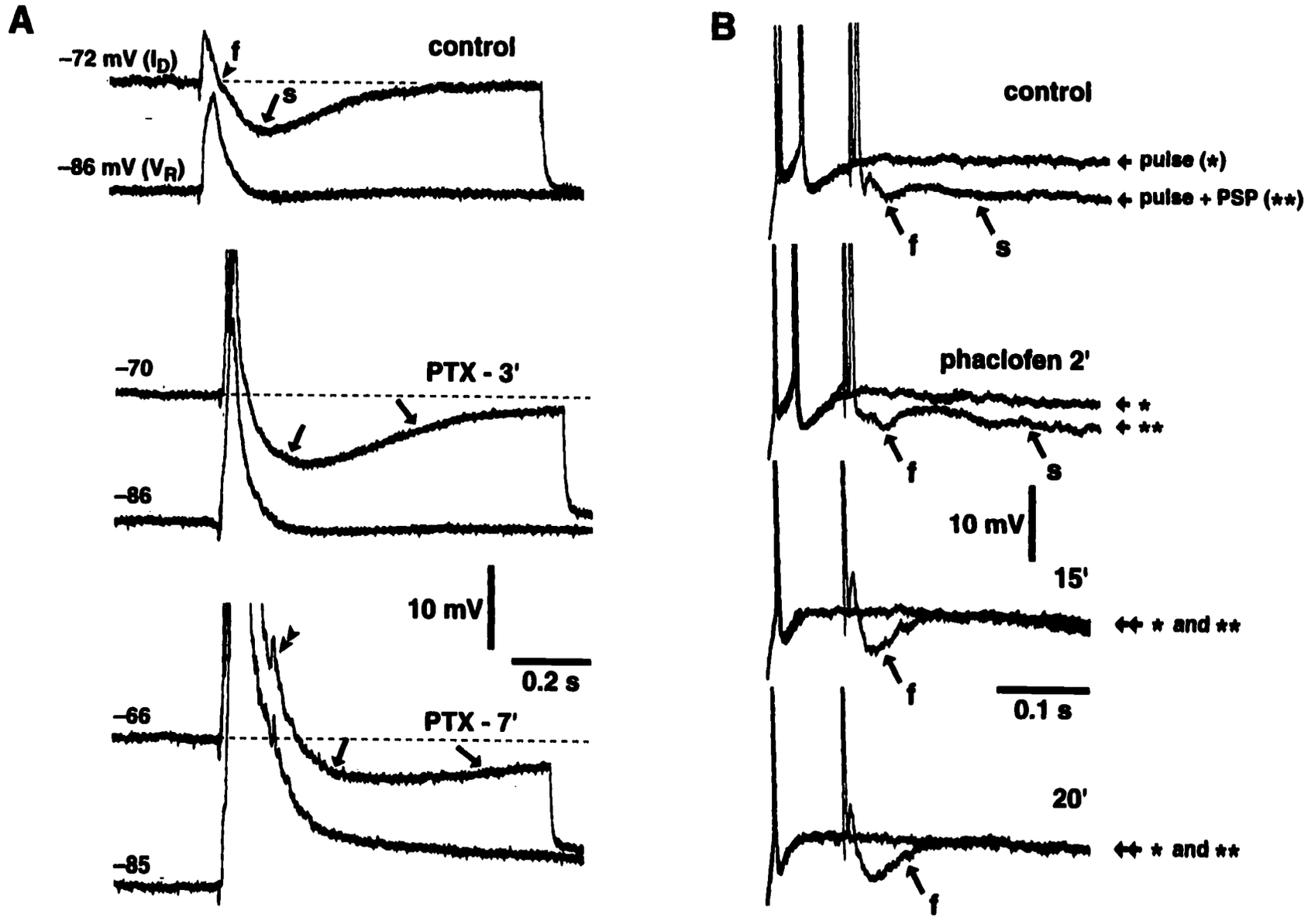
A
–72 mV (I_D)
f
control
s
–86 mV (V_R)
–70
PTX - 3'
–86
10 mV
0.2 s
–66
PTX - 7'
–85
B
control
pulse (*)
pulse + PSP (**)
f
s
phaclofen 2'
*
**
f
s
10 mV
15'
* and **
f
0.1 s
20'
* and **
f

Figure 12

Figure 13. Anoxic depolarization and changes in R_N. (A)–(B) Anoxic-evoked depolarization (AD) in two neocortical neurons produced by brief N_2 exposure. Hyperpolarizing pulses (0.2 nA—not shown) were injected throughout the recording to monitor R_N. AD was initiated at ≈ 1 min after N_2 exposure, when tissue O_2 levels (monitored with an O_2-sensitive microelectrode) were close to zero (dashed vertical line in A). In some cells, during recovery, AD was followed by postanoxic hyperpolarization (PAH in B). (C)–(D) In this cell, control R_N (●) decreased by 24% during anoxia (○). During recovery (▲) a transient small increase in R_N was observed. (C) A decrease in R_N during anoxia resulted in an elevation of the rheobase and a higher depolarizing pulse was necessary to elicit a single action potential (D). The rheobase recovered during reoxygenation (not shown).

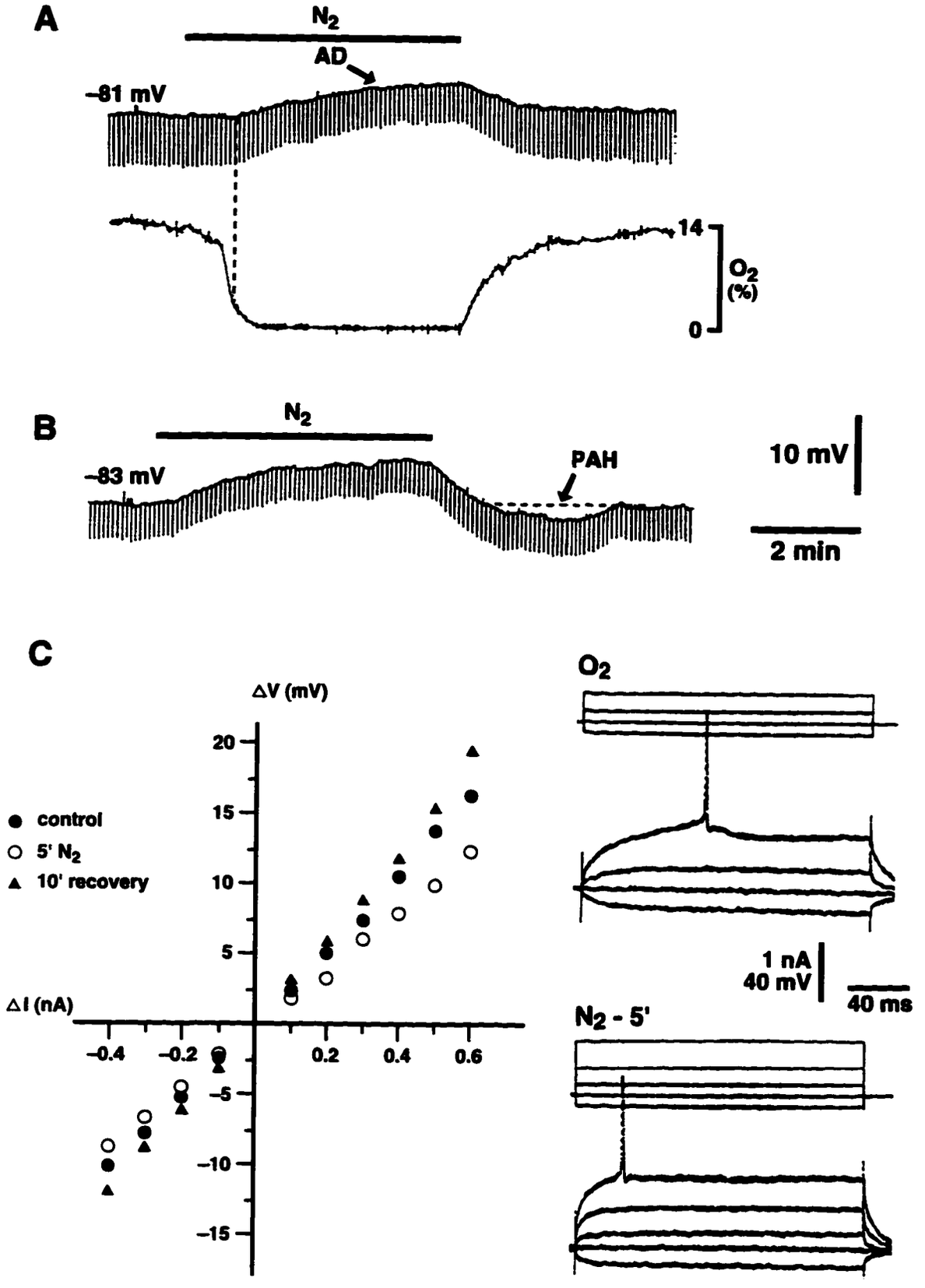
A
N2
AD
-81 mV
14
O2
(%)
0
B
N2
-83 mV
PAH
10 mV
2 min
C
ΔV (mV)
20
15
10
5
control
5' N2
10' recovery
ΔI (nA)
-0.4
-0.2
0.2
0.4
0.6
-5
-10
-15
O2
1 nA
40 mV
40 ms
N2 - 5'

Figure 13

Figure 14. E_{REV} of the anoxic depolarization (AD). For each of the 5 neurons illustrated here with different symbols, the plateau AD amplitude was measured from various starting membrane potentials (V_m), including V_R (for all 5 cells around – 80 mV—arrow) as well as during various amounts of steadily injected depolarizing/hyperpolarizing current; AD was plotted as a function of V_m. Note that in some cells AD amplitude increased in the – 70 to – 60 mV range of V_m; this corresponded to a pronounced anomalous (inward) rectification present in these neurons in this voltage range (see Fig. 8). The reversal potential of AD (E_{REV}), extrapolated from the straight portion of each plot (dotted lines) was approximately – 40 mV.

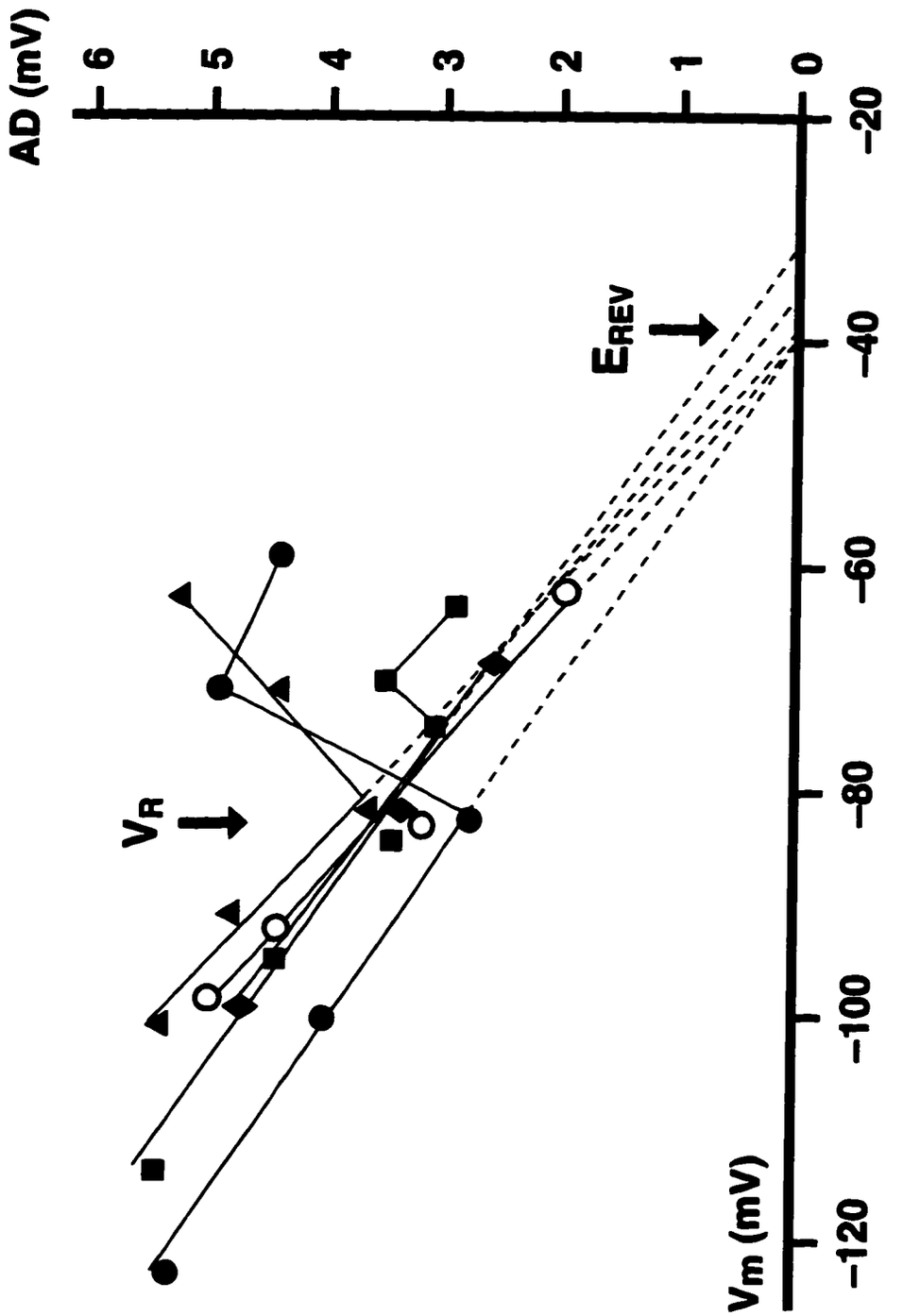

Figure 14

Figure 15. Effects of $[Na^+]_o$ replacement on the anoxic depolarization. Slice superfusion for 60 min with low-Na^+ ACSF (created by replacement of NaCl —corresponding to ≈ 72% of total $[Na^+]$—with an equimolar concentration of choline chloride) resulted in a significant reduction of the amplitude of AD (by 40% at 40 min exposure—mid trace, and by 77% at 60 min exposure—lower trace). In the upper trace, PSPs were continuously evoked at 0.1 Hz (upward voltage deflections), whereas in the mid- and lower traces, hyperpolarizing current pulses (0.2 nA at 0.2 Hz and 0.1 Hz, respectively) were continuously injected to monitor R_N (downward voltage deflections). Note also progressive decrease in amplitude of PAH, as $[Na^+]_o$ decreased. V_R of this neuron was – 76 mV.

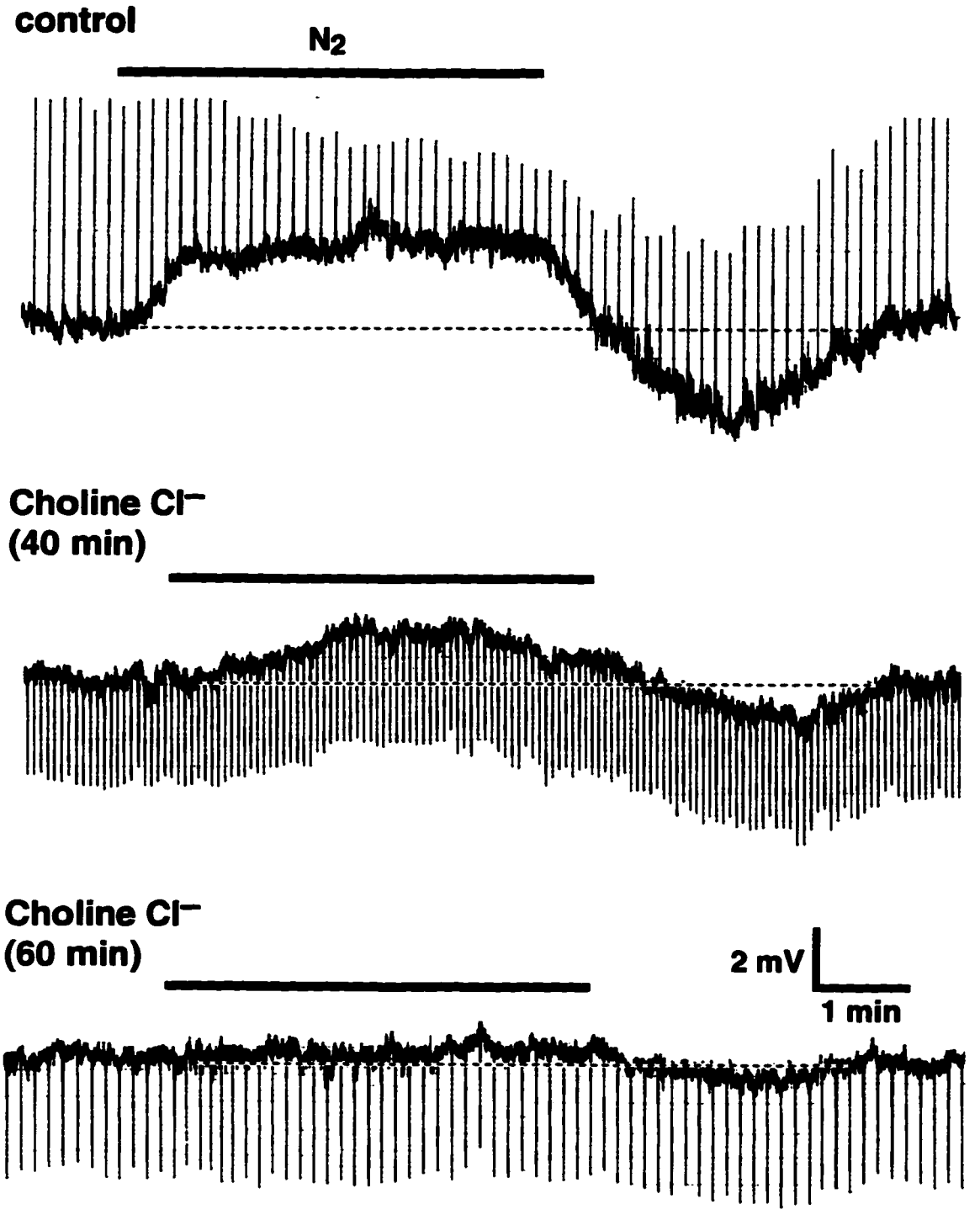

Figure 15

Figure 16. Effects of the Na^+ channel blocker, tetrodotoxin (TTX) on the anoxic depolarization. (A) Pre-treatment of the slice with 1 μM TTX for 10 min reduced the amplitude of AD by about 50%. (B) Change in E_{REV} of AD in another slice exposed to 1 μM TTX. Note the occurrence of anoxic hyperpolarization at V_m levels of – 57 and – 48 mV. The AD remaining in the presence of TTX at V_R (– 87 mV) had an estimated E_{REV} of – 65 mV. (Compare this value to the ≈ – 40 mV obtain in control ACSF—see Fig. 14).

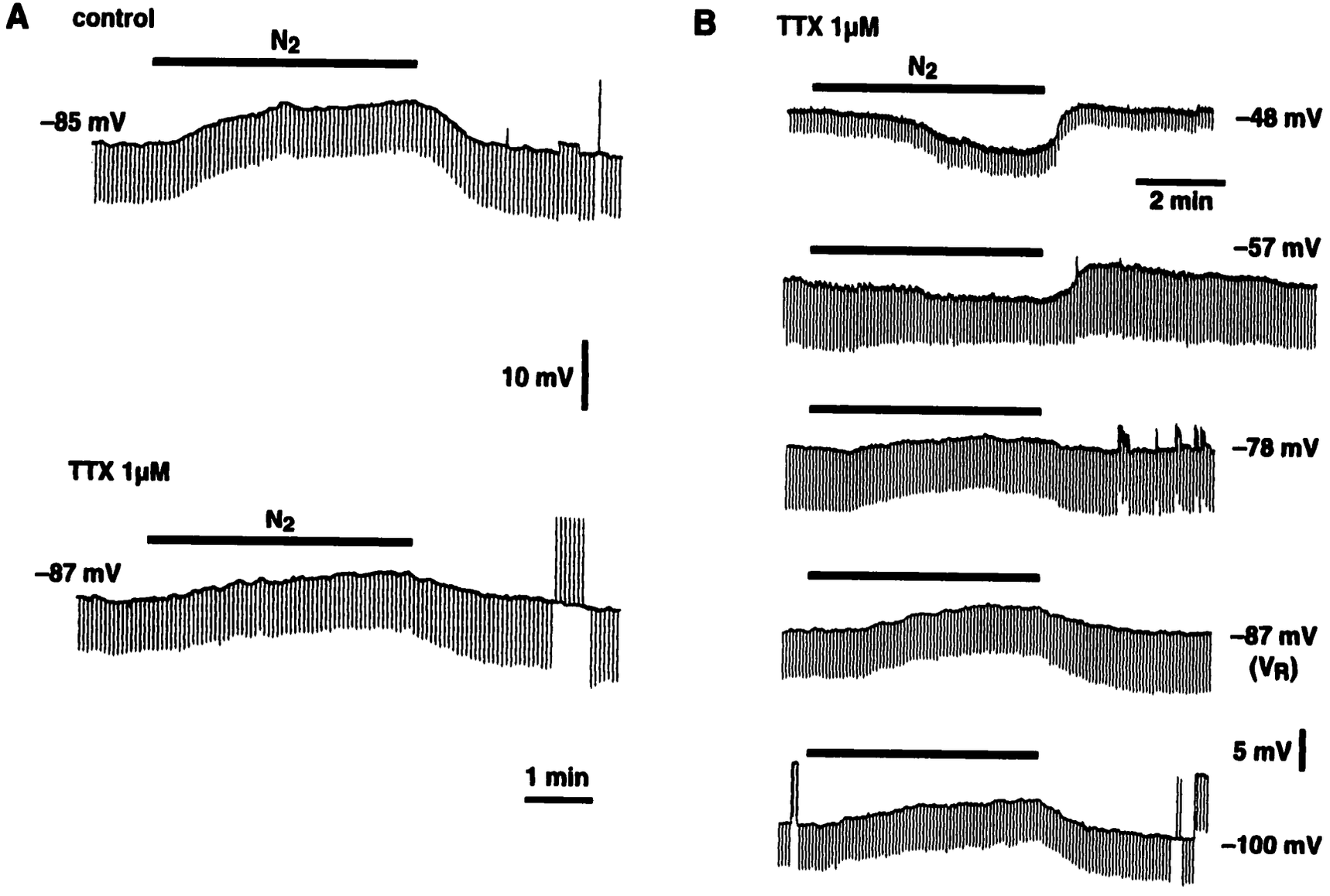
A
control
N2
–85 mV
10 mV
TTX 1μM
N2
–87 mV
1 min
B
TTX 1μM
N2
–48 mV
2 min
–57 mV
–78 mV
–87 mV
(VR)
5 mV
–100 mV

Figure 16

Figure 17. Effects of $[Ca^{2+}]_o$ influx blockade on anoxic depolarization. Succesive anoxic trials performed in the same neuron in control ACSF (upper trace), after 15 min exposure to a Ca^{2+}-free ACSF containing 2.3 mM $MnSO_4$ (middle trace), and after 20 min recovery in normal ACSF (lower trace). During the entire experiment, continuous orthodromic stimulation (0.05 Hz) was applied in layer IV (upward voltage deflections in upper and lower traces represent EPSPs). Note that abolishing Ca^{2+} influx through voltage dependent-channels (through the combined action of very low $[Ca^{2+}]_o$ and Mn^{2+}-induced channel blockade) resulted in complete blockade of EPSPs, but rather increased than diminished the amplitude of AD (middle trace).

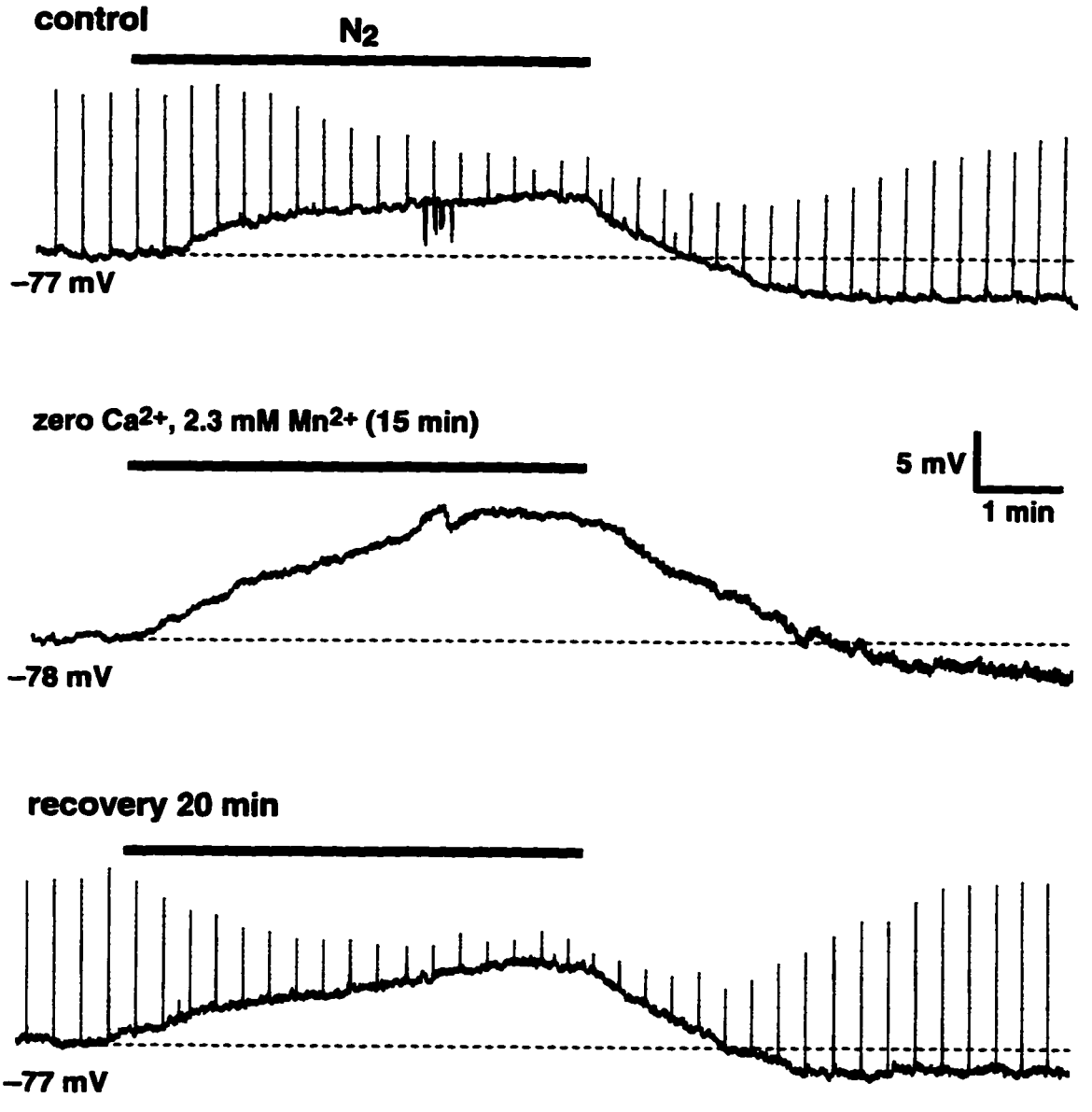
control
N_2
–77 mV
zero Ca^{2+}, 2.3 mM Mn^{2+} (15 min)
5 mV
1 min
–78 mV
recovery 20 min
–77 mV

Figure 17

Figure 18. $[K^+]_o$ changes during anoxic exposure. (A) Upper trace—continuous recording of E_K changes during a 5 min anoxic episode. At the recording site (100 μm depth), the control level of $[K^+]_o$, as plotted from the calibration curve of the K^+-sensitive microelectrode (see C), was 3.7 mM. At peak of anoxia, $[K^+]_o$ reached 4.8 mM, for a total increase of 1.1 mM. Note slight undershoot of E_K during early re-oxygenation (dotted line). Lower trace—recording of the extracellular potential, obtained from the reference barrel of the microelectrode. (B) First calibration (i.e. before the experiment—upper panel), and last calibration (after the experiment—lower panel) of the K^+-sensitive microelectrode used to record the traces in (A). In each panel, the upper trace represents the response of the ion-sensitive barrel and the lower trace represents the response of the reference barrel of the microelectrode. (C) Plot of the superimposed calibration curves for the two calibration runs showed in (B). (Valinomycin microelectrode, 12 μm tip diameter, resistance of the reference barrel: 2.7 MΩ .)

Note: Calibrations were recorded on the Grass polygraph—note curvilinear scale in (C), whereas K^+ measurements in the slice were recorded on the Gould chart recorder—note straight scales in (A).

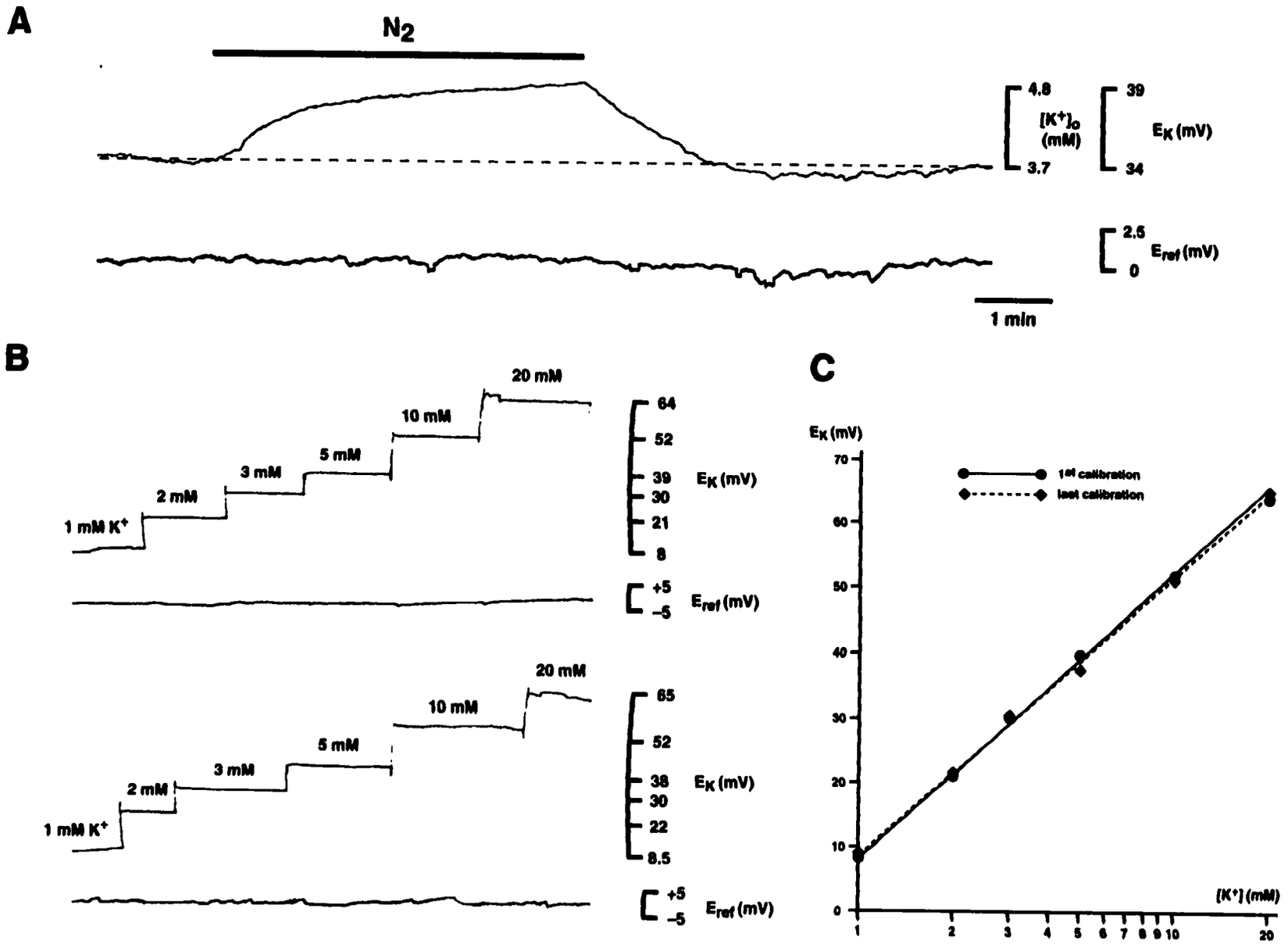
A
N2
4.8
[K+]o
(mM)
3.7
39
EK (mV)
34
2.5
Eref (mV)
0
1 min
B
20 mM
10 mM
5 mM
3 mM
2 mM
1 mM K+
64
52
39
30
21
8
EK (mV)
+5
–5
Eref (mV)
20 mM
10 mM
5 mM
3 mM
2 mM
1 mM K+
65
52
38
30
22
8.5
EK (mV)
+5
–5
Eref (mV)
C
EK (mV)
70
60
50
40
30
20
10
0
1st calibration
last calibration
[K+] (mM)
1
2
3
4
5
6
7
8
9
10
20

Figure 18

Figure 19. Effects of ouabain on the anoxic depolarization. (A)–(C) The depolarization elicited by 5 μM ouabain (B) was similar to that seen in the same cell during anoxia (A), although PAH was less prominent (arrows). Effects of anoxia and ouabain were additive (C).

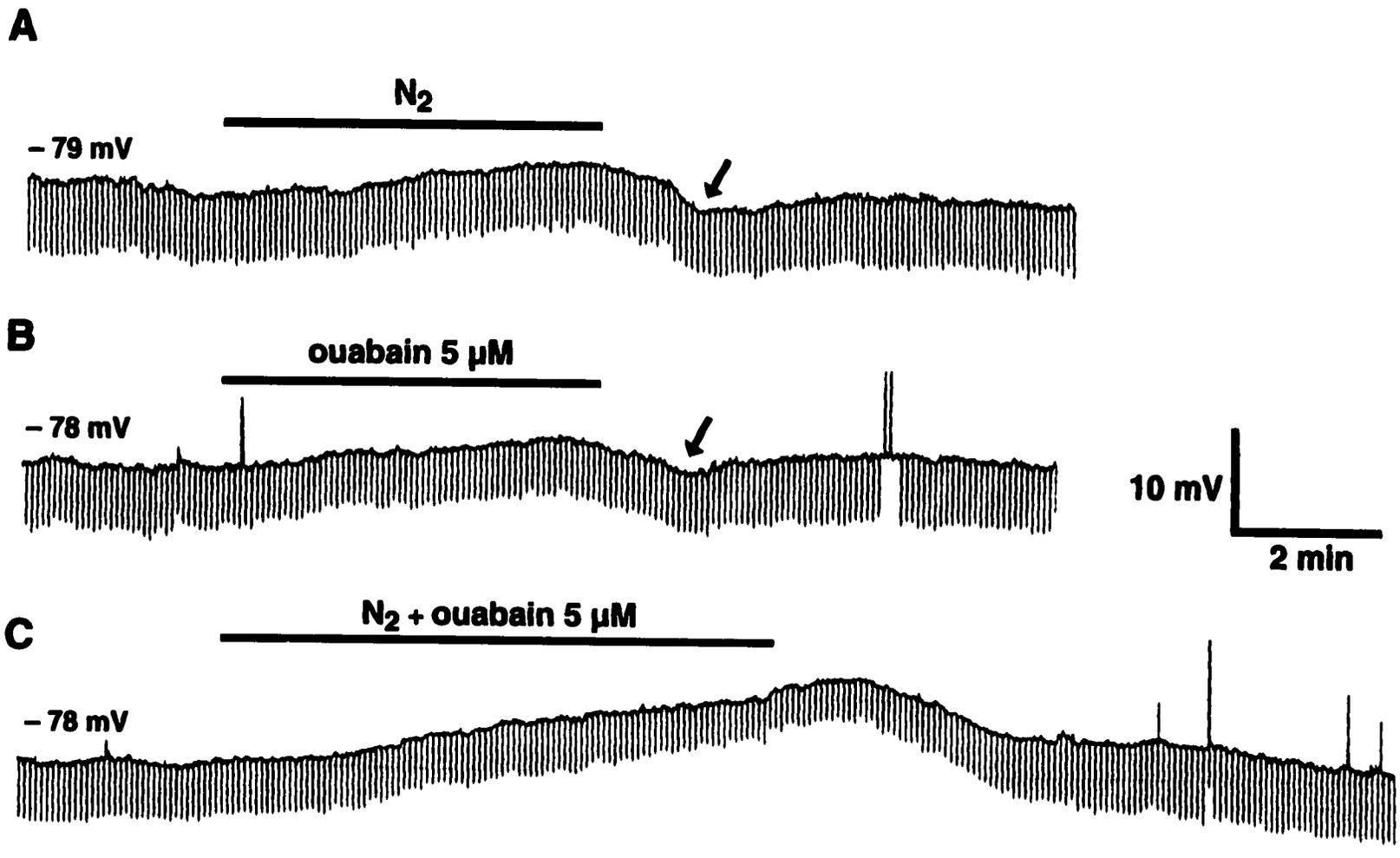

Figure 19

Figure 20. Effects of $[Cl^-]_o$ replacement on the anoxic depolarization. Slice superfusion for 35 min with low-Cl^- ACSF (created by replacement of NaCl —corresponding to almost 95% of total $[Cl^-]$—with an equimolar concentration of Na-methane sulphonate—NaMS), resulted in this neuron in a 18% increase of the amplitude of AD. Downward voltage deflections represent responses of V_m to hyperpolarizing current pulses (0.2 nA at 0.2 Hz), continuously injected to monitor R_N.

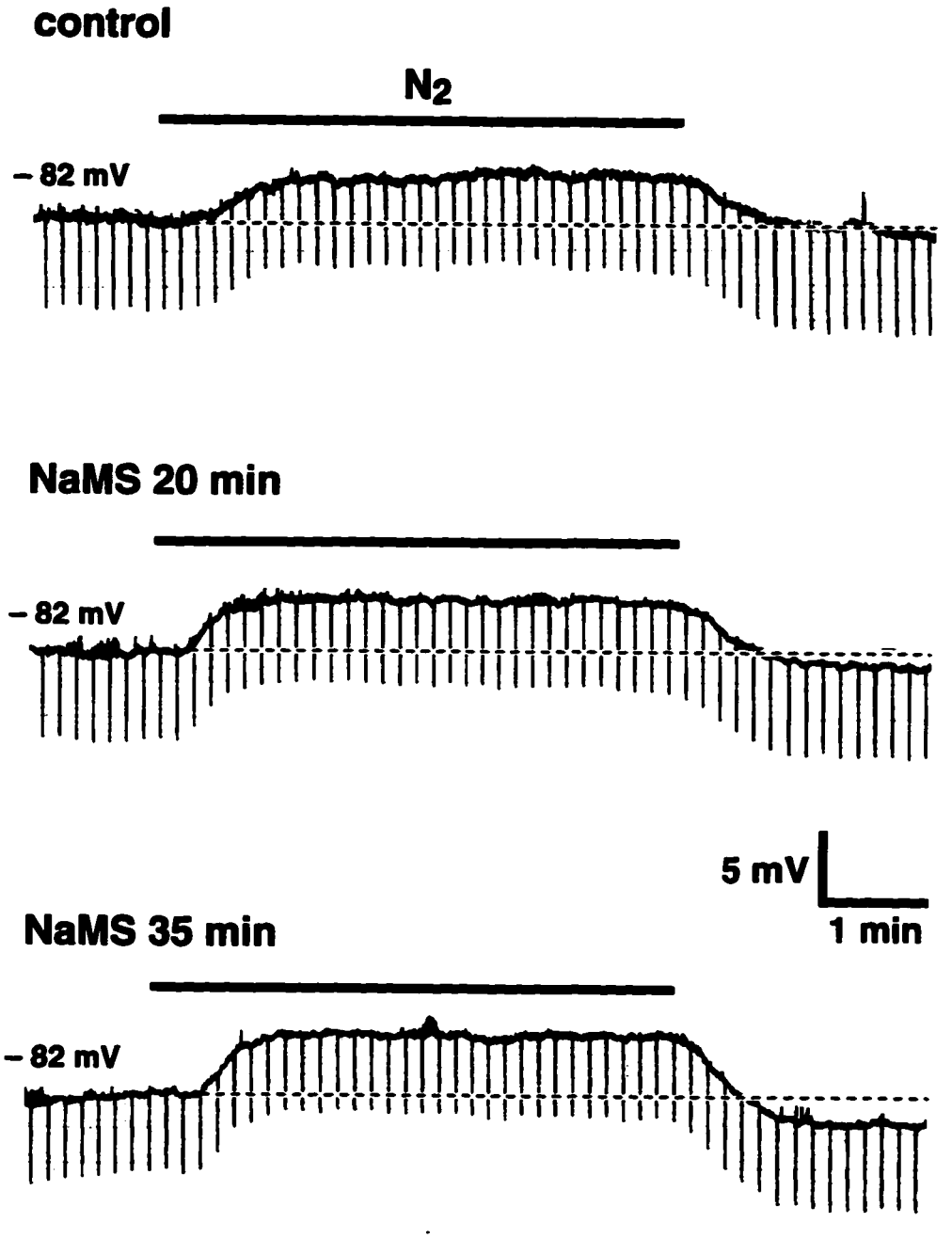

Figure 20

Figure 21. Effects of excitatory amino acid (EAA) receptor antagonists on anoxic depolarization (1). Succesive anoxic trials performed in the same neuron in control conditions (upper trace), after a 20 min exposure to 1 mM kynurenic acid (KYN—middle trace), and after 15 min washout of KYN (lower trace). Downward voltage deflections represent responses to hyperpolarizing pulses (– 0.2 mV), injected into the cell to monitor R_N. Note reduction in AD amplitude by 59% during exposure to KYN. V_R of the neuron was – 81 mV . Calibration bars refer to all traces.

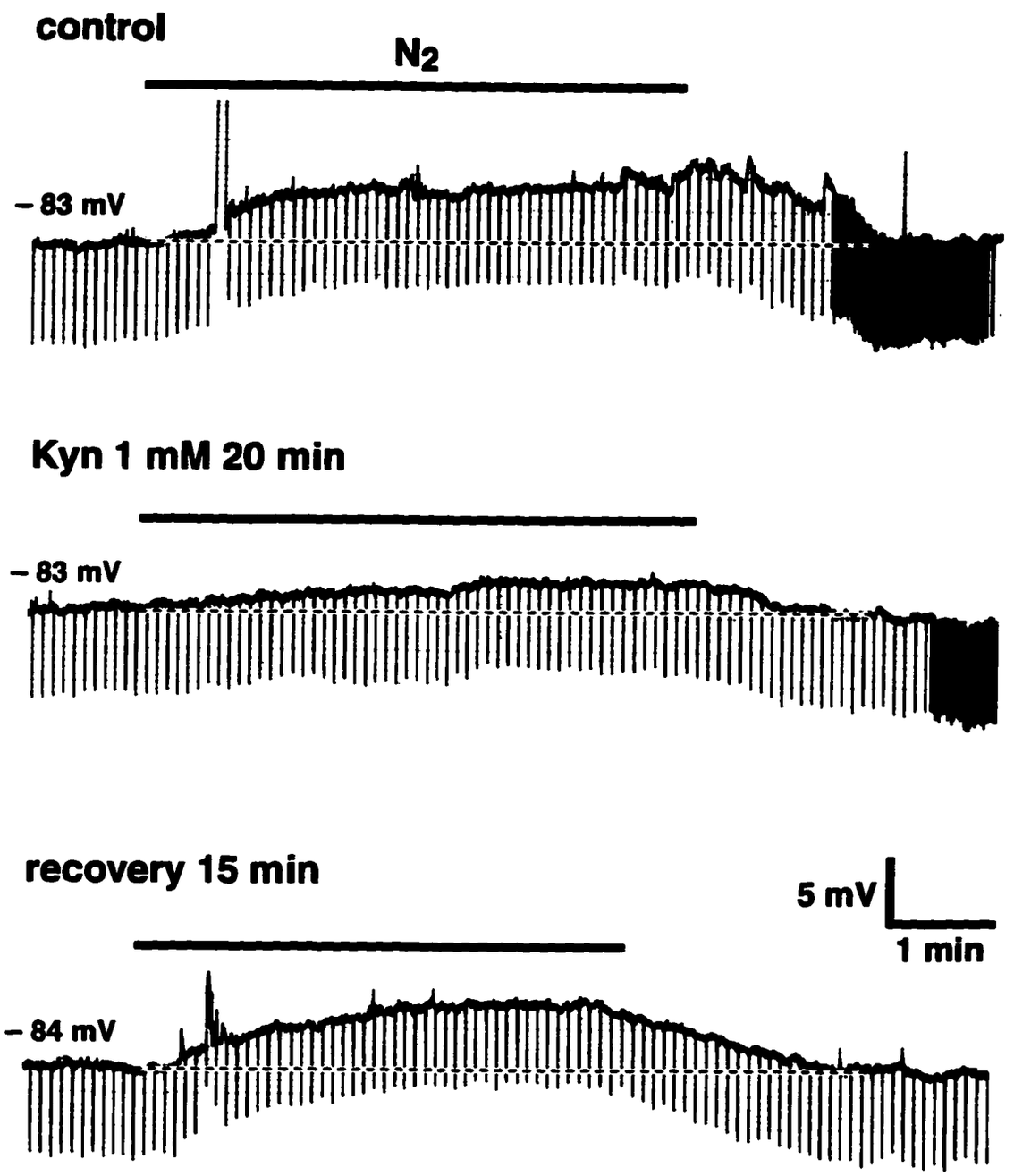
control
N2
– 83 mV
Kyn 1 mM 20 min
– 83 mV
recovery 15 min
5 mV
1 min
– 84 mV

Figure 21

Figure 22. Effects of excitatory amino acid (EAA) receptor antagonists on anoxic depolarization. (2) (A) Lack of effect of the specific NMDA receptor antagonist, DL-2-amino-5 phosphonovaleric acid (DL-APV) on AD. Although DL-APV (50 μM) was effective in blocking the *l* EPSP in a few minutes (see Fig. 10), it did not have any influence on the amplitude of AD even at 1h of exposure to high concentration (200 μM). (B) Lack of effect of the specific metabotropic receptor antagonist, (+)-methyl-4-carboxyphenyl-glycine (MCPG) on AD. Superfusion of the slice with 1mM MCPG did not affect the amplitude and course of AD. (C) Recordings from a different neuron, showing that the effect on AD of 1mM KYN did not change when 1 mM MCPG was added to the superfusing ACSF. Calibration for all traces is shown in (C).

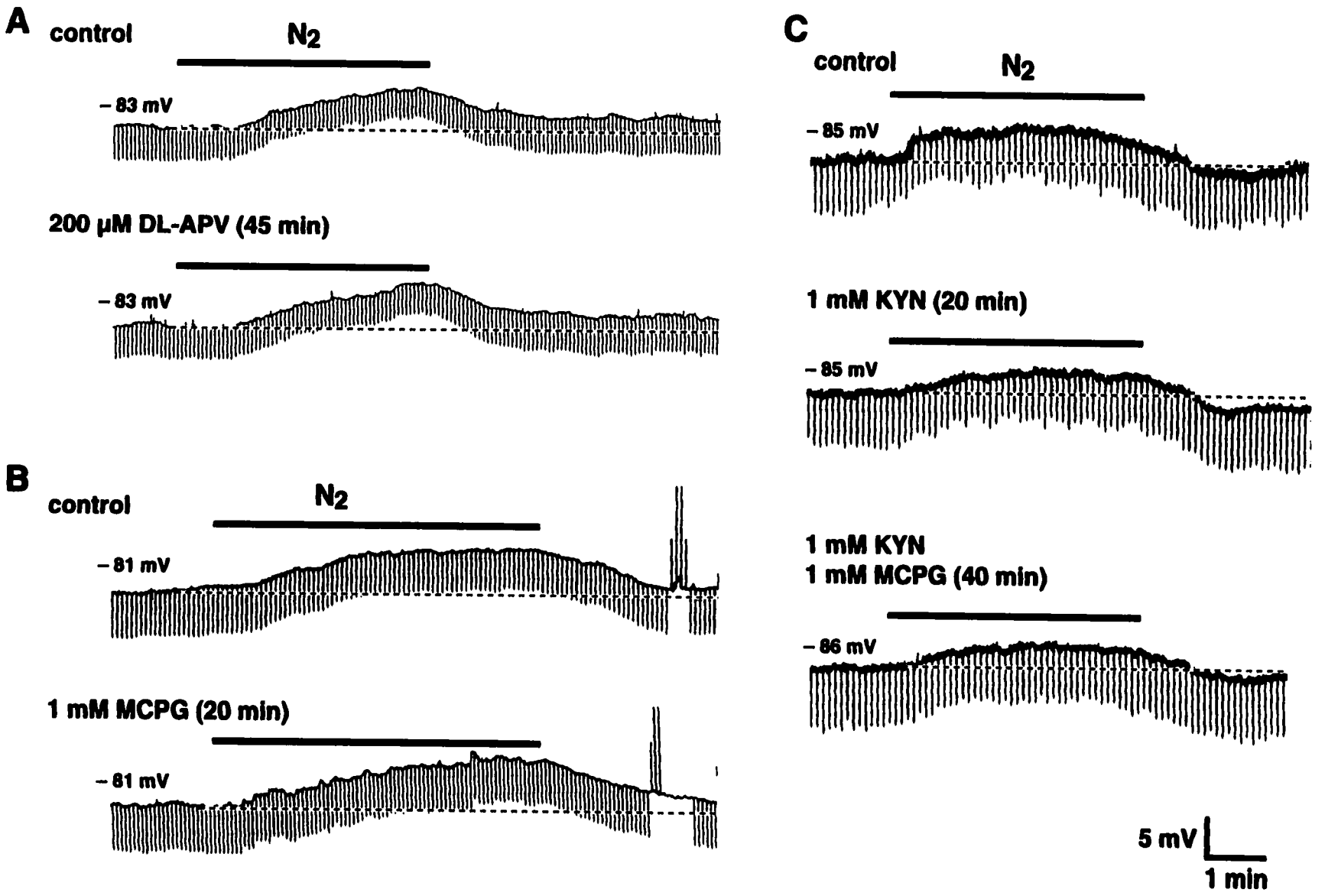
A
control
N2
– 83 mV
200 µM DL-APV (45 min)
– 83 mV
B
control
N2
– 81 mV
1 mM MCPG (20 min)
– 81 mV
C
control
N2
– 85 mV
1 mM KYN (20 min)
– 85 mV
1 mM KYN
1 mM MCPG (40 min)
– 86 mV
5 mV
1 min

Figure 22

Figure 23. Anoxic depression and postanoxic recovery of neocortical EPSPs (layer IV stimulation). (A) Neuron of the type shown in Fig. 9–A; stimulus strength, 0.62 T. Exposure to N_2 (4 min) induced a decrease in *e* EPSP (e) amplitude by 43% and the disappearance of the *l* EPSP (l). The depressed *e* EPSP was recorded during a transient restoration of V_R to – 81 mV using hyperpolarizing current (I_{HP}). Note reverse sequence of events during recovery. (B) Neuron of type shown in Fig 9–B; stimulus strength, 0.83 T. The amplitude of the *e* EPSP (e) decreased by 55% at 4 min N_2 exposure, and the *l* EPSP (l) disappeared within 3 min. Note the appearance of several subcomponents of the *l* EPSP during early anoxia and especially during re-oxygenation (arrows). Calibration for both A and B is shown in B.

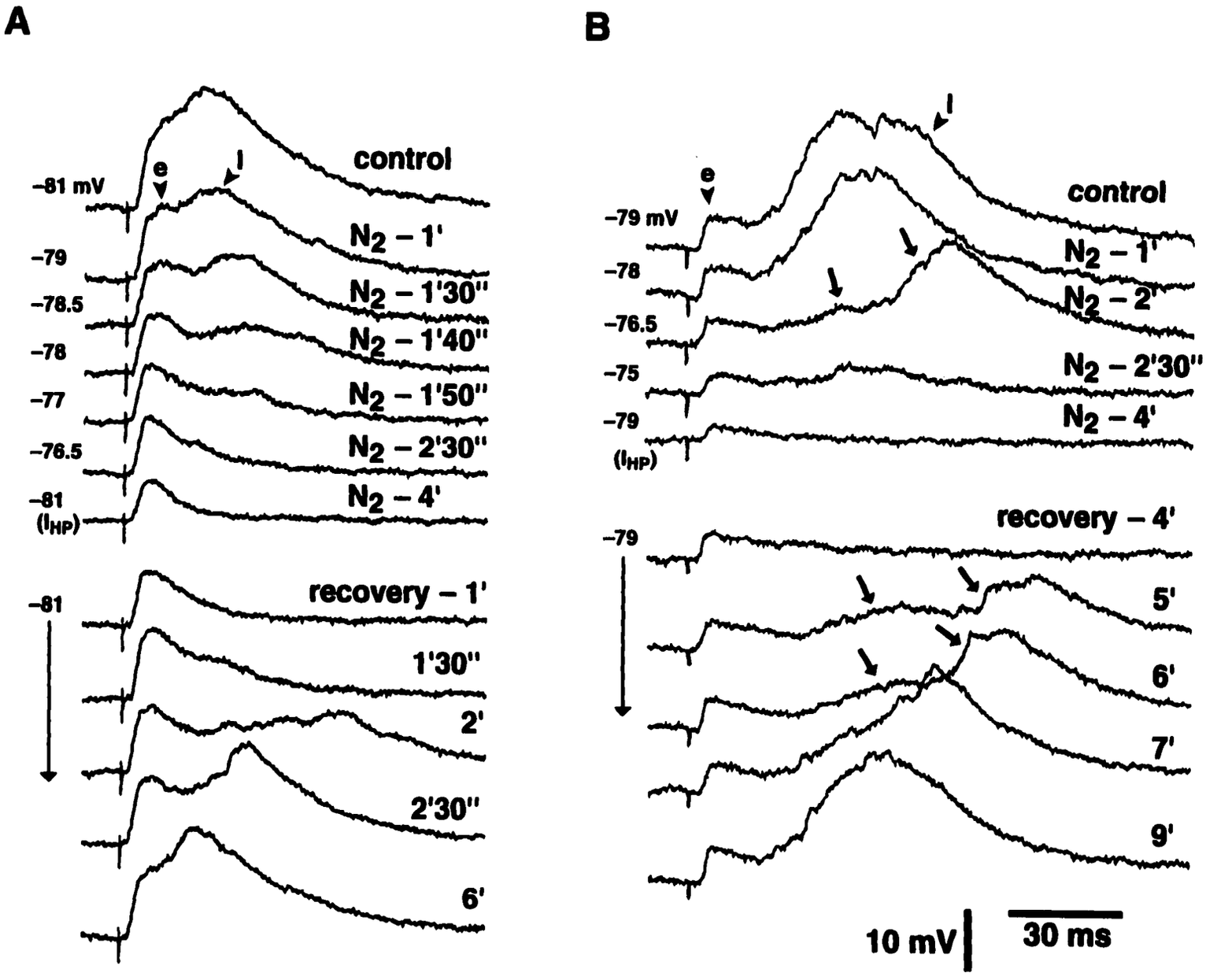
A
B
control
e
I
−81 mV
N2 – 1'
−79
N2 – 1'30"
−78.5
N2 – 1'40"
−78
N2 – 1'50"
−77
N2 – 2'30"
−76.5
N2 – 4'
−81
(IHP)
recovery – 1'
−81
1'30"
2'
2'30"
6'
−79 mV
N2 – 1'
−78
N2 – 2'
−76.5
N2 – 2'30"
−75
N2 – 4'
−79
(IHP)
recovery – 4'
−79
5'
6'
7'
9'
10 mV
30 ms

Figure 23

Figure 24. Anoxic depression and postanoxic recovery of neocortical IPSPs. (A)–(D) Recording of evoked responses in one neuron, WM stimulation; stimulus strength 1.4 T. (A) Anoxic exposure. Synaptic responses evoked during application of depolarizing pulses, superimposed on the responses to pulses alone. (Each panel shows first part of responses to 600 ms, 0.75 nA pulses.) Each EPSP was preceded by a non-synaptic AP (●) induced by the pulse of depolarizing current. Note disappearance of *f* IPSP (f), followed by that of the *s* IPSP (s). At 5 min anoxia, the only response evident was the current-induced spike and a prominent depolarizing afterpotential (arrow), which masked the depressed EPSP. (B) Recovery. By 15 min reoxygenation, the EPSP has recovered completely, whereas the IPSPs have reached ~ 90% of the control value. (C) and (D) Single synaptic responses recorded at V_R (–85 mV) during the same anoxic trial and at times close to those in (A) and (B). At ~ 5 min N_2 the EPSP was decreased by 75%. Note the slightly shallower *s* IPSP at ~ 15 min recovery, compared with control (refer to dotted line); this corresponds to the incomplete recovery seen at 15 min in (B). Calibration refers to all traces.

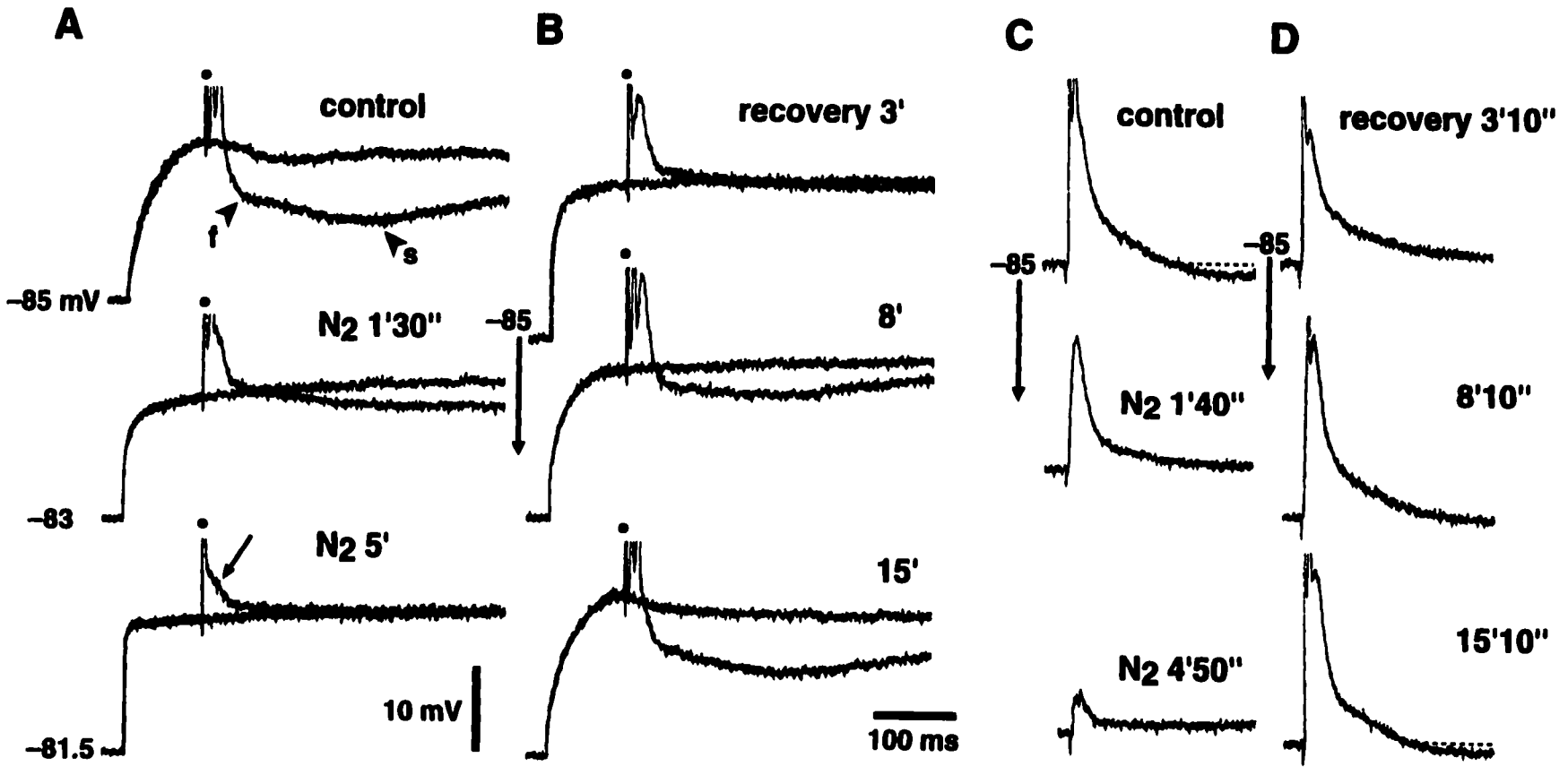
A
B
C
D
control
recovery 3'
control
recovery 3'10"
f
s
–85 mV
N2 1'30"
–85
8'
–85
8'10"
–83
N2 5'
15'
N2 1'40"
15'10"
10 mV
N2 4'50"
–81.5
100 ms

Figure 24

Figure 25. Reversal potential of s IPSP. (A)–(C) Reversal potential (E_{REV}) values of *s* IPSP in control (O_2, ○) and anoxic (N_2, ●) conditions, recorded in 3 different neurons. Note the similarity of E_{REV} values—paired for each neuron, which indicates that the IPSP depression was not an artifact due to a shift in E_{REV}.

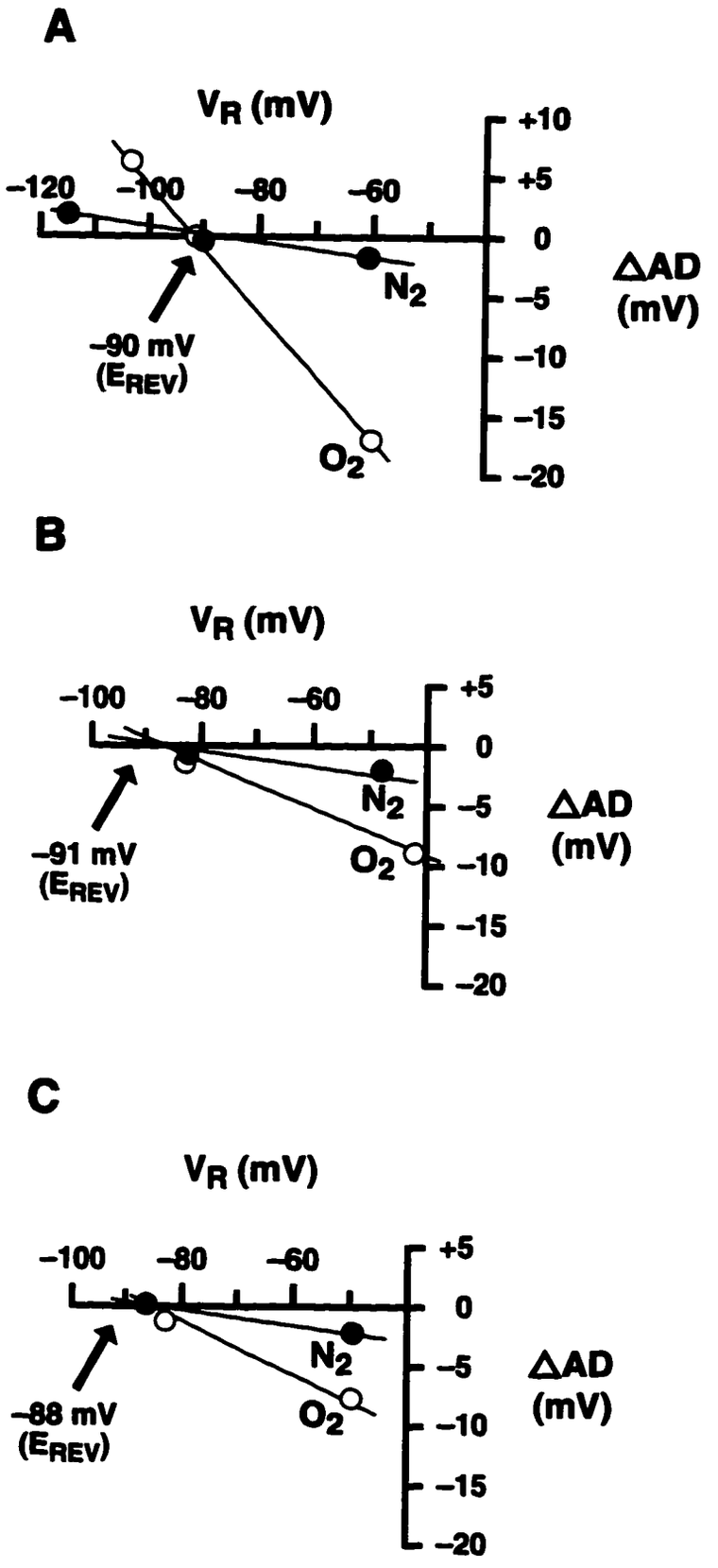
A
V_R (mV)
+10
+5
0
−5
−10
−15
−20
−120
−100
−80
−60
N_2
O_2
−90 mV
(E_{REV})
ΔAD
(mV)
B
V_R (mV)
−100
−80
−60
+5
0
−5
−10
−15
−20
N_2
O_2
−91 mV
(E_{REV})
ΔAD
(mV)
C
V_R (mV)
−100
−80
−60
+5
0
−5
−10
−15
−20
N_2
O_2
−88 mV
(E_{REV})
ΔAD
(mV)

Figure 25

Figure 26. Time course of PSP changes with anoxic exposure. (A) Changes in early (●) and late (■) EPSPs during a 5 min exposure to N_2. The *e* EPSP amplitude decreased by 70% and the *l* EPSP was abolished within < 3 min of N_2. The recovery of the *l* EPSP was delayed and still incomplete at 5 min re-oxygenation. (B) Changes in *e* EPSP (●) compared with the fast (■) and slow (❑) IPSPs in a different neuron, during a 5 min N_2 exposure; no *l* EPSP was recorded in this cell (WM stimulation). e EPSP amplitude (recorded at V_R of – 85 mV) decreased by 80%. The *f* IPSP and *s* IPSP (recorded during depolarizing pulses at V_m = – 55 mV) were abolished at 2.5 min N_2. Note the delayed recovery of both IPSPs. Dashed lines in A and B represent mean control values for each PSP.

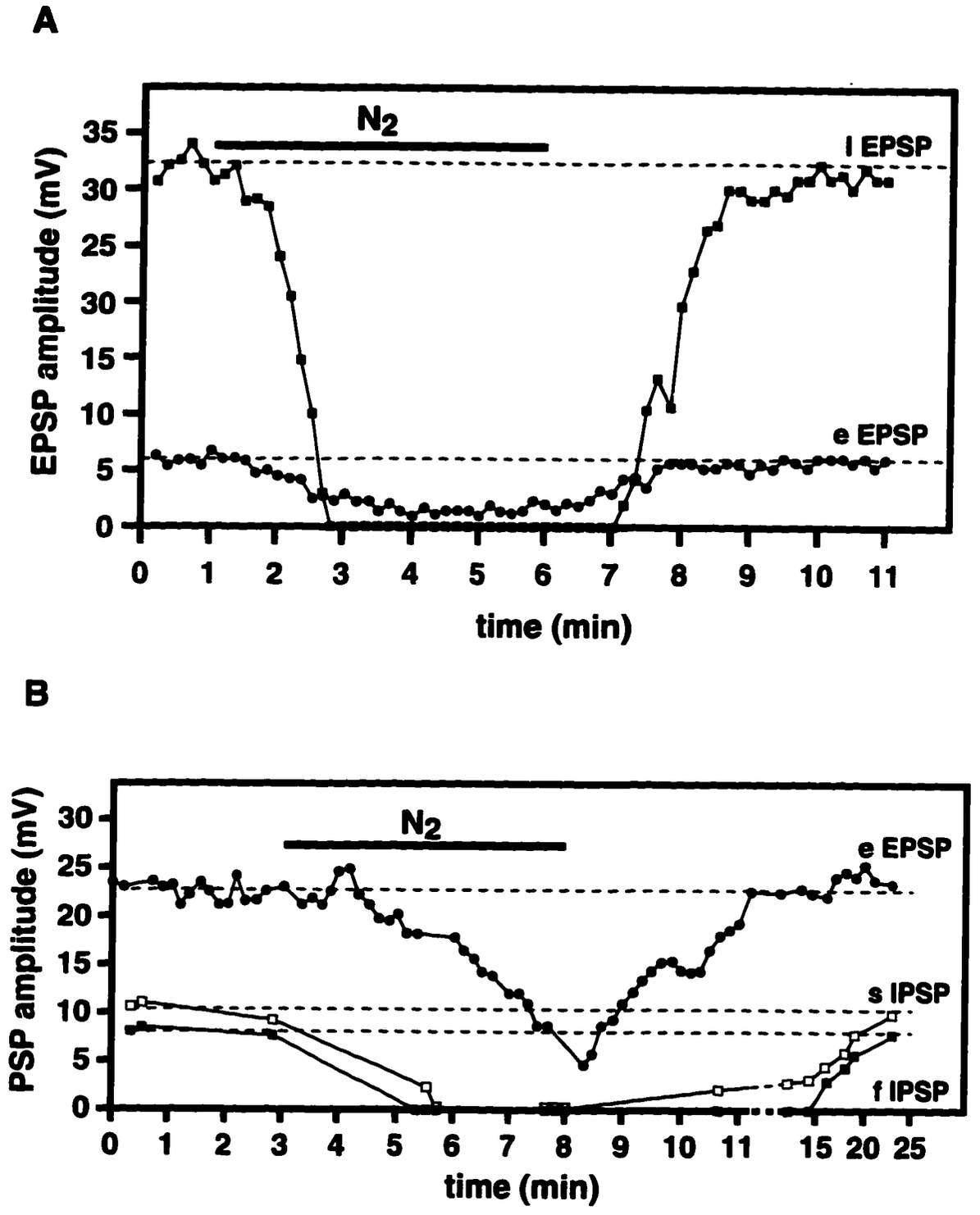
A
N2
I EPSP
e EPSP
EPSP amplitude (mV)
35
30
25
30
15
10
5
0
0 1 2 3 4 5 6 7 8 9 10 11
time (min)
B
N2
e EPSP
s IPSP
f IPSP
PSP amplitude (mV)
30
25
20
15
10
5
0
0 1 2 3 4 5 6 7 8 9 10 11 15 20 25
time (min)

Figure 26

Figure 27. Consequences of different PSP sensitivity to anoxia. (A) Opposite changes in amplitude of EPSP and IPSP during early phase of anoxia. Superimposed synaptic responses recorded in control (O_2) and anoxic (N_2, 1 min 45 s) conditions; each response was evoked by layer IV stimulation during application of a 500 ms, 1.0 nA depolarizing pulse. The early, almost complete disappearance of both fast (f) and slow (s) components of the IPSP resulted in an increase in amplitude and duration of the EPSP recorded at the same membrane potential (– 62 mV, dotted line). Inset: expanded view of the first 60 ms post-stimulus. Note the more robust EPSP, the delayed 1st AP (due to an increase in AP threshold), but a higher firing frequency (shorter inter-spike interval) due to lack of shunting effect of the *f* IPSP. (B)–(C) Transient increases in excitability during early anoxia and recovery. Synaptic potentials were evoked by layer IV stimulation (0.8 T); although the *s* IPSP was not visible at V_R, it was evident during transient depolarization of the membrane (not shown). (B) Occurrence of an AP on the *l* EPSP (2nd trace, N_2 30s) was independent of V_R and probably due to an early depression (and therefore less effective shunting) of the IPSPs. At 40 s N_2 exposure, the AP had a shorter latency due to membrane depolarization to – 86 mV. The remainder of the anoxic trial was characterized by the depression of the EPSPs. (C) Similar phenomenon occurring during reoxygenation (APs in 2nd trace, 2 min 10 s) due to *l* EPSP activation before *s* IPSP recovery. APs were truncated by the plotter. Calibrations for both B and C are shown in C.

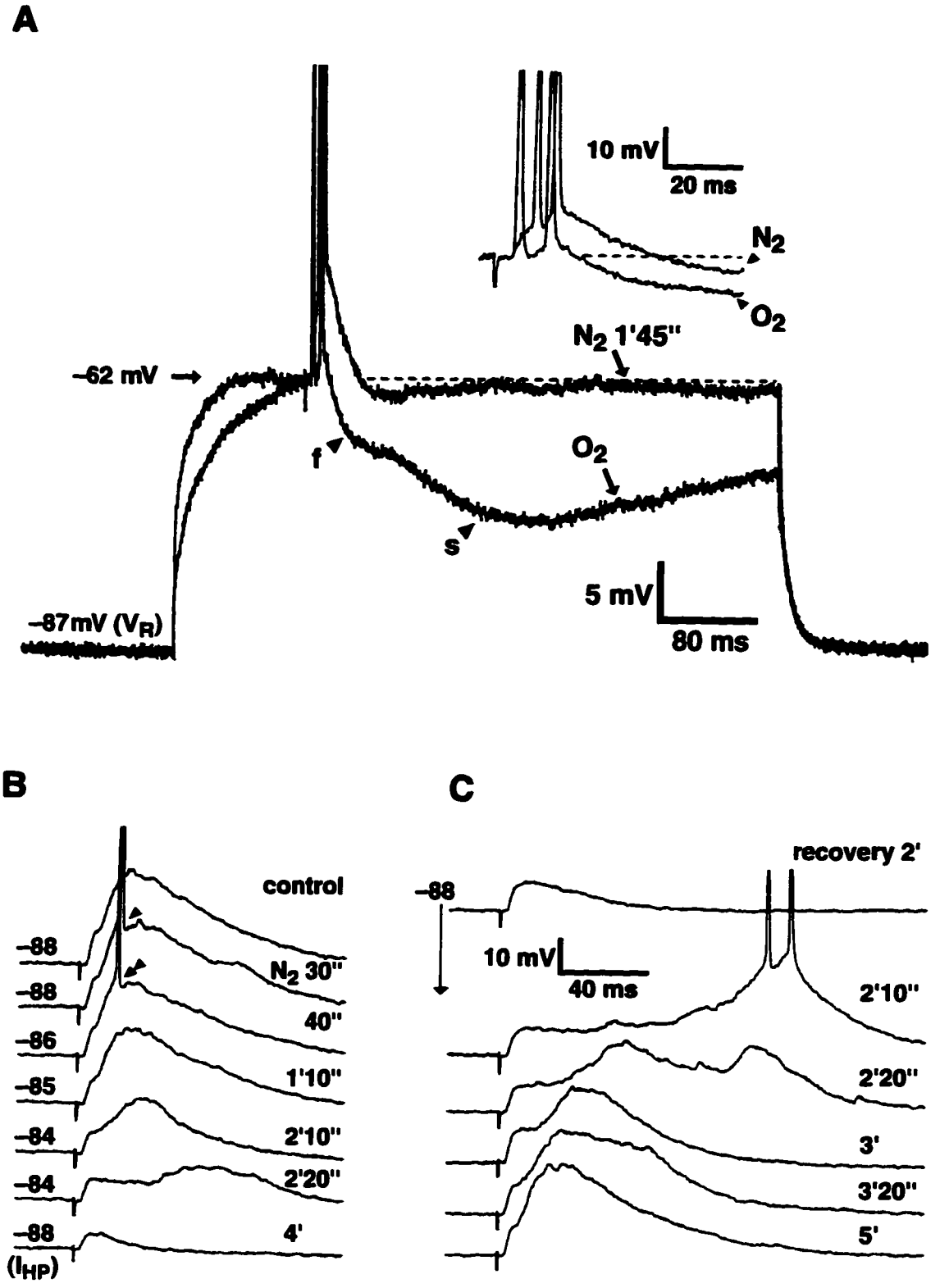
A
10 mV
20 ms
N2
O2
N2 1'45"
-62 mV
f
O2
s
5 mV
80 ms
-87mV (VR)
B
control
-88
N2 30"
-88
40"
-86
1'10"
-85
2'10"
-84
2'20"
-84
4'
-88
(IHP)
C
recovery 2'
-88
10 mV
40 ms
2'10"
2'20"
3'
3'20"
5'

Figure 27

Figure 28. Lack of dependence of the EPSP depression on the AD. (A) Selected synaptic responses (layer IV stimulation) recorded (from left to right) in control ACSF, during peak anoxia (at V_R and V_R + 5 mV), and at 4 min recovery. (B) Continuous recording of the same anoxic trial: each upward deflection of the membrane potential represents an EPSP, as recordeed at slow speed by the chart recorder. Arrows: time sequence of the four EPSPs expanded in A. I_{HP}: transient (~ 30 s) restoration of V_R at the peak of the anoxic response, using hyperpolarizing current injection. Note that the residual *e* EPSP recorded at V_R was almost identical to the *e* EPSP recorded during membrane depolarization (V_R + 5 mV). Records are from the same neuron as in Fig. 23–A.

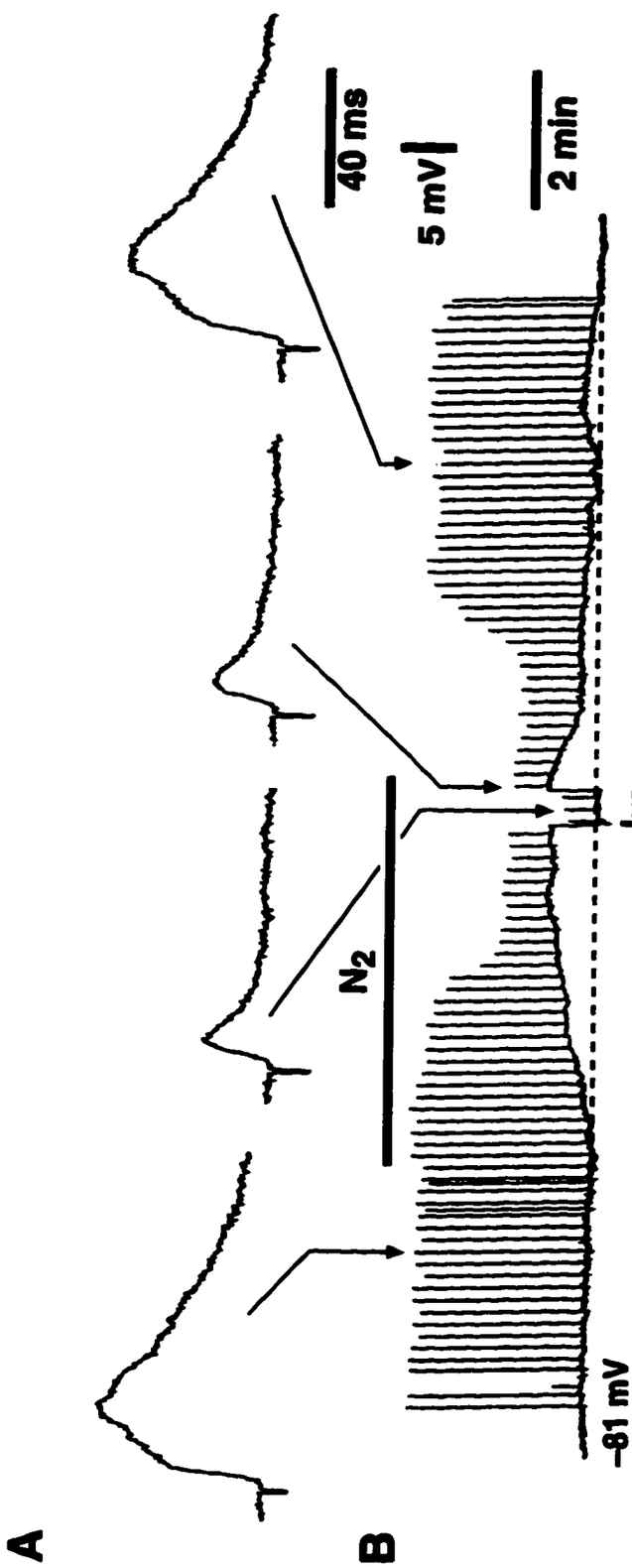

Figure 28

Figure 29. Lack of dependence of the EPSP depression on Na^+ pump inactivation. (A)–(E) Traces recorded from a single neuron. The upward deflections in A, C and E are EPSPs evoked at 0.05 Hz. Exposure to N_2 for 5 min (A) resulted in depression of the *e* EPSP and disappearance of the *l* EPSP, as shown in selected expanded traces in (B). Bath application of 5 μM ouabain for 8 min (C) induced a higher and longer depolarization than that produced by N_2, but did not have a significant influence upon the EPSPs (compare superimposed control and ouabain (Ou) traces in D). Exposure to ouabain in C induced *l* EPSP-like depolarizations with multiple components and nearly symmetrical time course. These occurred as single or double discharges (arrowheads), which correspond to sequence of expanded traces, (from *top* down, in *left inset*) or sustained bursts (*right inset*: sequence of events marked with bar and arrow), which followed closely ($\leq$ 2 s) some evoked EPSPs. (E) Anoxic trial in the same cell after 12 min of ouabain washout. The depolarizations (arrowheads) were still present, disappeared during N_2 exposure, and reappeared during reoxygenation. In A, C and E, V_R level is shown by dotted lines. Calibrations for A, C and E are shown in E; note separate calibration (25 mV, 150 ms) for *insets* in C. Calibrations for B and D are shown in D. Records are from the same neuron as in Fig. 23–B.

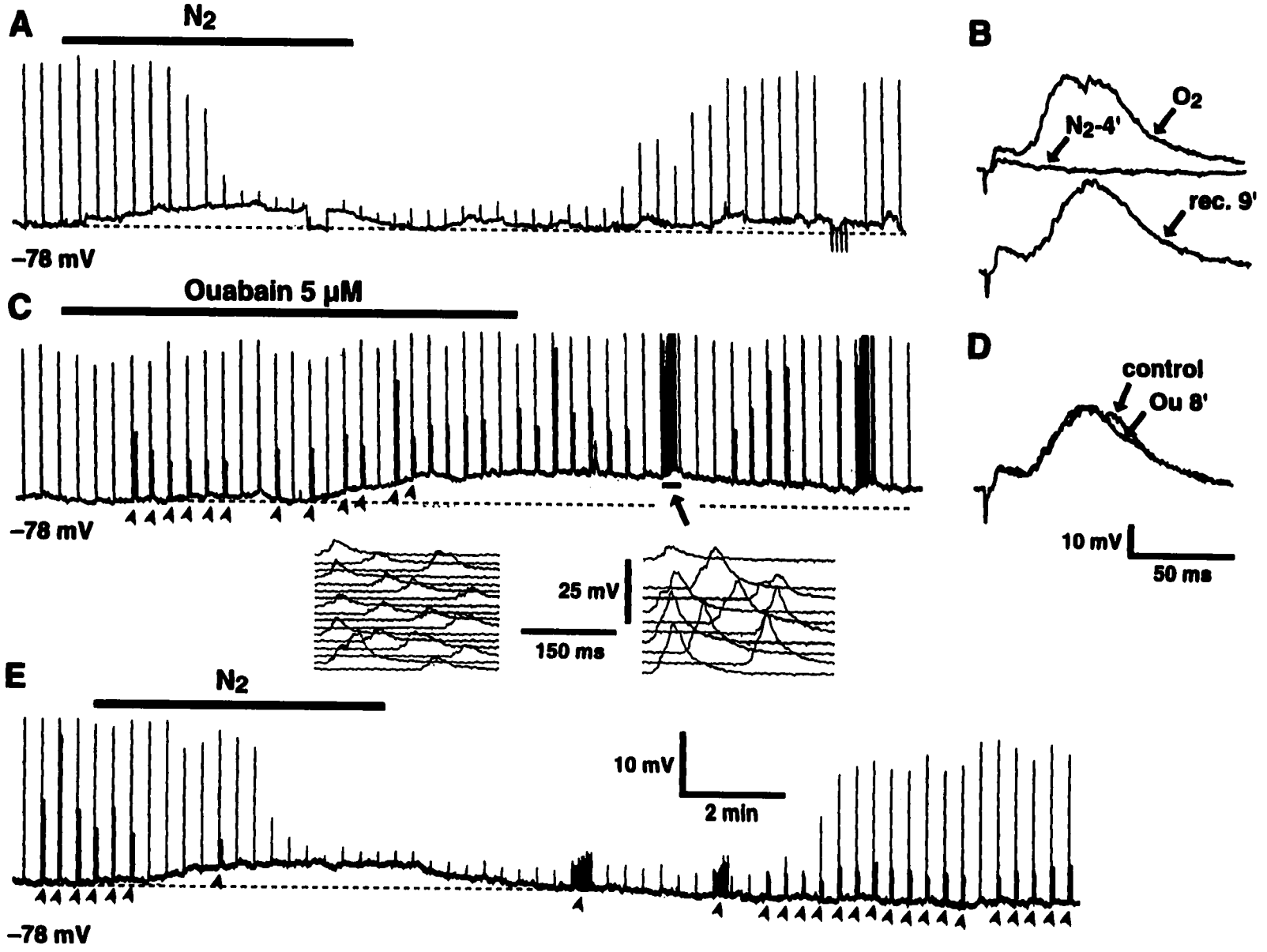
A
N2
−78 mV
B
O2
N2-4'
rec. 9'
C
Ouabain 5 µM
−78 mV
25 mV
150 ms
D
control
Ou 8'
10 mV
50 ms
E
N2
10 mV
2 min
−78 mV

Figure 29

Figure 30. Postsynaptic responses to local applications of neurotransmitter agonists. (A) Response to a QUIS pulse (100 μM, 15 ms, 20 psi) recorded in control ACSF. (B) Responses of a different neuron to GABA ejection (500 μM, 50 ms, 20 psi) recorded in control ACSF at V_m values of – 56, – 62, – 72 mV (obtained with steady depolarizing current injection–I_D), and at – 83 mV (V_R). Hyperpolarizing pulses of – 0.2 nA, 100 ms, 5 Hz (downward deflections) were continuously injected to monitor R_N (current trace not shown). Upward deflections in traces recorded at – 56 mV and – 62 mV represent APs triggered at the end of each hyperpolarizing pulse (anode break phenomenon). The terminal phase of the GABA response reversed at about – 70 mV. C Anoxic effect on response to QUIS (same neuron and ejection parameters as in A) in the presence of 1 μM TTX (35 min). The amplitude of the QUIS-induced depolarization decreased by 23% at 4 min anoxia. I_{HP}: hyperpolarizing current injected to temporarily restore V_R during the ejection. Last trace shows recovery at 4 min. (D) Anoxic effect on responses to GABA (1 mM, 150 ms, 30 psi). The slice (different from that shown in B) was bathed for 27 min in 1 μM TTX and 1 mM KYN. Downward deflections are responses of V_m to hyperpolarizing current pulses (0.2 nA, 150 ms, 0.2 Hz, current trace not shown), injected to monitor R_N. The amplitude of GABA-induced depolarization (trace was expanded in those portions—see dual time base) decreased by 24% at 3.5 min of anoxia. The depression was not dependent on V_R or R_N, because it persisted at 3 min recovery (arrow), when V_R and R_N reached control values. Arrowheads in all traces: times of drug ejection. Dotted lines indicate interruption in record display as marked (2 and 3 min).

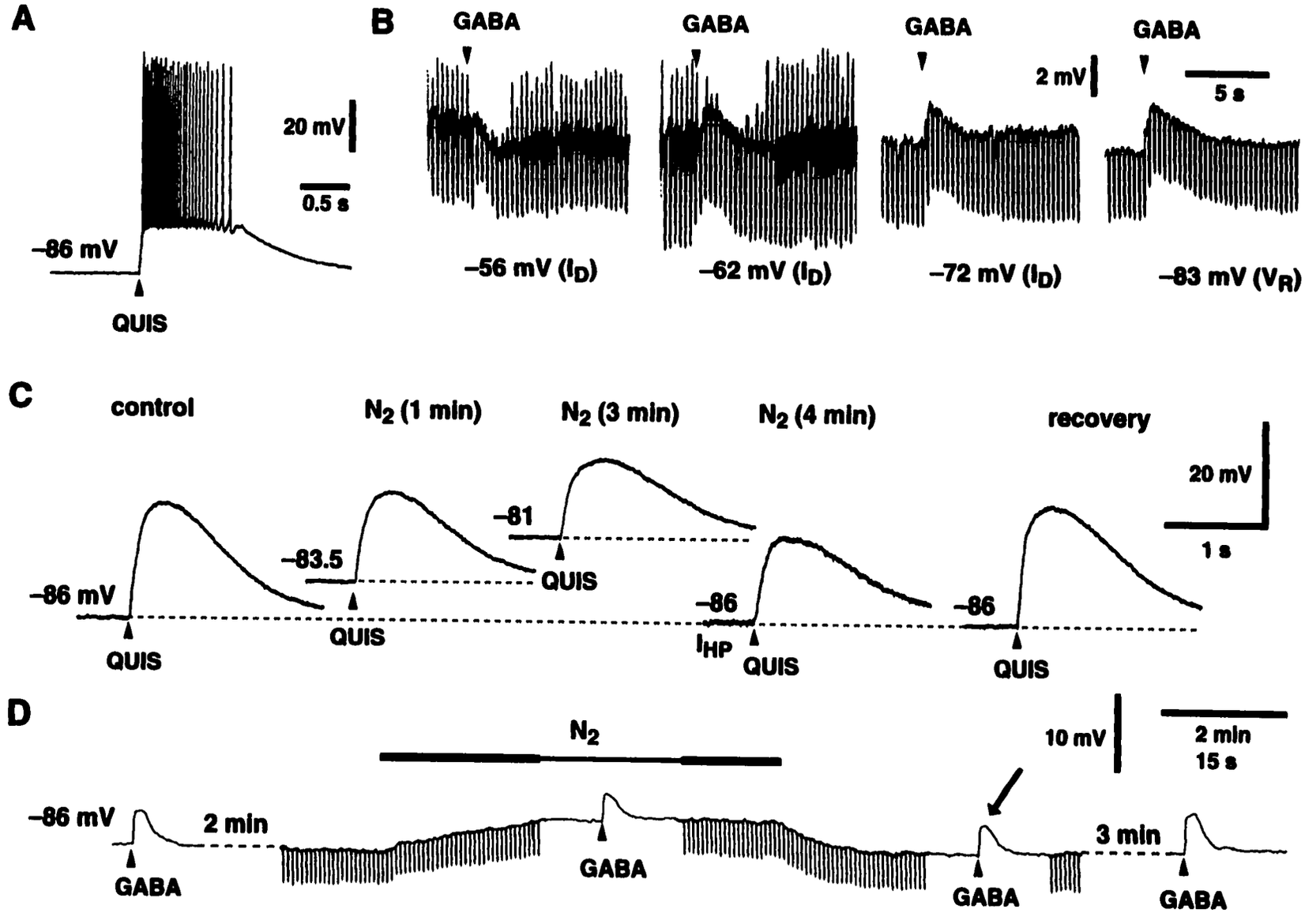
A
20 mV
0.5 s
–86 mV
QUIS
B
GABA
GABA
GABA
GABA
2 mV
5 s
–56 mV (I_D)
–62 mV (I_D)
–72 mV (I_D)
–83 mV (V_R)
C
control
N2 (1 min)
N2 (3 min)
N2 (4 min)
recovery
20 mV
1 s
–86 mV
–83.5
–81
–86
–86
QUIS
QUIS
QUIS
QUIS
QUIS
I_HP
D
N2
10 mV
2 min
15 s
–86 mV
2 min
3 min
GABA
GABA
GABA
GABA

Figure 30

Figure 31. Effects of anoxia on miniature PSPs (mpsps). (A) The effect of anoxia on mpsps (neuron recorded in standard ACSF). The frequency of mpsps decreased by 75% (mid panel). (B) Decrease of mpsps frequency in 5 neurons recorded in standard ACSF vs. 5 neurons recorded in 1 μM TTX. Although TTX reduced drastically the control values of 1 min-count of mpsps, the degree of anoxia–induced frequency reduction was preserved.

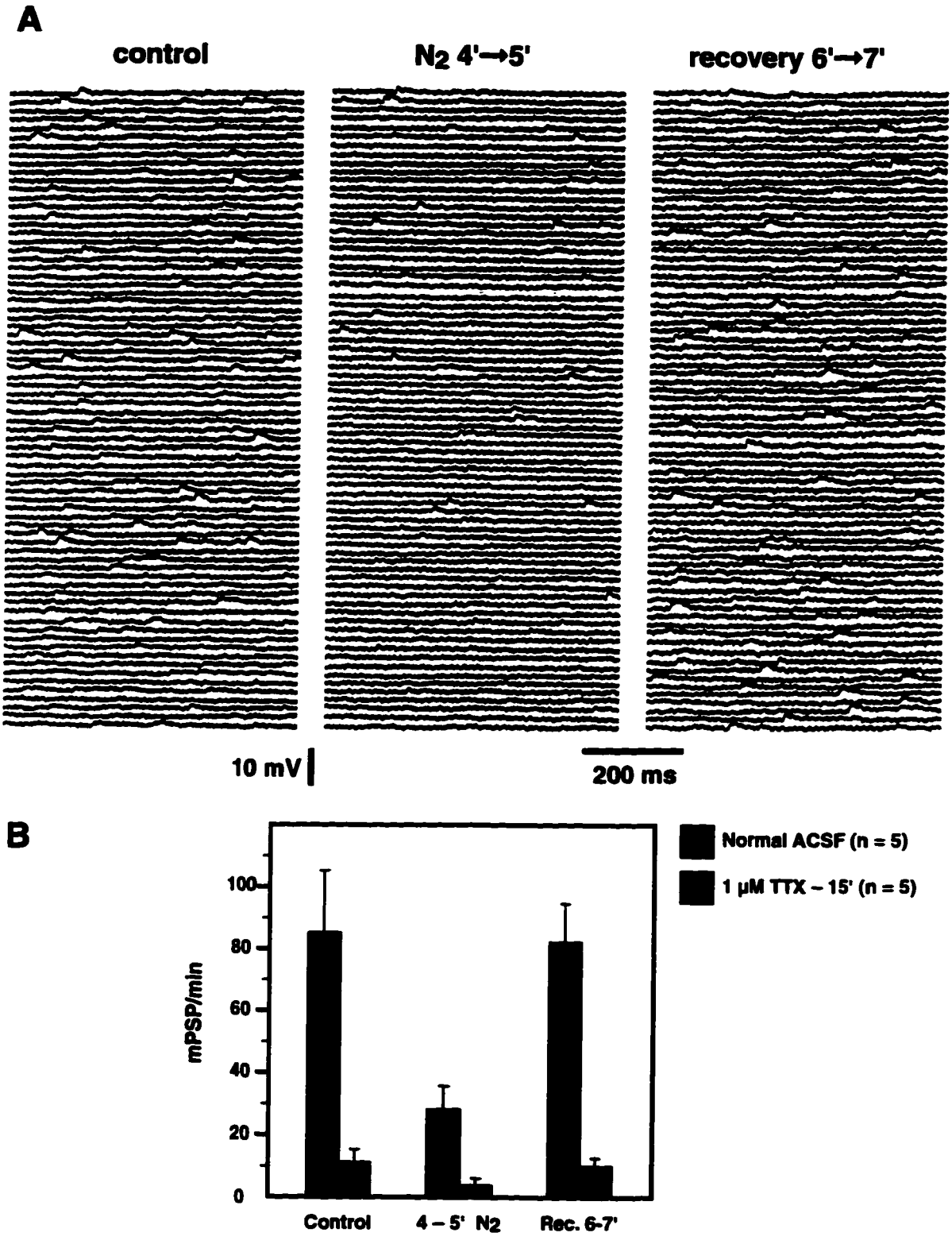
A
control
N2 4'→5'
recovery 6'→7'
10 mV
200 ms
B
Normal ACSF (n = 5)
1 μM TTX – 15' (n = 5)
mPSP/min
100
80
60
40
20
0
Control
4 – 5' N2
Rec. 6-7'

Figure 31

Figure 32. Effects of the adenosine antagonist 8-CPT on anoxic changes. In both traces, upward deflections represent EPSPs evoked at 0.1 Hz. Pre-treatment of the slice with 1 μM 8-cyclopentyltheophylline (8-CPT), a potent A_1 receptor antagonist did not influence significantly the anoxic depolarization, but protected the neuron against synaptic depression.

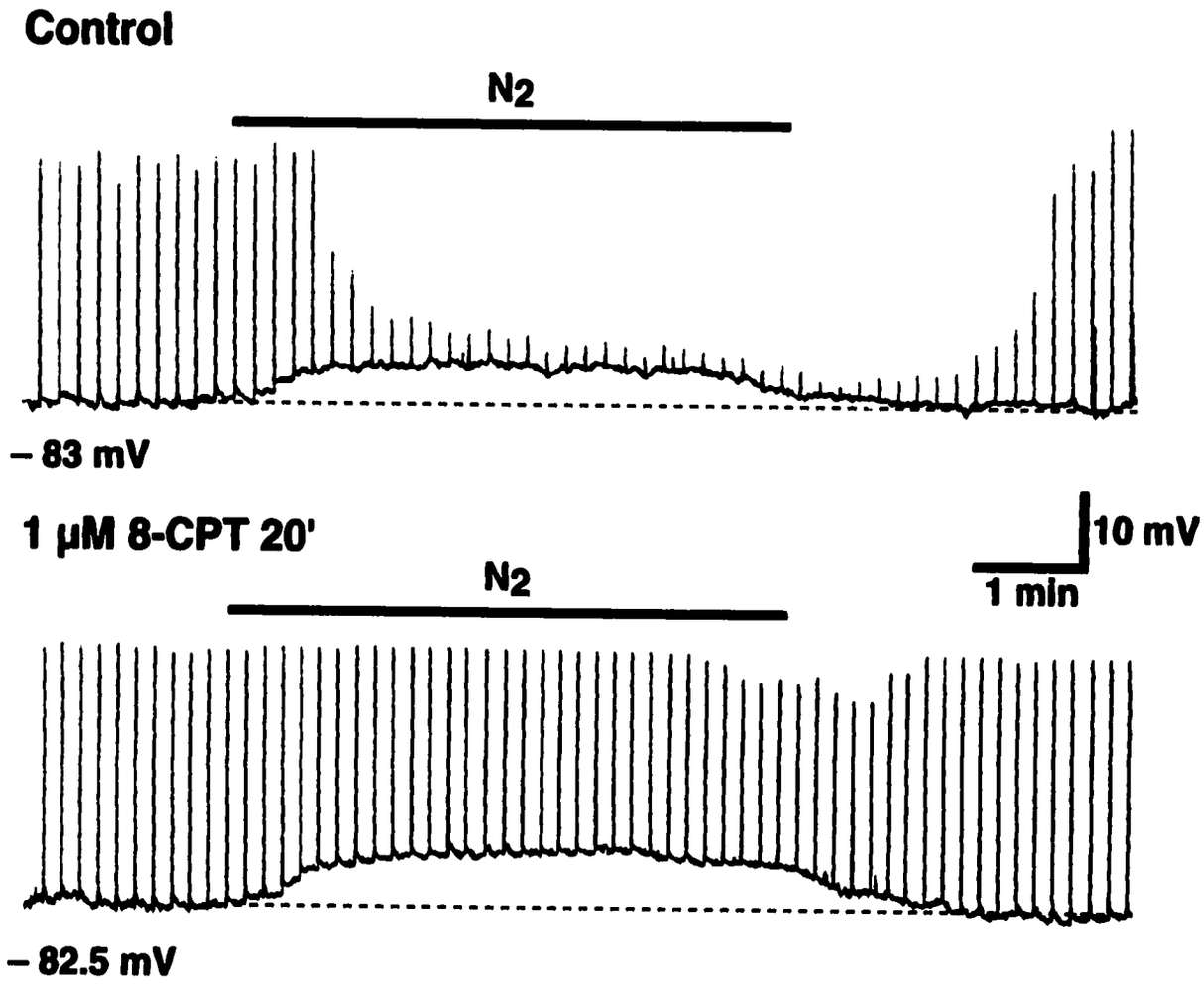

Figure 32

Figure 33. Effects of creatine pre-incubation on the anoxic depolarization and EPSP depression. (A) Control anoxic response (anoxic depolarization of about 5 mV—see dotted line, and significant synaptic depression) of a neocortical neuron exposed to N_2 for 5 min. The cell was continuously stimulated at 0.1 Hz (EPSPs are seen as upward deflections from the baseline). Corresponding inset shows from top to bottom nine expanded successive synaptic responses (arrowhead marks the stimulus artifact), corresponding to the bracketed portion of the main trace and representing the initial phase of the synaptic depression. Note the presence of both early (e) and late (l) EPSP; the latter elicited a spike, truncated by the oscilloscope screen. (B) Anoxia recorded in a different slice from the same animal. The slice was pre-incubated for over 1.5 h in ACSF containing 25 mM creatine. In normoxic conditions, the continuously evoked EPSPs (0.05 Hz) showed a high amplitude, bursting late component of almost epileptiform appearance (see upper response in inset). Anoxia (5 min.) evoked a much more accentuated depolarization ($\approx$ 70% increase—see dotted line) and synaptic depression. Corresponding inset (note different calibration) shows from top to bottom 7 expanded successive synaptic responses (arrowhead marks the stimulus artifact), corresponding to the bracketed portion of the main trace and representing the initial phase of the synaptic depression. Note the rapid disappearance (20 s—between the first and second responses) of the *l* EPSP (l) in an "all-or-none" fashion. Note also the prolonged depolarizing shift during EPSP recovery (main trace—arrow), due to an extra stimulus applied shortly after a preceding EPSP. Calibration for both main traces is shown at right in A.

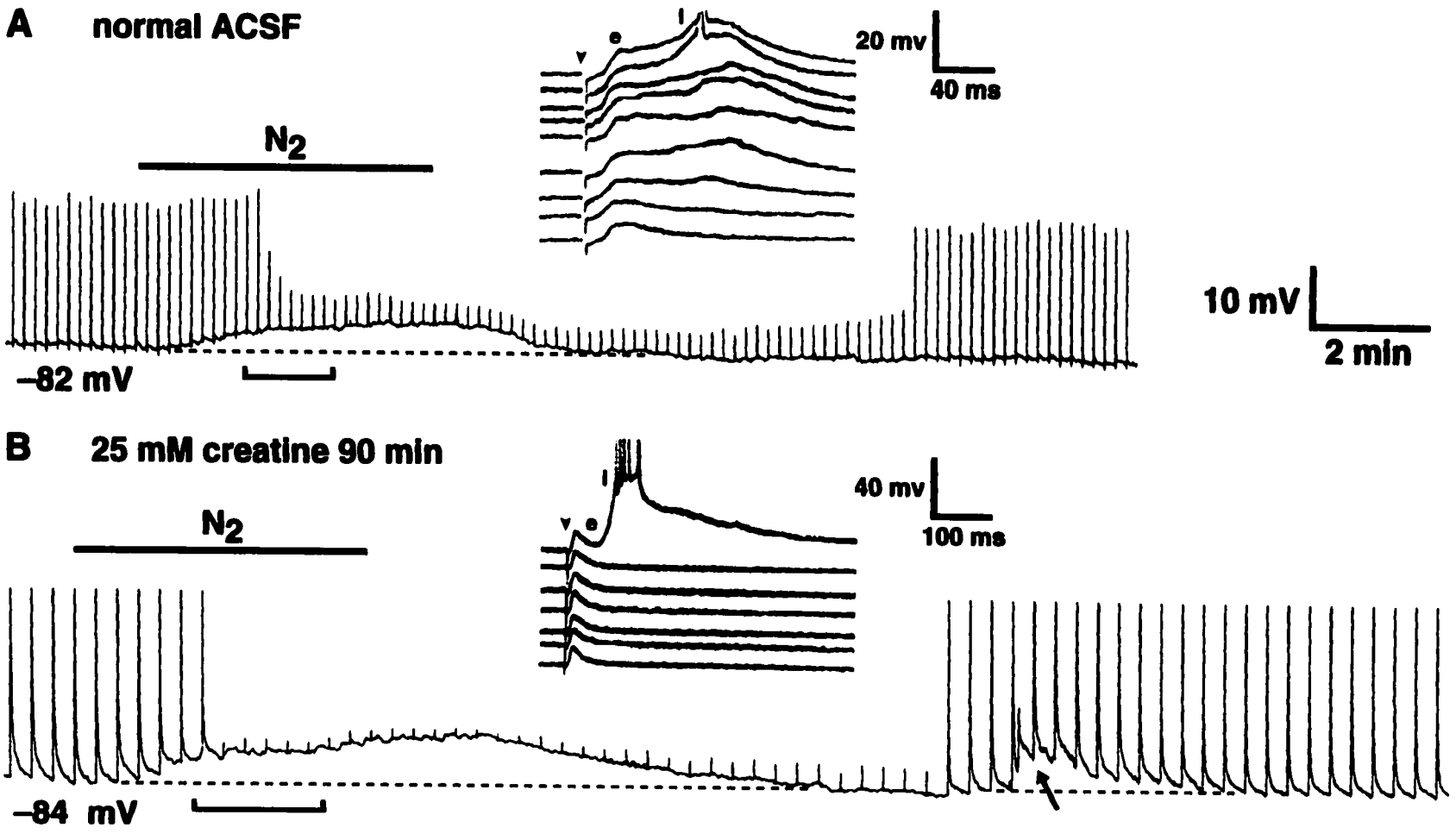
A
normal ACSF
20 mv
40 ms
N2
10 mV
2 min
-82 mV
B
25 mM creatine 90 min
40 mv
100 ms
N2
-84 mV

Figure 33

Figure 34. Effects of temperature changes on synaptic potentials in normoxic conditions. (A)–(C) are records from three different neurons. Asterisks mark the aligned stimulus artifacts. (A) The latency of the *e* EPSP (e) was decreased (dotted lines) and the initial slope of the *e* EPSP appeared slightly steeper at 36°C. (B), (C) Cooling increased *e* EPSP latency (dotted lines) and induced a significant decrease in steepness of the rising phase of the *e* EPSP (arrows) and of its amplitude (arrowheads in C). Upon return to control temperature, recovery of the EPSP latency was obtained in all cases—not shown for B and C.

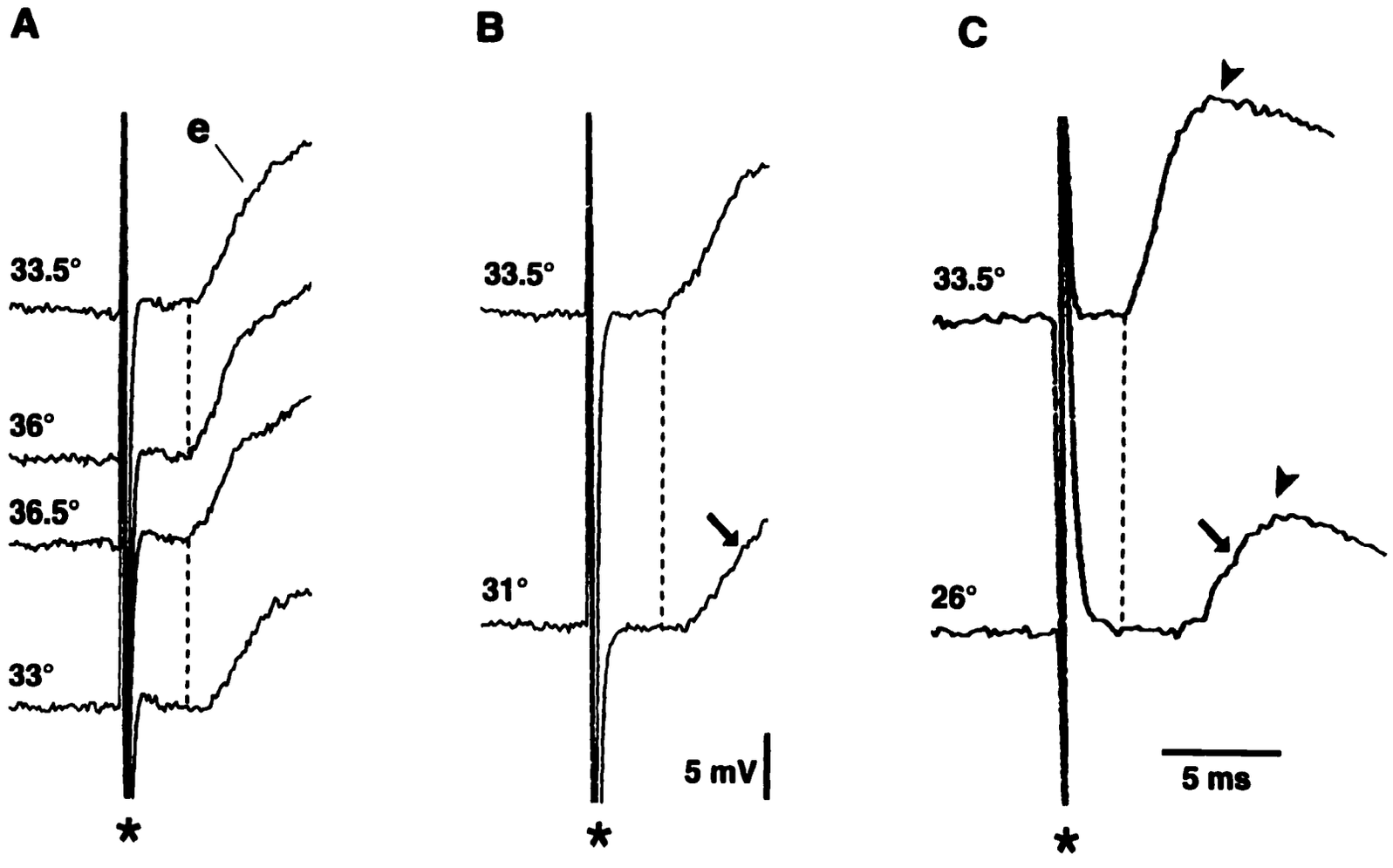

Figure 34

Figure 35. Effects of increased temperature on anoxic changes. All records are from the same neuron. Upward deflections from the baseline represent compound postsynaptic potentials elicited by continuous stimulation (0.1 Hz), as seen at the slow speed of the chart recorder. Upper trace: control anoxic trial (N_2), showing the anoxic depolarization and synaptic depression. When temperature was raised above 35°C (middle trace, left), the cell depolarized and steady hyperpolarizing current injection (I_{hp}) was needed to keep V_R at control level. Note a more accentuated anoxic depolarization followed by postanoxic fluctuations of V_R, a more pronounced PSP depression and the occurrence of rare spontaneous brief depolarizations (arrowheads). These depolarizations increased in frequency and amplitude as the temperature was raised above 36°C (expanded trace in inset at right). Lower trace: at 37.3°C, the cell depolarized further and the same amount of hyperpolarizing current was not sufficient to keep V_R at control level. The EPSP depression was faster and deeper and the recovery delayed. The anoxic depolarization was also slow to recover, although it was briefly interrupted by a postanoxic repolarization (arrow). The spontaneous depolarizations were more frequent (some marked by arrowheads).

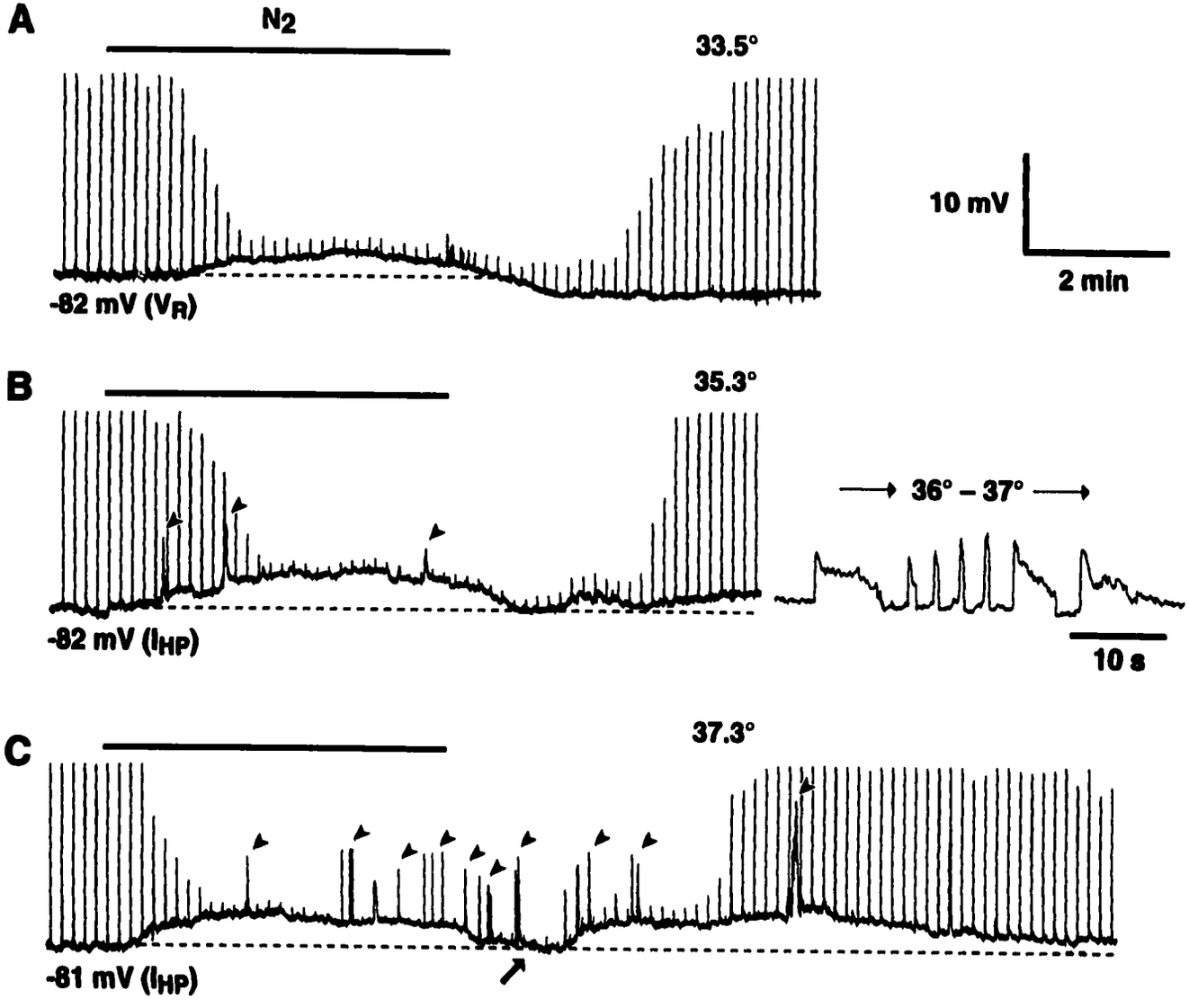

Figure 35

Figure 36. Effects of increased temperature on PSP anoxic depression. All traces were recorded from the same neuron. (A)–(C) Left panels show traces superimposed on their baselines at increased intervals, in order to compare control EPSP amplitude (O_2) with EPSP amplitude at various moments during the anoxic trial (N_2). Right panels show postanoxic recovery. (A) Anoxic trial at control temperature. Note that EPSP amplitude began to decrease significantly only after 2 min of anoxia. Note also the presence of a *s* IPSP (sag under the baseline, at left), which fully recovered (arrow, at right). (B) At 36.5°C, the control EPSP was smaller, the synaptic depression started during the first minute of anoxia and was more accentuated, and the recovery was delayed (9 min vs. 6.5 min). Note absence of *s* IPSP at this temperature. (C) Lowering the ACSF temperature back to 33.5°C resulted in the recovery of all characteristics seen in A.

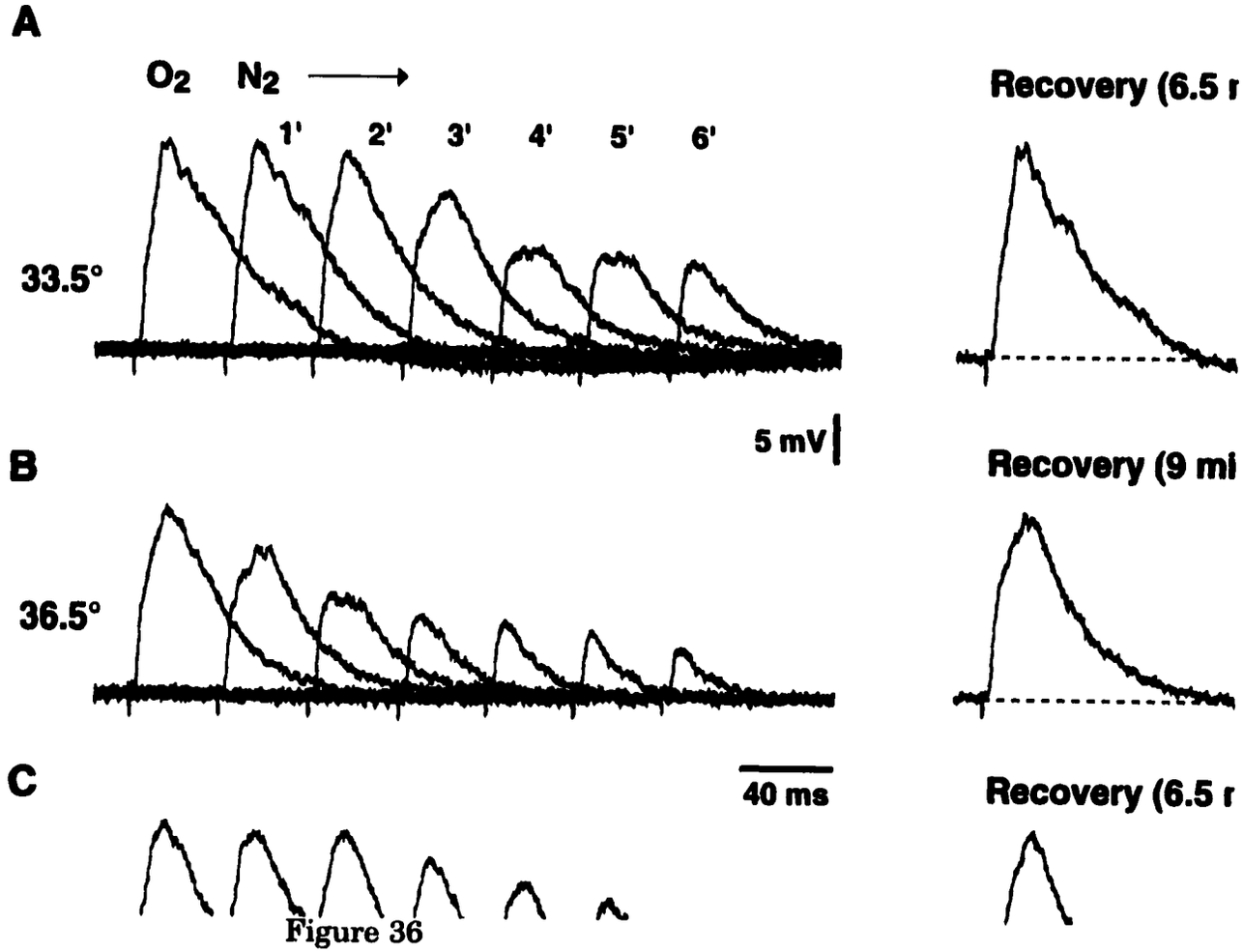
A
O2 N2
1' 2' 3' 4' 5' 6'
Recovery (6.5 r
33.5°
5 mV
B
Recovery (9 mi
36.5°
C
40 ms
Recovery (6.5 r

Figure 36

Figure 37. Effects of decreased temperature on PSP anoxic depression. All traces were recorded from the same neuron (cell also illustrated in Figure 1C). (A)–(C) show each: control, anoxic and recovered EPSPs, as marked in A. An important reduction of EPSP anoxic depression occurred at 31°C (B) as compared with 33.5°C (A). At 26°C, EPSP amplitude was practically un-affected by anoxia (C). Note also the progressive decrease in amplitude of the control EPSP, as temperature decreased. I_{HP}: hyperpolarizing current injected at peak anoxia, in order to bring V_m to resting level, for proper *e* EPSP comparison.

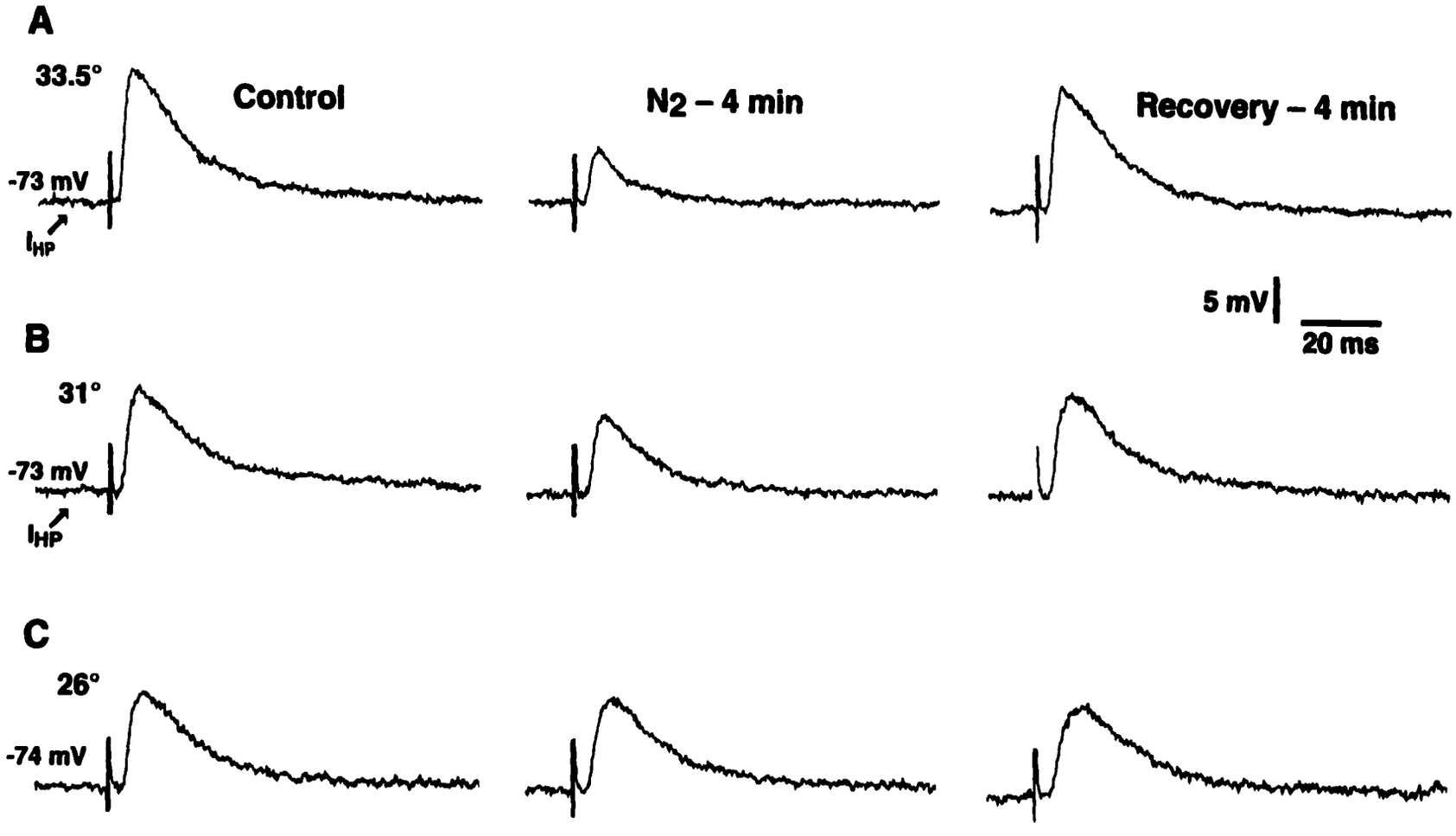

Figure 37

Figure 38. Variation of anoxic depression of *e* and *l* EPSPs (± S.E.M.) with temperature; (n = 58 anoxic trials in 22 neurons.) From control trials at 33.5°C (n = 30), temperature was increased or decreased and anoxic responses were recorded at various values between 26 and 37.5°C (n = 1–5 observations at each temperature point). The *e* EPSP depression was measured at 2 min of anoxia (▲) and 5 min of anoxia (i.e. during the plateau of the anoxic depolarization) (●). The *l* EPSP depression (○) was measured at 2 min N_2 exposure (i.e. before *l* EPSP disappearance, as recorded during the initial control trial at 33.5°C). Note the almost complete preservation of the *e* EPSP and *l* EPSP amplitude during anoxic trials performed at 26–27°C. For temperatures above 35°C, there was an accelerated depression of the *l* EPSP with warming, which resulted in its disappearance within the first 2 min.

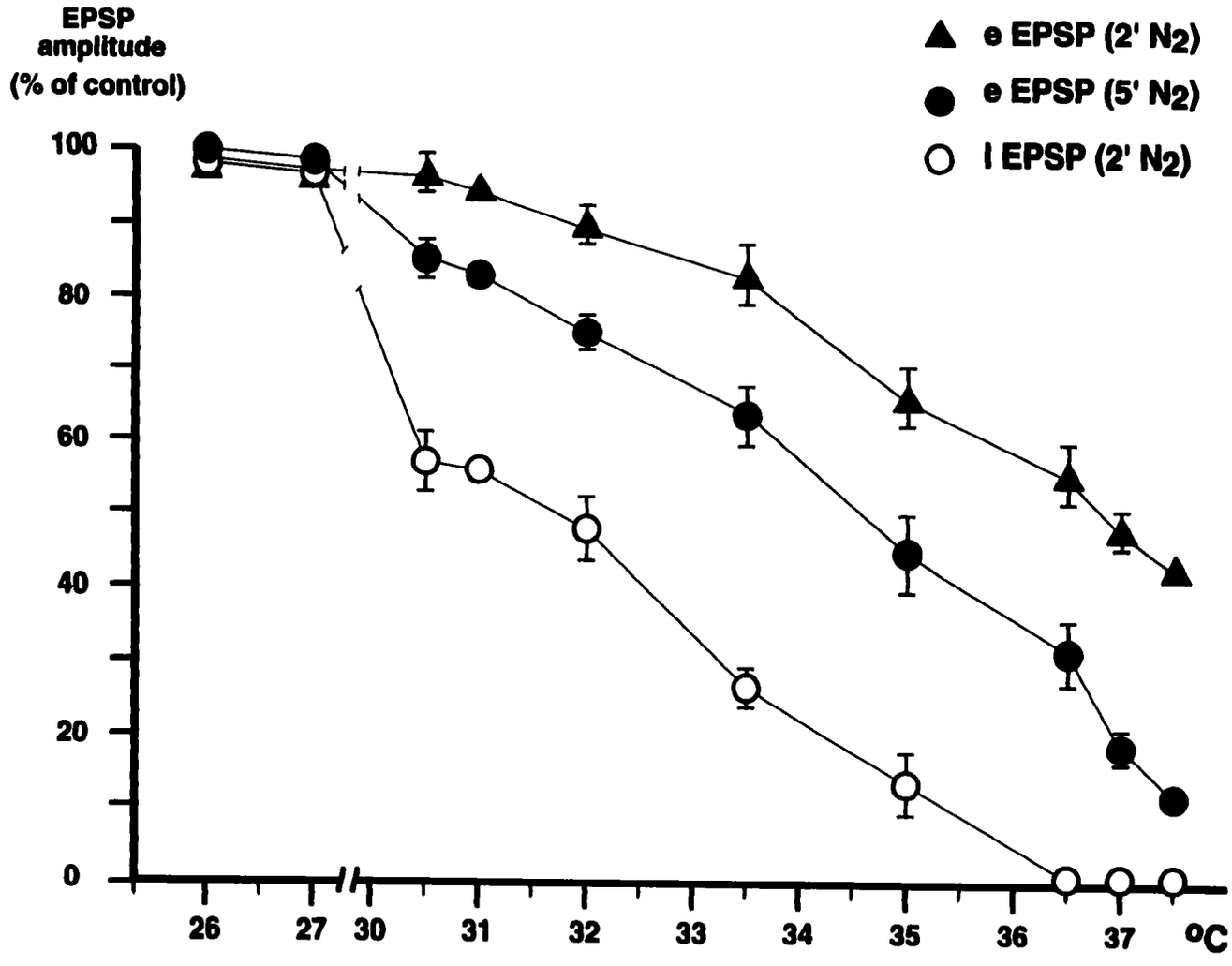
EPSP
amplitude
(% of control)
e EPSP (2' N2)
e EPSP (5' N2)
I EPSP (2' N2)
100
80
60
40
20
0
26
27
30
31
32
33
34
35
36
37
°C

Figure 38

DISCUSSION

A. PROPERTIES OF NEOCORTICAL NEURONS

1. Passive membrane properties (V_R and R_N)

V_R and R_N values (– 83 mV and 29 MΩ) recorded in the present experiments are consistent with the figures obtained from the same preparation during earlier studies (– 85 mV and 32 MΩ—Rosen and Andrew, 1990), confirming that this model of neocortical slice gives reproducible results. The values are also comparable with those reported for other *in vitro* experiments in the neocortex (– 79 mV and 35 MΩ—Luhmann and Heinemann, 1992).

The V_R values obtained in slices are more negative than those usually recorded *in vivo* (Bindmann et al., 1988; Pockberger, 1991). This is thought to be due to a decrease of the tonic excitatory synaptic input (Stafstrom et al., 1982) and the increased stability of the recordings performed *in vitro* (Connors et al., 1982).

In vitro studies have reported mean R_N values of 25–40 MΩ for neocortical neurons (Connors et al., 1982; Connors and Gutnick, 1984; McCormick et al., 1985; Bindmann et al., 1988; Luhmann and Heinemann, 1992). The variation is probably due to the diversity of neurons recorded in different layers and regions of the neocortex. These values are consistently higher than 6–18 MΩ recorded *in vivo* (Bindman et al., 1988). This discrepancy may be explained by shrinkage and uncoupling of neurons *in vitro* (Alger et al., 1984) or reduced mean cell size, caused by slicing of the dendrites (Bindman et al., 1988).

2. Synaptic potentials

The findings of the current study show that in most respects the *l* EPSP had characteristics similar to those originally described by Sutor & Hablitz (1989a,b): a presynaptically NMDA-dependent polysynaptic event (unable to follow higher stimulation frequencies and blocked by the specific NMDA receptor antagonist DL-2-amino-5 phosphonovaleric acid (DL-APV —Fig. 10). However, in the experiments reported here, the *l* EPSP had more diversity. In about 25% of cases, the polysynaptic excitatory circuits were exceptionally active, eliciting low-threshold, robust *l* EPSP capable of evoking APs. Together with the small preceding *e* EPSP, as well as the characteristic long and invariable latency to peak, this suggests a distinct activatory pathway for this variant of *l* EPSP. Although slight differences in the placement of the stimulating electrode or in the cortical area selected for recording may also play a role, it is more likely that the occurrence of these responses was due to the complexity of the preparation. In contrast to the small, wedge-shaped, unilateral slices used by Sutor and Hablitz (see Sutor and Zieglgänsberger, 1987) , these larger, bilateral slices (Figs. 1, 5) allowed an increased chance of preservation of intact neuronal processes. This explanation is in accordance with the occasional absence of layer IV–elicited *l* EPSPs in the small slices (Sutor and Hablitz, 1989a), as opposed to their presence in all the large, bilateral slices.

B. ANOXIC DEPOLARIZATION

In the present experiments, the most characteristic feature of the anoxic response (besides synaptic depression—see below) was the occurrence at V_R

of the small to moderate anoxic depolarization (AD) in all recorded neurons. This is in contrast with the changes in CA1 pyramidal neurons which, due to the activation of K^+ conductance(s), have been described as mainly hyperpolarizing (Krnjevic and Xu, 1989, 1990; Leblond and Krnjevic, 1989) and even with some neocortical studies which have reported hyperpolarization (Glötzner, 1967) or mixed responses (Luhmann and Heinemann, 1992). A careful study of these reports reveals that in fact, even in the cortical regions described as typically showing hyperpolarizing responses, there are numerous examples of depolarizing cells. For example, Leblond and Krnjevic (1989) reported that among CA1 cells, 50% of those with APs > 90 mV were depolarizing and among neurons with APs < 90 mV, 25% showed AD. Morris et al., (1995) have shown that during brief anoxia (4 min), depolarization is more common that hyperpolarization in pyramidal neurons from the CA2/CA1c/CA1b regions, as compared to neurons from the CA1a/subicular regions. Luhmann and Heinemann (1992) found depolarizing responses in 37% of the somato-sensory pyramidal neurons from layers II–III. Furthermore, mixed (hyperpolarizing/ depolarizing) responses were described in CA3 hippocampal neurons (Ben Ari, 1990; Ben Ari et al., 1990), while hippocampal granule cells show a depolarizing response to anoxia (Ben Ari and Lazdunski, 1989; Krnjevic and Ben Ari, 1989), very similar to the AD from the present experiments. These findings show that there is a great diversity of responses to anoxia among various cortical neuronal populations and that, even among related neurons, there is no such a thing as a "typical, unique anoxic response".

It is more reasonable to consider that the anoxic insult affects concomitantly multiple conductances and that for a given type of neuron, the anoxic response is a compound result of the depolarizing and hyperpolarizing

tendencies created by various transmembrane ionic currents being depressed or activated by lack of O_2.

This study showed that for the pyramidal neurons of layers II–III from the fronto-parietal neocortex, the depolarizing events represent by far the predominant process during brief anoxia, and that a significant component contributing to their production is a Na^+ influx through glutamate-dependent synaptic channels of the non-NMDA (AMPA/kainate) type. This does not exclude, however, that other processes involving Na^+ influx and intracellular accumulation (Na^+-Ca^{2+} exchanger, TTX-insensitive non-inactivating Na^+ currents (Catterall, 1992; Taylor, 1993)) could be involved in the anoxic response. A reversed transmembrane passive chloride movement (Cl^- efflux), due to the hyperpolarized V_R of these cells (i. e. more negative than E_{Cl}) could add to the depolarization, as suggested by the Cl^- substitution experiments. These issues should be addressed in future experiments, in order to narrow down the possible factors contributing to the AD.

Another issue which remains to be clarifed is the relative importance of GLU release/accumulation processes in the production of anoxic effects. It is of importance to ascertain if the increased anoxic interactivity GLU–GLU receptors is due to (1) increased transmitter release (the inefficiency of low Ca^{2+} treatment seems to eliminate at least an increased vesicular release), (2) increased extracellular accumulation (depressed/reversed re-uptake mechanisms?), or (3) a combination of increased release (possibly non-vesicuular) and decreased uptake.

The experiments strongly suggest that, at least in this group of neurons, K^+ conductances play a minimal role in the response to anoxia. Since slice incubation in KYN and/or TTX, or in KYN and BMI (not shown), as well as Na^+ replacement were followed by significant depression of AD, but failed

to induce hyperpolarization at V_m values up to – 65 mV, it is unlikely that the activation of a K^+ conductance (even minimal and masked by AD) would be of importance in this type of anoxic response. The consistency of the absence of any anoxic hyperpolarizing events in the present experiments constitutes perhaps the most important regional difference between this type of neocortical neurons and the CA1 hippocampal neurons, which have been the object, by far, of most of the recent studies involving effects of brief anoxia.

The dynamics of intracellular $[Ca^{2+}]$ and its role in the anoxic events leading to cellular damage is well documented (Siesjö, 1988; Siesjö and Bengtsson, 1989; Kostyuk and Verkhratsky, 1994; Simpson et al., 1995) (see **BACKGROUND**). Interestingly, the present experiments using DL-APV, MCPG, Ca^{2+}-free solution and metallic blockers, suggest that Ca^{2+} influx through NMDA-receptor activated channels or through voltage-dependent channels is not likely to occur in these group of neocortical neurons, at least in the first few minutes of anoxic exposure. Similarly, mechanisms implicating the activation of mGLU do not seem to play a role in the occurrence of AD.

Clearly, the experiments did not investigate all possible mechanisms which could induce an increase in $[Ca^{2+}]_i$. It is important to mention, however, that since several of the mechanisms responsible for intracellular Ca^{2+} accumulation involve relatively "slow" processes, dependent on intracellular second messengers, Ca^{2+} was implicated mostly in the delayed anoxic events (neuronal degeneration), rather than the immediate changes, induced mostly by Na^+/Cl^- influx and cell swelling (Choi, 1988; Choi and Rothman, 1990). Indeed, the fact that at 33°C the changes in $[Ca^{2+}]o$ during brief (3–4 min) anoxia in rat CA1 pyramidal neurons are minimal (0.058 ± 0.12 mM) (Morris et al., 1991), suggest that a significant extracellular Ca^{2+} influx is not likely to occur in the first few minutes of O_2 deprivation *in vitro*. Krnjevic and

Leblond (1987, 1989) have shown that in CA1 slowly inactivating L-type voltage-dependent Ca^{2+} currents are in fact *blocked* by anoxia. These findings do not, however, eliminate the possibility that the process of intracellular Ca^{2+} accumulation may start early during anoxia, through Ca^{2+} release from the internal stores (endoplasmic reticulum) caused by ATP reduction. It has been shown in CA1 neurons (Krnjevic and Xu, 1989) that dantrolene-Na, which blocks Ca^{2+} release from the endoplasmic reticulum, reduces the amplitude of the anoxic hyperpolarization and that intracellular Ca^{2+} chelators cause a variable depression of anoxic changes in R_N (Leblond and Krnjevic, 1989). Extending and detailing these experiments, Belousov et al. (1995) confirmed that in CA1 neurons recorded with the whole-cell patch clamp technique, dantrolene sodium (10 μM) suppresses the anoxic hyperpolarization and the change in R_N. Moreover, the *sensitivity* of the anoxic changes to heparin and thapsigargin (blockers of inositol triphosphate–induced Ca^{2+} release and of Ca^{2+} uptake, respectively) and *insensitivity* to ryanodine and procaine (blockers of Ca^{2+}–induced Ca^{2+} release) suggested that the anoxic response is initiated predominantly by an inositol triphosphate–induced Ca^{2+} release from the internal stores, rather than by a Ca^{2+}–induced Ca^{2+} release.

Therefore, a more detailed study, involving selective blockade of various types of Ca^{2+} channels known to be present in neocortical neurons (Sayer et al., 1993), blockade of intracellular Ca^{2+} release (with dantrolene, ryanodine, procaine), intracellular chelation using ethylene glycol-bis (β-aminoethyl ether (EGTA) and/or newer buffers, such as *bis*-(o-aminophenoxy)-ethane-N,N,N,N-tetraacetic acid (BAPTA) and *bis*-(o-aminophenoxy)-ethane-N,N,N,N-tetraacetic acid aminoethoxy (BAPTA-AM) (Scharfman and Schwartzkroin, 1989; Niesen et al., 1991), would prove useful for clarifying the role of Ca^{2+} in the early phase of anoxia in neocortical neurons.

C. ANOXIA-INDUCED SYNAPTIC DEPRESSION

1. Differential synaptic sensitivity to anoxia

This study demonstrates the differential anoxic depression of the *e* EPSPs and *l* EPSPs, as well as the extreme sensitivity to anoxia of both types of IPSPs in neocortical pyramidal neurons. An important factor likely to contribute to the high sensitivity to anoxia of the *l* EPSP and the IPSPs is their multisynapticity. Both types of PSPs are elicited through polysynaptic pathways that have at least one excitatory synapse involving "non-NMDA" (AMPA/kainate) receptors. This is supported by the finding that 6-cyano-7-nitroquinoxaline-2,3-dione (CNQX), an AMPA receptor antagonist, is effective in blocking not only the *e* EPSP but also the *l* EPSP and both types of IPSPs (Hablitz and Sutor, 1990). Consequently, even if a simple, non-NMDA synaptic event such as the *e* EPSP is only moderately depressed by anoxia, the effect would be augmented in a polysynaptic pathway and result in failure of discharge of the last neuron(s) in the chain. The rapid blockade of spike-generating, multisynaptic events such as the *l* EPSP may be a significant mechanism underlying the early loss of consciousness that is induced by anoxia and has been related to an impaired ability of neocortical neurons to fire repetitively (Krnjevic, 1986).

One cannot dismiss, however, the possibility that different synapses may have different sensitivities to anoxia. NMDA-evoked inward currents in mature CA1/CA3 neurons are reversibly suppressed by anoxia, whereas those in immature neurons are highly resistant (Krnjevic et al., 1989). Other preliminary experiments have shown that NMDA-mediated synaptic responses in CA1 are rapidly abolished by anoxia, as opposed to only a modest decrease

in the non-NMDA response during the same time interval (Hershkowitz and Veregge, 1991). This would represent an additional factor in determining the high sensitivity of the neocortical *l* EPSP, which is dependent on NMDA receptors at a presynaptic level (Sutor and Hablitz, 1989b).

The results illustrate the rapid disappearance and delayed recovery of both fast and slow IPSPs with anoxia and are in agreement with experiments performed in CA1 pyramidal neurons which have reported early blockade of the undifferentiated IPSP (Fujiwara et al., 1987; Leblond and Krnjevic, 1989) and fast (< 80 s) depression of inhibitory postsynaptic currents (Hershkowitz and Veregge, 1991), as well as with the neocortical study of the primary somatosensory cortex (Luhmann and Heinemann, 1992), which reported a significantly larger depression of both IPSPs, as compared to the EPSP. Although the underlying cause is not yet known, the experiments using QUIS and GABA suggest that the higher N_2 sensitivity of the IPSP is not attributable to a differential vulnerability of postsynaptic processes. Moreover, in a recent study (Khazipov et al., 1993) it was shown that monosynaptic $GABA_A$-receptor mediated currents are resistant to anoxia, suggesting that the inhibition of the multisynaptic chloride-dependent (fast) IPSPs is due mainly to the depression of the excitatory glutamate–activated neurons in the chain.

Because of the non-uniform progression of the depression and/or recovery of the IPSPs/EPSPs, both neocortex and hippocampus have the potential of developing transient increases in excitability during the early anoxic and early recovery phases. The net effect would be modulated by additional factors such as the initial slope of the anoxic depolarization, the presence of the anomalous rectification, intrinsic bursting properties of the neuron and the degree of increase in AP threshold. Given the brevity of this effect in neocortical slices, its *in vivo* significance is uncertain, but it is conceivable that in the

presence of intact and spontaneously active synaptic circuitry, both membrane depolarization and enhanced excitability due to loss of IPSPs may induce significant cation (Na^+, Ca^{2+}) influx and anoxic damage (Choi, 1988). In the hippocampus, where, the contrast between the anoxic effects on IPSP vs. EPSP appears greater than in the neocortex, the extremely high vulnerability of the CA1 neurons to hypoxia-induced seizures and degeneration may be importantly determined by the EPSP/IPSP differential sensitivity.

2. Mechanisms of synaptic depression

a. Postsynaptic mechanisms

It must be emphasized that the present experiments reflect changes recorded at the level of the neuronal soma. It is possible that anoxia induces different variations in V_R and R_N in the dendrites. This is important, because most of the excitatory synapses are located in these neurons on the spines and dendritic shafts (Douglas and Martin, 1990), and it has been shown that the *e* EPSP origin is most probably in the distal dendrites (Sutor and Hablitz, 1989a). The manipulation of V_m and decrease in R_N at the soma would not be able to influence the *e* EPSP changes, and therefore postsynaptic occlusion and/or shunting cannot be excluded as contributing factors to the depression of the *e* EPSP. On the other hand, the *l* EPSP and most of the IPSPs are generated at or close to the soma (Douglas and Martin, 1990; Sutor and Hablitz, 1989a). The present results show that at least for these types of PSPs, somatic postsynaptic occlusion or shunting does not seem to play a role in anoxic depression.

Further demonstration of only a moderate anoxic effect on postsynap-

tic receptors is shown by the 25–26% decrease in amplitude of the responses to locally applied QUIS and GABA. Due to the reproducibility of the responses to exposure to these substances prior to anoxia, as well as the low frequency of ejections, it is conceivable that this represents a true anoxic depression, rather than being an effect of receptor de-sensitization due to repeated and prolonged exposure to the transmitters. The postsynaptic mechanism(s) of the anoxic depression of the excitatory synaptic transmission are not known—a decrease in receptor-channel phosphorylation, or a shift in equilibrium potential for Na^+ and Ca^{2+} may constitute possible explanations. However, the effect on QUIS responses would not seem extensive enough to account for the large depression of amplitude (about 70%) of the monosynaptic *e* EPSP, although it may be important for a polysynaptic pathway such as that supporting the *l* EPSP. Furthermore, the similarity between the anoxic effects of GABA and QUIS responses suggests that postsynaptic depression may not be the mechanism responsible for the increased sensitivity of the IPSPs to anoxia.

b. Presynaptic mechanisms

The observation that the frequency of mpsps decreased significantly (65–70%) during anoxic exposure suggests that presynaptic mechanisms constitute the major factor determining the synaptic depression. This is in agreement with the finding that N_2 blocks the decreases in $[Ca^{2+}]_o$ evoked in CA1 stratum radiatum by orthodromic stimulation (Young and Somjen, 1991). The mechanism producing this presynaptic inhibition appears to be the activation of the A_1 presynaptic adenosine receptors. Although glutamate continues to accumulate extracellularly due to a reversal of its uptake mechanisms

(Szatkowski and Attwell, 1994), by blocking presynaptic Ca^{2+} influx and vesicular transmitter release, adenosine depresses coherent synaptic transmission and limits energy expenditure. This effect is thought to account for the neuroprotective anti-anoxic role of endogenously released adenosine in neurons rich in glutamate receptors (Rudolphi et al., 1992; Lee and Löwenkopf, 1993; Kennedy and Ijzerman, 1994).

It is important to mention that, due to the hyperpolarized V_R values for the neocortical neurons, the recorded mpsps represented in fact a mixture of excitatory mpsps (mepsps) and reversed inhibitory mpsps (mipsps), and therefore, these experiments did not take into account the differential sensitivity to anoxia between the two types of synaptic inputs. In the event that IPSPs may be more sensitive to lack of O_2 than EPSPs due to specific pre-synaptic characteristics, it is possible that the overall observed effect on mpsps could be due to a predominant mipsps presynaptic depression, and the real effect of anoxia on mepsps has been overestimated.

D. PROTECTIVE MEASURES

1. Creatine

It is not known why pre-incubation in creatine failed to protect the fronto-parietal neocortical neurons against anoxic–induced synaptic depression and/or depolarization. The dose and pre-incubation period were similar to those previously described (Whittingham and Lipton, 1981; Leblond and Krnjevic, 1989; Luhmann and Heinemann, 1992), which resulted in a prominent protective effect, with preservation of synaptic transmission during anoxia. It is possible that ATP stores are less vulnerable in the parietal neo-

cortex than in other neuronal groups (Lipton and Whittingham, 1979, 1982). Conversely, the increased excitability with bursting discharges, observed in normoxic conditions in our experiments has not been described in the other studies.

2. ATP-sensitive K^+ channels

Apart from pancreatic beta cells and myocytes (Henquin and Meissner, 1982; Ashcroft, 1988), ATP-dependent K^+ channels have been described in both hippocampal CA1 and (especially) CA3 regions (mossy fibers terminals—Krnjevic and Leblond, 1988; Krnjevic, 1990) and in neocortex (Cook, 1988; Quast and Cook, 1989).

Since in physiological conditions these channels are kept closed by the normal levels of ATP, a decrease in ATP such as in anoxia is expected to open them and result in (1) a direct K^+ efflux and hyperpolarization of the postsynaptic neuron if the channels are present postsynaptically, or (2) a K^+ efflux and hyperpolarization of the terminal with potentially either increased or decreased transmitter release and hyperpolarization of the postsynaptic neuron, if the channels are also present presynaptically. Interestingly, this is not the case for neurons in CA1, where the hyperpolarizing response to anoxia is determined (at least in the largest part) by another type of K^+ conductance (possibly Ca^{2+}-activated? M current?). However, the presence of the ATP-dependent K^+ channels in CA3 neurons which are depolarized by anoxia raises the therapeutic possibility of using channel openers (diazoxide, galanin) to counteract the anoxic depolarization.

Several hippocampal studies demonstrate that these channel openers are indeed able to suppress CA3 anoxic depolarization, whereas ATP-sensitive

K^+ channel inhibitors (tolbutamide, glibenclamide) augment it (Ben Ari and Krnjevic, 1989; Ben Ari and Lazdunski, 1989; Ben Ari, 1990; Ben Ari et al., 1990). It appears that, in the hippocampal slices, brief anoxia implicates ATP-dependent K^+ channels differently in hyperpolarizing neurons (CA1) as compared to depolarizing neurons (CA3). These findings have been partially confirmed by *in vivo* experiments which have shown a lack of effect of gliquidone (a sulphonylurea believed to be selective for the ATP-dependent K^+ channels) on hypoxia-induced rise in $[K^+]_o$ in CA1 neurons (Zetterström et al. 1995).

It could have been expected that neocortical neurons, which in many respects behave quite similarly to CA3 cells (depolarization), would manifest a sensitivity to pharmacological manipulation of ATP-sensitive K^+ channels (i.e. an activation of these channels would trigger a hyperpolarizing component that could counteract the anoxic depolarization). The present study failed to demonstrate the ability of ATP-sensitive K^+ channels to be activated as an either endogenous (decrease in ATP levels) or exogenous (diazoxide) potential antidepolarizing measure. On the other hand, Luhmann and Heinemann (1992) found in the somato-sensory cortex that the ATP-dependent K^+ channel blocker, gliquidone shifted E_{REV} of anoxic hyperpolarization towards more depolarized levels, which suggests that these channels may play a direct role in the hyperpolarization seen in that type of neurons. However, in their study gliquidone did not increase AD in depolarizing neurons, which behave in the same way as fronto-parietal neocortical neurons. This suggests that (1) in very similar neurons of neighboring neocortical regions, ATP-sensitive K^+ channels have a non-uniform distribution and (2) depolarizing pyramidal neurons from different types of neocortex do not manifest the same ability of recruiting antidepolarizing mechanisms during early anoxia.

3. Changes in temperature

Temperature can be easily controlled in the slice preparation (Andersen et al., 1972; Schiff and Somjen, 1985) and cortical slices have in many instances been used to study the effects of temperature on neuronal physiology in control and anoxic/ischemic conditions (Thompson et al., 1985; Tanimoto and Okada, 1987; Morris et al., 1988, 1991; Taylor and Weber, 1993, Kurihara et al., 1996). These studies focused on hippocampal CA1 neurons and although neocortical neurons are also known to be particularly sensitive to anoxia, the effects of temperature on neocortical anoxic changes, especially at intracellular level, have been studied far less often.

a. Normoxic conditions

Data from the literature regarding effects of temperature on V_R and synaptic potentials are not entirely in agreement. This may be due in part to the fact that various authors used different control temperatures (with different ranges of "warming" and "cooling") and because temperature effects do not seem to vary linearly over the wide range between room temperature (about 21°C) and 37°C. For example, our findings are partially in agreement with the hippocampal study of Schiff and Somjen (1985) who also found that at 33°C, the extracellularly recorded focal EPSP increased as compared with 29°C. However, they reported a further increase of the EPSP at 37°C and explained it through a warming-induced hyperpolarization of the postsynaptic neurons, again in disagreement with our finding that warming above 35°C induces depolarization. Another hippocampal study (Thompson et al., 1985) reported the increase of a Ca^{2+}-activated K^+ conductance by cooling the slice from 37

to 27–33°C —in agreement with changes in population spike duration and $[K^+]_o$ measurements recorded by others (Morris et al., 1991) and also with the more hyperpolarized, stable V_R values seen in our experiments. However, Thompson et al., (1985) described a K^+-dependent *s* IPSP which became prominent only at low temperature, whereas our experiments show that IPSPs are highly sensitive to temperature changes in both directions.

It is not clear if these discrepancies are due to functional differences between cortical regions (hippocampus vs. neocortex), recording conditions (interface vs. submerged preparations), or other factors which could affect the viability of the slice and its capability of coping with the increased energy demands brought about by raised temperature.

Some of the effects of increasing temperature seen in our experiments (slow membrane depolarization, spontaneous depolarizing shifts and decrease in PSP amplitude) may be due to the induction of a relatively hypoxic state; however, these changes were limited, since V_R shifts were minimal and neurons never discharged bursts of APs. Indeed, our relatively low control temperatures of about 34°C are frequently used in similar hippocampal and neocortical in vitro studies (Connors et al., 1988; Leblond and Krnjevic, 1989; Sutor and Hablitz, 1989a,b; Taylor and Weber, 1993) in order to promote viability and improve the quality of recording (Thompson et al., 1985).

b. Anoxic conditions

The results show that increased temperature can accelerate the hypoxic-anoxic induced changes in neocortical neuronal excitability. This confirms similar observations in other brain regions/preparations (Tanimoto and Okada, 1987; Krnjevic and Walz, 1990; Morris et al., 1991; Taylor and Weber,

1993; Kurihara et al., 1996). The more pronounced effect of warming upon the anoxic depression of IPSPs and *l* EPSP, as compared with *e* EPSP, is consistent with the polysynaptic nature of both IPSPs and the *l* EPSP—a feature which is also responsible for their increased sensitivity to anoxia at control temperature (see **RESULTS**). Functionally, there is augmented disruption of normal neuronal communication—with the enhancement of the depression of the synaptic transmission and the occurrence of spontaneous activity. Moreover, phenomena related to the enhanced depolarization (increased transmitter release, Na^+-K^+ pump failure and increased $[K^+]_o$ (Morris et al., 1991) can summate, resulting in further metabolic deleterious effects. Conversely, cooling, especially under 30°C, appears to represent an efficient protective measure against the early anoxic response.

SUMMARY AND CONCLUSIONS

The object of this study was to characterize the response of neocortical pyramidal neurons to brief periods of anoxia. Experiments were carried out *in vitro,* using a rat brain slice preparation and inducing anoxic episodes by total replacement of O_2 with N_2. Membrane properties and synaptic responses of fronto-parietal pyramidal neurons from layers II-III were tested using intracellular recording techniques (current clamp mode) and were compared in normoxic and anoxic conditions. Various pharmacological and physical manipulations (drug bath application and pressure ejection, ion replacement, temperature variation) were used to define the mechanisms underlying the observed anoxia-induced changes and to investigate some possible anti-anoxia protective measures. These experimental procedures helped in determining the following:

(1) Brief (5 min) anoxia induced a reversible small ***depolarization*** (3-5 mV), which was present in all tested neurons and was not contaminated by hyperpolarizing tendencies. The anoxic depolarization was accompanied by a small /moderate ***decrease in input resistance*** (by at most 20% of the control value).

(2) The principal ionic mechanism underlying the anoxic depolarization is an intracellular ***Na^+ influx***. This is supported by the strong suppressive effect elicited by ***tetrodotoxin*** and extracellular ***Na^+ replacement*** on the depolarization.

(3) An important source of Na^+ influx is constituted by the ***non-NMDA*** (AMPA/kainate) synaptic receptors, (as opposed to NMDA and metabotropic receptors), since the depolarization is also supresssed by ***kynurenic acid***, but not by APV and MCPG.

(4) Extracellular K^+ accummulation and extracellular Ca^{2+} influx are most probably ***not significantly involved*** in the depolarization, as suggested by K^+ bath changes and bath application of metallic calcium blockers and APV. ***Chloride*** efflux, (not mediated by the $GABA_A$ receptors), seems to contribute to some extent to the depolarization. Additional experiments are necessary in order to fully ascertain the role of Ca^{2+} (especially regarding possible Ca^{2+} release from internal stores).

(5) Anoxia strongly ***depresses*** all synaptic events (***EPSPs*** and ***IPSPs***). IPSPs and polysynaptic ("late") EPSPs are particularly sensitive (complete block), whereas monosynaptic ("early") EPSP are depressed by 60–70%. These changes are reversible upon re-oxygenation. The accentuated sensitivity of the IPSPs may result in transient ***increases in excitability*** during early anoxia and early recovery.

(6) The mechanisms responsible for synaptic depression appear to be mainly of ***presynaptic*** origin—presynaptic inhibition through ***adenosine A_1*** receptors, as suggested by the decreased mepsps frequency and the protective role of the A_1 receptor antagonist 8–CPT. However, a small ***postsynaptic*** contribution could also be demonstrated by the anoxic depression of the response to quisqualate application on synaptically-isolated neurons.

(7) The electrophysiological changes induced by N_2 exposure (particularly the synaptic depression), show a strong correlation with variations of ***temperature*** (26–37°C)—hyperthermia accentuates, while hypothermia protects against the effects of anoxia.

REFERENCES

Alger, B.E. and Nicoll, R.A. (1982). Pharmacological evidence for two kinds of GABA receptor on rat hippocampal pyramidal cells studied *in vitro*. J. Physiol. 328: 125–141.

Alger, B.E., Dhanjal, S.S., Dingledine, R., Garthwaite, J., Henderson, G., King, G.L., Lipton, P., North, A., Schwartzkroin, A., Sears, T.A., Segal, M.,Whittingham, T.S. and Williams, J. (1984). Brain slice methods. In: *Brain Slices*, edited by R. Dingledine. New York: Plenum, pp. 381–437.

Andersen, P. (1984). Brain slice work: some prospects. In: *Brain Slices*, edited by R. Dingledine. New York: Plenum, pp. 375–380.

Andersen, P., Gjerstad, L. and Pasztor, E. (1972). Effect of cooling on synaptic transmission through the cuneate nucleus. Acta Physiol. Scand. 84: 433–447.

Andersen, P., Dingledine, R., Gjerstad, L., Langmoen, I.A. and Mosfeldt Laursen, A. (1980). Two different responses of hippocampal pyramidal cells to application of γ-aminobutyric acid. J. Physiol. 305: 279–296.

Aram, J.A., Michelson, H.B. and Wong, R.K.S. (1991). Synchronized GABAergic IPSPs recorded in the neocortex after blockade of synaptic transmission mediated by excitatory amino acids. J. Neurophysiol. 65(5): 1034–1041.

Ashcroft, F.M. (1988). Adenosine 5'-triphosphate-sensitive potassium channels. Ann. Rev. Neurosci. 11: 97–118.

Balesterino, M. and Somjen, G.G. (1986). Chlorpromazine protects brain tissue in hypoxia by delaying spreding depression-mediated calcium influx. Brain Res. 385: 219–226.

Barolet, A.W., Andrews, R. and Morris, M.E. (1989). Calibration of ion-selec tive microelectrodes: flow-system and analysis program for the IBM PC. J. Neurosci. Methods 30: 263–266.

Bashir, Z.I., Bortolotto, Z.A., Davies, C.H., Berretta, N., Irving, A.J., Seal, A.J., Henley, J.M., Jane, D.E., Watkins, J.C. and Collingridge, G.L. (1993). Induction of LTP in the hippocampus needs synaptic activation of glutamate metabotropic receptors. Nature 363: 347–350.

Baskys, A. (1992). Metabotropic receptors and "slow" excitatory actions of glutamate agonists in the hippocampus. Trends Neurosci. 15(2): 92–96.

Belousov, A.B., Godfraind, J.-M. and Krnjevic, K. (1995). Internal Ca^{2+} stores involved in anoxic responses of rat hippocampal neurons. J. Physiol. 486.3: 547–556.

Bendo, A.A., Kass, I.S. and Cottrell, J.E. (1987). Anesthetic protection against anoxic damage in the rat hippocampal slice. Brain. Res. 403: 136–141.

Ben Ari, Y. (1990). Galanin and glibenclamide modulate the anoxic release of

glutamate in rat CA3 hippocampal neurons. Eur. J. Neurosci. 2: 62–68.

Ben Ari, Y. and Krnjevic, K. (1989). The ATP–sensitive K^+ channel opener diazoxide reduces anoxic depolarization in rat CA3 hippocampal neurones in isolated slices. J. Physiol. 418: 192P.

Ben Ari, Y., Krnjevic, K. and Crépel, V. (1990). Activators of ATP–sensitive K^+ channels reduce anoxic depolarization in CA3 hippocampal neurons. Neuroscience 37(1): 55–60.

Ben Ari, Y. and Lazdunski, M. (1989). Galanin protects hippocampal neurons from the functional effects of anoxia. Eur. J. Pharmacol. 165: 331–332.

Bindman, L.J., Meyer, T., Prince, C.A. (1988). Comparison of the electrical properties of neocortical neurones in slices *in vitro* and in the anæsthetized rat. Exp. Brain Res. 69: 489–496.

Boening, J.A., Kass, I.S., Cottrell, J.E. and Chambers, G. (1989). The effect of blocking sodium influx on anoxic damage in the rat hippocampal slice. Neuroscience 33(2): 263–268.

Bonanno, G. and Raiteri, M. (1993). Multiple $GABA_B$ receptors. Trends Pharmacol. Sci. 14: 259–261.

Bormann, J. (1988). Electrophysiology of $GABA_A$ and $GABA_B$ receptor subtypes. Trends Neurosci. 11(3):

Boxer, A.P., Cordon, J.J., Mann, M.E., Rodolosi, R.C., Vartanian, M.G., Rock, D.M.,Taylor, C.P. and Marcoux, F.W. (1990). Comparison of phenytoin with non–competitive N-methyl-D-aspartate antagonists in a model of focal brain ischemia in rat. Stroke 21: (Suppl.III) 47–51.

Brown, R.E. and Reymann, K.G. (1995). Class I metabotropic glutamate receptor agonists do not facilitate the induction of long-term potentia tion in the dentate gyrus of the rat in vitro. Neurosci. Lett. 202: 73–76.

Burke, J.P. and Hablitz, J.J. (1994). Metabotropic glutamate receptor activation decreases epileptiform activity in rat neocortex. Neurosci. Lett. 174: 29–33.

Catterall, W.A. (1992). Cellular and molecular biology of voltage-gated sodium channels. Physiol. Rev. 72(4-suppl.): S15–S48.

Choi, D.W. (1988). Glutamate neurotoxicity and diseases of the nervous system. Neuron 1: 623–634.

Choi, D.W. and Rothman, S.M.(1990). The role of glutamate neurotoxicity in hypoxic–ischemic neuronal death. Annu. Rev. Neurosci. 13: 171–182.

Clark, G.D. and Rothman, S.M. (1987). Blockade of excitatory amino acid receptors protects anoxic hippocampal slices. Neuroscience 21(3): 665–671.

Connors, B.W. and Gutnick, M.J. (1984). Neocortex—cellular properties and

intrinsic circuitry. In: *Brain Slices*, edited by R. Dingledine. New York: Plenum, pp. 313–339.

Connors, B.W. and Gutnick, M.J. (1990). Intrinsic firing patterns of diverse neocortical neurons. Trends Neurosci. 13(3): 99–104.

Connors, B.W., Gutnick, M.J. and Prince, D.A. (1982). Electrophysiological properties of neocortical neurons in vitro. J. Neurophysiol. 48: 1302–1320.

Connors, B.W., Malenka, R.C. and Silva, L.R. (1988). Two inhibitory postsynaptic potentials, and $GABA_A$ and $GABA_B$ receptor-mediated responses in neocortex of rat and cat. J. Physiol. 406: 443–468.

Cook, N.S. (1988). The pharmacology of potassium channels and their therapeutic potential. Trends Pharmacol. Sci. 9: 21–28.

Cotman, C.W. and Iversen, L.L. (1987). Excitatory amino acids in the brain—focus on NMDA receptors. Trends Neurosci. 10(7): 263–272.

Doll, C.J., Hochachka, P.W. and Reiner, P.B. (1991). Effects of anoxia and metabolic arrest on turtle and rat cortical neurons. Am. J. Physiol. 260: R747–R755.

Douglas, R.J. and Martin, K.A.C. Neocortex. In: *The Synaptic Organization of the Brain*, edited by G.M. Shepherd. New York: Oxford Univ. Press, pp. 389–438.

Dutar, P. and Nicoll, R.A. (1988). A physiological role for $GABA_B$ receptors in the central nervous system. Nature 332: 156–158.

Erecinska, M. and Silver, I.A. (1994). Ions and energy in mammalian brain. Prog. Neurobiol. 43: 37–71.

Fowler, J.C. (1989). Adenosine antagonists delay hypoxia–induced depression of neuronal activity in hippocampal brain slice. Brain Res. 490: 378–384.

Fried, E., Amorim, P., Chambers, G., Cottrell, J.E. and Kass, I.S. (1995). The importance of sodium for anoxic transmission damage in rat hippocam pal slices: mechanisms of protection by lidocaine. J. Physiol. 489.2: 557–565.

Fujiwara, N., Higashi, H., Shimoji, K. and Yoshimura, M. (1987). Effects of hypoxia on rat hippocampal neurones *in vitro*. J. Physiol. 384: 131–151.

Globus, M. Y-T., Busto, R., Martinez, E., Valdés,I. and Dietrich, W.D. (1990). Ischemia induces release of glutamate in regions spared from histopathologic damage in the rat. Stroke 21: (Suppl.III) 43–46.

Glötzner, F. (1967). Intracelluläre potentiale, EEG und korticale Gleichspannung an der sensorimotorischen Rinde der Katze bei akuter Hypoxie. Arch. Psychiatr. Nervenkr. 210: 274–296.

Godfraind, J.M. and Krnjevic, K. (1993). Tolbutamide suppresses anoxic out

ward current of hippocampal neurons. Neurosci. Lett. 162: 101–104.

Grace, A.A. and Llinas, R. (1985). Morphological artifacts induced in intracellularly stained neurons by dehydration: circumvention using rapid dimethyl sulfoxide clearing. Neuroscience 16: 461–475.

Graham, S.H., Chen, J., Sharp, F.R. and Simon, R.P. (1993). Limiting ischemic injury by inhibition of excitatory amino acid release. J. Cereb. Blood Flow Metab. 13: 88–97.

Graham, S.H., Shiraishi, K., Panter, S.S., Simon, R.P. and Faden, A.I. (1990). Changes in extracellular amino acid neurotransmitters produced by focal cerebral ischemia. Neurosci. Lett. 110: 124–130.

Gribkoff, V.K., Bauman, L.A. and VanderMaelen, C.P. (1990). The adenosine antagonist 8-cyclopentyltheophylline reduces the depression of hippocampal neuronal response during hypoxia. Brain Res. 512: 353–357.

Hablitz, J.J. and Sutor, B. (1990). Excitatory postsynaptic potentials in rat neocortical neurons in vitro. III. Effects of a quinoxalinedione non-NMDA receptor antagonist. J. Neurophysiol. 64(4): 1282–1290.

Haddad, G. and Donnelly, D.F. (1990). O_2 deprivation induces a major depolarization in brain stem neurons in the adult but not in the neonatal rat. J. Physiol. 429: 411–428.

Hansen, A.J. (1985). Effect of anoxia on ion distribution in the brain. Physiol. Rev. 65(1): 101–148.

Hansen, A.J., Hounsgaard, J. and Jahnsen, H. (1982). Anoxia increases potassium conductance in hippocampal nerve cells. Acta Physiol. Scand. 115: 301–310.

Hauptman, M., Nelson, D., Wilson, D.F. and Erecinska, M. (1984). Neurotransmitter amino acids in the CNS. II. Some changes in amino acid levels in rat brain synaptosomes during and after in vitro anoxia and simulated ischemia. Brain Res. 304: 23–35.

Henquin, J-C. and Meissner, H.P. (1982). Opposite effects of tolbutamide and diazoxide on $^{86}Rb^{+}$ fluxes and membrane potential in pancreatic B cells. Biochem. Pharmacol. 31(7): 1407–1415.

Hershkowitz, N. and Veregge, S. (1991). Effects of hypoxia on spontaneous and evoked synaptic currents in the hippocampus. Soc. Neurosci. Abstr. 17:1269.

Hollmann, M., Hartley, M. and Heinemann, S. (1991). Ca^{2+} permeability of KA-AMPA-gated glutamate receptor channels depends on subunit composition. Science 252: 851–853.

Hollmann, M. and Heinemann, S. (1994). Cloned glutamate receptors. Annu. Rev. Neurosci. 17: 31–108.

Hossmann, K–A. and Zimmermann, V. (1974). Resuscitation of brain after one hour of complete ischemia. I. Physiological and morphological observations. Brain Res. 81: 59–74.

Howe, J.R., Sutor, B. and Zieglgänsberger, W. (1987). Characteristics of long-duration inhibitory postsynaptic potentials in rat neocortical neurons *in vitro*. Cell. Mol. Neurobiol. 7(1): 1–18.

Huntley, G.W., Vickers, J.C. and Morrison, J.H. (1994). Cellular and synaptic localization of NMDA and non–NMDA receptor subunits in neocortex: organizational features related to cortical circuitry, function and disease. Trends Neurosci. 17(12): 536–543.

Inoue, M., Matsuo, T. and Ogata, N. (1985a). Baclofen activates voltage-dependent and 4-aminopyridine sensitive K^+ conductance in guinea-pig hippocampal pyramidal cells maintained *in vitro*. Br. J. Pharmacol. 84: 833–841.

Inoue, M., Matsuo, T. and Ogata, N. (1985b). Characterization of pre- and post-synaptic actions of (–)-baclofen in the guinea-pig hippocampus *in vitro*. Br. J. Pharmacol. 84: 843–851.

Inoue, M., Matsuo, T. and Ogata, N. (1985c). Possible involvement of K^+ conductance in the action of γ-aminobutyric acid in the guinea-pig hippocampus. Br. J. Pharmacol. 86: 515–524.

Jane, D.E., Jones, P.L.St.J., Pook, P.C-K., Tse, H–W. and Watkins, J.C.

(1994). Actions of two new antagonists showing selectivity for different sub-types of metabotropic glutamate receptor in the neonatal rat spinal cord. Br. J. Pharmacol. 112: 809–816.

Jacobson, I., Hagberg, H., Sandberg, M. and Hamberger, A. (1986). Ouabain-induced changes in extracellular aspartate, glutamate and GABA levels in the rabbit olfactory bulb in vivo. Neurosci. Lett. 64: 211–215.

Kass, I.S. and Lipton, P. (1982). Mechanisms involved in irreversible anoxic damage to the *in vitro* rat hippocampal slice. J. Physiol. 332: 459–472.

Kass, I.S., Chambers, G. and Cottrell, J.E. (1989). The *N*-methyl-D-aspartate antagonists aminophosphonovaleric acid and MK-801 reduce anoxic damage to dentate granule and CA1 pyramidal cells in the rat hippocampal slice. Exp. Neurol. 103: 116–122.

Kemp, J.A., Foster, A.D. and Wong, E.H.F. (1987). Non-competitive antagonists of excitatory amino acid receptors. Trends Neurosci. 10(7): 294–298.

Kennedy, C. and Ijzerman, A. (1994). Adenosine and ATP: from receptor structure to clinical applications. Trends Pharmacol. Sci. 15: 311–316.

Khazipov, R., Bregestovski, P. and Ben Ari, Y. (1993). Hippocampal inhibitory interneurons are functionally disconnected from excitatory inputs by anoxia. J. Neurophysiol. 70(6): 1–9.

Kostyuk, P. and Verkhratsky, A. (1994). Calcium stores in neurons and glia. Neurosci. 63: 381–404.

Krnjevic, K. (1986). Cellular and synaptic effects of general anesthetics. In: *Molecular and Cellular Mechanisms of Anesthetics*. Edited by S.H. Roth and K.W. Miller. New York: Plenum, pp. 3–16.

Krnjevic, K. (1987). GABAergic inhibition in the neocortex. J. Mind Behaviour 8(4): 537[61]–548[72].

Krnjevic, K. (1990). Adenosine triphosphate-sensitive potassium channels in anoxia. Stroke 21(11) Suppl.III: 190–193.

Krnjevic, K. and Ben Ari, Y. (1989). Anoxic changes in dentate granule cells. Neurosci. Lett. 107: 89–93.

Krnjevic, K., Cherubini, E. and Ben Ari, Y. (1989). Anoxia on slow inward currents of immature hippocampal neurons. J. Neurophysiol. 62: 896–906.

Krnjevic, K. and Leblond, J. (1987). Anoxia reversibly depresses neuronal Ca^{2+} currents in rat hippocampal slices. Can. J. Physiol. Pharmacol. 65: 2157–2161.

Krnjevic, K. and Leblond, J. (1988). Are there hippocampal ATP-sensitive K channels that are activated by anoxia? Pflügers Arch. 411: Suppl. R145.

Krnjevic, K. and Leblond, J. (1989). Changes in membrane currents of hippocampal neurons evoked by brief anoxia. J. Neurophysiol. 62: 15–30.

Krnjevic, K. and Schwartz, S. (1967). The action of γ-aminobutyric acid on cortical neurons. Exp. Brain Res. 3: 320–336.

Krnjevic, K. and Walz, W. (1990). Acidosis and blockade of orthodromic responses caused by anoxia in rat hippocampal slices at different temperatures. J. Physiol. 422: 127–144.

Krnjevic, K. and Xu, Y.Z. (1989). Dantrolene suppresses the hyperpolarization or outward current observed during anoxia in hippocampal neurons. Can. J. Physiol. Pharmacol. 67: 1602–1604.

Krnjevic, K. and Xu, Y.Z. (1990). Mechanisms underlying anoxic hyperpolarization of hippocampal neurons. Can. J. Physiol. Pharmacol. 68: 1609–1613.

Kurihara, E., Ishikawa, A., Tamaki, N. and Okada, Y. (1996). The protective effect of hypothermia on the recovery of neural activity after depriva tion of oxygen and glucose: study of slices from the hippocampus and superior colliculus. Neurosci. Lett. 204: 197–200.

Landis, D.M.D. (1994). The early reactions of non-neuronal cells to brain injury. Annu. Rev. Neurosci. 17: 133–151.

Leblond, J. and Krnjevic, K. (1989). Hypoxic changes in hippocampal neurons. J. Neurophysiol. 62: 1–14.

Lee, K.S. and Löwenkopf, T. (1993). Endogenous adenosine delays the onset of hypoxic depolarization in the rat hippocampus in vitro via an action at A_1 receptors. Brain Res. 609: 313–315.

Lipton, P. and Whittingham, T.S. (1979). The effect of hypoxia on evoked potentials in the *in vitro* hippocampus. J. Physiol. Lond. 287: 427–438.

Lipton, P. and Whittingham, T.S. (1982). Reduced ATP concentration as a basis for synaptic transmission failure during hypoxia in the *in vitro* guinea-pig hippocampus. J. Physiol. 325: 51–65.

Lipton, P. and Whittingham, T.S. (1984). Energy metabolism and brain slice function. In: *Brain Slices*, edited by R. Dingledine. New York: Plenum, pp.113–153.

Luhmann, H.J. (1996). Ischemia and lesion induced imbalances in cortical function. Progr. Neurobiol. 48: 131–166.

Luhmann, H.J. and Heinemann, U. (1992). Hypoxia–induced functional alterations in adult rat neocortex. J. Neurophysiol. 67(4): 798–811.

Manzoni, O.J., Manabe, T. and Nicoll, R.A. (1994). Release of adenosine by activation of NMDA receptors in the hippocampus. Science 265: 2098–2101.

Martin, R.L., Lloyd, H.G.E. and Cowan, A.I. (1994). The early events of oxy gen and glucose deprivation: setting the scene for neuronal death? Trends Neurosci. 17(6): 251–257.

McCarren, M. and Alger, B.E. (1987). Sodium-potassium pump inhibitors increase neuronal excitability in the rat hippocampal slice: role of a Ca^{2+}–dependent conductance. J. Neurophysiol. 57(2): 496–509.

McCormick, D.A. (1989). GABA as an inhibitory neurotransmitter in human cerebral cortex. J. Neurophysiol. 62(5): 1018–1027.

McCormick, D.A., Connors, B.W., Lighthall, J.W. and Prince, D.A. (1985). Comparative electrophysiology of pyramidal and sparsely spiny stellate neurons of the neocortex. J. Neurophysiol. 54: 782–806.

Meldrum, B.S., Swan, J.H., Leach, M.J., Millan, M.H., Gwinn, R., Kadota, K., Graham, S.H., Chen, J. and Simon, R.P. (1992). Reduction of glutamate release and protection against ischemic brain damage by BW-1003C87. Brain Res. 593: 1–6.

Mody, I. and MacDonald, J.F. (1995). NMDA receptor-dependent excitotoxicity: the role of intracellular Ca^{2+} release. Trends Pharmacol. Sci. 16: 356–359.

Mody, I., De Koninck, Y., Otis, T.S. and Soltesz, I. (1994). Bridging the cleft at GABA synapses in the brain. Trends Neurosci. 12: 517–525.

Morris, M.E., Baimbridge, K.G., El-Beheiry, H., Obrocea, G.V. and Rosen, A.S. (1995). Correlation of anoxic neuronal responses and calbindin-D_{28k} localization in stratum pyramidale of rat hippocampus. Hippocamp. 5: 25–39.

Morris, M.E., Leblond, J., Agopyan, N. and Krnjevic, K. (1991). Temperature dependence of extracellular ionic changes evoked by anoxia in hippocampal slices. J. Neurophysiol. 65(2): 157–167.

Morrisett, R.A., Mott, D.D., Lewis, D.L., Swartzwelder, H.S. and Wilson, W.A. (1991). $GABA_B$ -receptor-mediated inhibition of the *N*-methyl-D-aspartate component of synaptic transmission in the rat hippocampus. J. Neurosci. 11(1): 203–209.

Müller, W., Misgeld, U. and Lux, H.D. (1989). γ–aminobutyric acid-induced ion movements in the guinea pig hippocampal slice. Brain Res. 484: 184–191.

Niesen, C., Charlton, M.P. and Carlen, P.L. (1991). Postsynaptic and presynaptic effects of the calcium chelator BAPTA on synaptic transmission in rat hippocampal dentate granule neurons. Brain Res. 555: 319–325.

Nowak, L., Bregestovski, P. and Ascher, P. (1984). Magnesium gates gluta mate-activated channels in mouse central neurones. Nature (London) 307: 462–465.

Pockberger, H. (1991). Electrophysiological and morphological properties of rat motor cortex neurons in vivo. Brain Res. 539: 181–190.

Quast, U. and Cook, N.S. (1989). Moving together: K^+ channel openers and ATP-sensitive K^+ channels. Trends Pharmacol. Sci. 10: 431–435.

Rader, R.K. and Lanthorn, T.H. (1989). Experimental ischemia induces a persistent depolarization blocked by decreased calcium and NMDA antagonists. Neurosci. Lett. 99: 125–130.

Raichle, M.E. (1983). The pathophysiology of brain ischemia. Ann. Neurol. 13:2–10.

Robinson, M.E., Anderson, K.D. and Koerner J.F. (1984). Kynurenic acid as an antagonist of hippocampal excitatory transmission. Brain. Res. 309: 119–126.

Rosen, A.S. and Andrew, D.R. (1990). Osmotic effects upon excitability in rat neocortical slices. Neuroscience 38: 579–590.

Rosen, A.S. and Morris, M.E. (1990). Anoxic depolarization of neocortical pyramidal neurons in vitro. Soc. Neurosci. Abstr. 16: 277.

Rosen, A.S. and Morris, M.E. (1991a). Depolarizing effects of anoxia on pyramidal cells of rat neocortex. Neurosci. Lett. 124: 169–173.

Rosen, A.S. and Morris, M.E. (1991b). Anoxic depression of neocortical synap-

tic potentials. Soc. Neurosci. Abstr. 17: 1079.

Rosen, A.S. and Morris, M.E. (1991c). Decreased synaptic activation during anoxia in neocortex. Can. J. Physiol. Pharmacol. 69: Axxviii.

Rosen, A.S. and Morris, M.E. (1993). Anoxic depression of excitatory and inhibitory postsynaptic potentials in rat neocortical slices. J. Neurophysiol. 69 (1): 109–117.

Rosen, A.S. and Morris, M.E. (1994). Influence of temperature on anoxic responses of neocortical pyramidal neurons. Neuroscience 63(4): 949–955.

Rothman, S.M. (1983). Synaptic activity mediates death of hypoxic neurons. Science 220: 536–537.

Rothman, S.M. (1984). Synaptic release of excitatory amnio acid transmitter mediates anoxic neuronal death. J. Neurosci. 4(7): 1884–1891.

Rothman, S.M. (1985) The neurotoxicity of excitatory amnio acids is produced by passive chloride influx. J. Neurosci. 5(6): 1483–1489.

Rothman, S.M. and Olney, J.W. (1986). Glutamate and the pathophysiology of hypoxic-ischemic brain damage. Ann. Neurol. 19(2): 105–111.

Rothman, S.M. and Olney, J.W. (1987). Excitotoxicity and the NMDA receptor. Trends Neurosci. 10(7): 299–302.

Rothman, S.M. and Samaie, M. (1985). The physiology of excitatory synaptic transmission in cultures of dissociated rat hippocampus. J. Neurophysiol. 54: 701–713.

Rudolphi, K.A., Schubert, P., Parkinson, F.E. and Fredholm, B.B. (1992). Neuroprotective role of adenosine in cerebral ischæmia. Trends Pharmacol. Sci. 13: 439–445.

Sayer, R.J., Brown, A.M., Schwindt, P.C. and Crill, W.E. (1993). Calcium currents in acutely isolated human neocortical neurons. J. Neurophysiol. 69(5): 1596–1606.

Scharfman, H.E. and Schwartzkroin, P.A. (1989). Protection of dentate hilar cells from prolonged stimulation by intracellular calcium chelation. Science 246: 257–260.

Schatzki, A., McMillian, M. and Miller, L.G. (1990). Glutamate, kainate and quisqualate enhance GABA–dependent chloride uptake in cortex. Brain. Res. Bull. 25: 239–243.

Schiff, S.J. and Somjen, G.G. (1985). The effects of temperature on synaptic transmission in hippocampal tissue slices. Brain Res. 345: 279–284.

Schmidt-Kastner, R. and Freund, T.F. (1991). Selective vulnerability of the hippocampuus in brain ischemia. Neurosci. 40:599–636.

Schoepp, D.D. and Conn, P.J. (1993). Metabotropic glutamate receptors in

brain function and pathology. Trends Pharmacol. Sci. 14: 13–20.

Schoepp, D.D., Bockaert, J. and Sladeczek, F. (1990). Pharmacological and functional characteristics of metabotropic excitatory amino acid receptors. Trends Pharmacol. Sci. 11: 608–514.

Seeburg, P.H. (1993). The molecular biology of mammalian glutamate receptor channels. Trends Pharmacol. Sci. 14: 297–303.

Shaw, C. and Teyler, T.J. (1982). The neural circuitry of the neocortex examined in the in vitro brain slice preparation. Brain Res. 243: 35–47.

Shimizu, H., Mizuguchi, A. and Aoki, M. (1996). Differential responses between CA1 pyramidal cells and granule cells to ischemic insult in rat hippocampal slices. Neurosci. Lett. 203: 195–198.

Siesjö, B.K. (1988). Historical overview – calcium, ischemia and death of brain cells. Ann. N.Y. Acad. Sci. 522: 638–661.

Siesjö, B.K. and Bengtsson, F. (1989). Calcium fluxes, calcium antagonists, and calcium–related pathology in brain ischemia, hypoglycemia and spreading depression: a unifying hypothesis. J. Cereb. Blood Flow Metab. 9(2): 127–140.

Silver, I.A. and Erecinska, M. (1990). Intracellular and extracellular changes of $[Ca^{2+}]$ in hypoxia and ischemia in rat brain in vivo. J. Gen. Physiol. 95: 837–866.

Simpson, R.E., Walter, G.A. and Phillis, J.W. (1991). The effects of hypothermia on amino acid neurotransmitter release from the cerebral cortex. Neurosci. Lett. 124: 83–86.

Simpson, P.B., Challiss, J.R.A. and Nahorski, S.R. (1995). Neuronal Ca^{2+} stores: activation and function. Trends Neurosci. 18: 299–306.

Soltesz, I., Haby, M., Leresche, N. and Crunelli, V. (1988). The $GABA_B$ antagonist phaclofen inhibits the late K^+–dependent IPSP in cat and rat thalamic and hippocampal neurones. Brain Res. 448: 351–354.

Sommer, B., Keinänen, K., Verdoorn, T.A., Wisden, W., Burnashev, N., Herb, A., Köhler, M., Takagi, T., Sakmann, B. and Seeburg, P.H. (1990). Flip and flop: a cell-specific functional switch in glutamate-operated channels of the CNS. Science 249: 1580–1585.

Stafstrom. C.E., Schwindt, P.C. and Crill. W.E. (1982). Negative slope conductance due to a persistent subthreshold sodium current in cat neocortical neurons in vitro. Brain Res. 236: 221–226.

Sutor, B. and Hablitz, J.J. (1989a). EPSPs in rat neocortical neurons *in vitro*. I. Electrophysiological evidence for two distinct EPSPs. J. Neurophysiol. 61: 607–620.

Sutor, B. and Hablitz, J.J. (1989b). EPSPs in rat neocortical neurons *in vitro*. II. Involvement of *N*-Methyl-D-aspartate receptors in the generation of EPSPs. J. Neurophysiol. 61: 621–634.

Sutor, B. and Zieglgänsberger, W. (1987). A low-voltage activated, transient calcium current is responsible for the time–dependent depolarizing inward rectification of rat neocortical neurons in vitro. Pflügers Arch. 410: 102–111.

Szatkowski, M. and Attwell, D. (1994). Triggering and execution of neuronal death in brain ischæmia: two phases of glutamate release by different mechanisms. Trends Neurosci. 17(9): 359–365.

Taft, W.C., Clifton, G.L., Blair, R.E. and DeLorenzo, R.J. (1989). Phenytoin protects against ischemia-produced neuronal cell death. Brain Res. 483: 143–148.

Tan, A.T., Erdemli, G. and Krnjevic, K. (1995). Metabotropic-glutamate recep tor activation does not cause anoxic hyperpolarization of hippocampal neurons. Soc. Neurosci. Abstr. 21: 996.

Tanimoto, M. and Okada, Y. (1987). The protective effect of hypothermia on hippocampal slices from guinea pig during deprivation of oxygen and glucose. Brain Res. 417: 239–246.

Taylor, C.P. (1993). Na^+ currents that fail to inactivate. Trends Neurosci. 16(11): 455–460.

Taylor, C.P. and Weber, M.L. (1993). Effect of temperature on synaptic function after reduced oxygen and glucose in hippocampal slices. Neuroscience 52: 555–562.

Thompson, S.M. (1994). Modulation of inhibitory synaptic transmission in the hippocampus. Prog. Neurobiol. 42: 575–609.

Thompson, S.M., Deisz, R.A. and Prince, D.A. (1988). Relative contributions of passive equilibrium and active transport to the distribution of chloride in mammalian cortical neurons. J. Neurophysiol. 60(1): 105–124.

Thompson, S.M., Masukawa, L.M. and Prince, D.A. (1985). Temperature dependence of intrinsic membrane properties and synaptic potentials in hippocampal CA1 neurons *in vitro*. J. Neurosci. 5: 817–824.

Thomsen, C., Boel, E. and Suzdak, P.D. (1994). Actions of phenylglycine analogs at subtypes of the metabotropic glutamate receptor family. Eur. J. Pharmacol. Mol. Pharmacol. 267: 77–84.

Vogt, B.A. and Gorman, A.L.F. (1982). Responses of cortical neurons to stimulation of corpus callosum in vitro. J. Neurophysiol. 48(6): 1257–1273.

Watkins, J. and Collingridge, G. (1994). Phenylglycine derivatives as antagonists of metabotropic glutamate receptors. Trends Pharmacol. Sci. 15: 333–342.

Whittingham, T.S. and Lipton,P. (1981). Cerebral synaptic transmission during anoxia is protected by creatine. J. Neurochem. 37(6): 1618–1621.

Yamamoto, C. and Kurokawa, M. (1970). Synaptic potentials recorded in brain

slices and their modification by changes in the level of tissue ATP. Exp. Brain Res. 10: 159–170.

Young, J.N. and Somjen, G.G. (1991). Suppression of presynaptic calcium currents by hypoxia in hippocampal tissue slices. Soc. Neurosci. Abstr. 17:1271.

Zhang, L. and Krnjevic, K. (1993). Whole-cell recording of anoxic effects on hippocampal neurons in slices. J. Neurophysiol. 69 (1): 118–127.

Zetterström, T.S.C., Vaughan-Jones, R.D. and Grahame-Smith, D.G. (1995). A short period of hypoxia produces a rapid and transient rise in $[K^+]_e$ in rat hippocampus *in vivo* which is inhibited by certain K^+-channel block ing agents. Neurosci. 67 (4): 815–821.